USGS
science for a changing world

Prepared in cooperation with Missouri Department of Transportation

Bathymetric and Velocimetric Surveys at Highway Bridges Crossing the Missouri and Mississippi Rivers on the Periphery of Missouri, June 13–22, 2022

Scientific Investigations Report 2024–5032

U.S. Department of the Interior
U.S. Geological Survey

Cover. Structure A5076 on State Highway 34 at Cape Girardeau, Missouri. Photograph by U.S. Geological Survey

Bathymetric and Velocimetric Surveys at Highway Bridges Crossing the Missouri and Mississippi Rivers on the Periphery of Missouri, June 13–22, 2022

By Richard J. Huizinga

Prepared in cooperation with Missouri Department of Transportation

Scientific Investigations Report 2024–5032

U.S. Department of the Interior
U.S. Geological Survey

U.S. Geological Survey, Reston, Virginia: 2024

Suggested citation:
Huizinga, R.J., 2024, Bathymetric and velocimetric surveys at highway bridges crossing the Missouri and Mississippi Rivers on the periphery of Missouri, June 13–22, 2022: U.S. Geological Survey Scientific Investigations Report 2024–5032, 82 p., https://doi.org/10.3133/sir20245032.

Associated data for this publication:
Huizinga, R.J., and Rivers, B.C., 2023, Bathymetry and velocity data from surveys at highway bridges crossing the Missouri and Mississippi Rivers on the periphery of Missouri, June 13–22, 2022: U.S. Geological Survey data release, https://doi.org/10.5066/P9K66GYC.

U.S. Geological Survey, 2023, USGS water data for the Nation: U.S. Geological Survey National Water Information System database, https://doi.org/10.5066/F7P55KJN.

ISSN 2328-0328 (online)

Acknowledgments

The author would like to acknowledge Bryan Hartnagel, Travis Stump, and Jennifer Harper at the Missouri Department of Transportation for their role in funding and supporting the work of the project detailed in this report.

The author also wishes to gratefully acknowledge Benjamin C. Rivers and Aaron L. Walsh of the U.S. Geological Survey for their assistance in collecting and processing the data for this project.

Contents

Figures

Tables

Conversion Factor

Multiply	By	To obtain
	Length	
foot (ft)	0.3048	meter (m)
mile (mi)	1.609	kilometer (km)
	Area	
square foot (ft^2)	0.09290	square meter (m^2)
	Volume	
cubic yard (yd^3)	0.7646	cubic meter (m^3)
	Flow rate	
foot per second (ft/s)	0.3048	meter per second (m/s)
cubic foot per second (ft^3/s)	0.02832	cubic meter per second (m^3/s)

Datums

Vertical coordinate information is referenced to the North American Vertical Datum of 1988 (NAVD 88).

Horizontal coordinate information is referenced to the North American Datum of 1983 (NAD 83).

Supplemental Information

In this report, the words “left” and “right” refer to directions that would be reported by an observer facing downstream.

Distance on the Missouri River is given in river miles (RM) upstream from the confluence with the Mississippi River at St. Louis, Missouri, at RM 195.2 of the Upper Mississippi River. Distance on the Upper Mississippi River is given in RM upstream from the confluence with the Ohio River at Cairo, Illinois, at RM 953.5 of the Lower Mississippi River. Distance on the Lower Mississippi River is given in RM upstream from the mouth of the Mississippi River at the Gulf of Mexico.

Frequency is given in kilohertz (kHz).

Data were collected, processed, and output in the International System of Units, and converted to U.S. customary units for presentation in the maps at the request and for the convenience of the cooperator.

Abbreviations

ADCP	acoustic Doppler current profiler
AEP	annual exceedance probability
CUBE	Combined Uncertainty and Bathymetry Estimator
DEM	digital elevation model
DoD	digital elevation model of difference
GCD	Geomorphic Change Detection
GNSS	Global Navigation Satellite System
IHO	International Hydrographic Organization
IMU	inertial measurement unit
INS	inertial navigation system
MBES	multibeam echosounder
MBMS	multibeam echosounder mapping system
MMS	Mobile Mapping Suite
MoDOT	Missouri Department of Transportation
NAVD 88	North American Vertical Datum of 1988
POS MV	Position Orientation Solution for Marine Vessels
RM	river mile
RTK	real-time kinematic
SBET	smoothed best estimate of trajectory
TIN	triangulated irregular network
USACE	U.S. Army Corps of Engineers
USGS	U.S. Geological Survey

Bathymetric and Velocimetric Surveys at Highway Bridges Crossing the Missouri and Mississippi Rivers on the Periphery of Missouri, June 13–22, 2022

By Richard J. Huizinga

Abstract

Bathymetric and velocimetric data were collected by the U.S. Geological Survey, in cooperation with the Missouri Department of Transportation, near seven bridges at six highway crossings of the Missouri and Mississippi Rivers on the periphery of Missouri from June 13–22, 2022. A multibeam echosounder mapping system was used to obtain channel-bed elevations for river reaches about 1,640 feet longitudinally and generally extending laterally across the active channel from bank to bank during minor flood-flow conditions. These surveys provided channel geometry and hydraulic conditions at the time of the surveys and provided characteristics of scour holes that may be useful in developing or verifying predictive guidelines or equations for computing potential scour depth. These data also may be useful to the Missouri Department of Transportation as a minor flood-flow assessment of the bridges for stability and integrity issues with respect to bridge scour during floods.

Bathymetric data were collected around every in-channel pier. Scour holes were present at most piers for which bathymetry could be obtained, except those on banks or surrounded by riprap. Occasionally, scour holes were minor and difficult to discern from nearby dunes and ripples. All bridge sites in this study were surveyed and documented in previous studies. Although partial exposure of substructural support elements was observed at several piers, at most sites the exposure most likely is minimal compared to the overall substructure that remains buried in bed material at these piers. The notable exceptions are piers 12 and 13 at structure L0135 on State Highway 51 at Chester, Illinois, where the bedrock material was fully exposed around the piers.

The average difference between the bathymetric surfaces between 2022 and 2018 varied from 0.41 foot higher to 1.86 feet lower. Between 2022 and 2014, the average difference between the bathymetric surfaces varied from 1.02 feet higher to 4.69 feet lower. Only the two sites on the Missouri River and the Caruthersville site were surveyed in 2011; for those sites, the average difference between the bathymetric surfaces varied from 5.83 feet higher to 1.34 feet lower. The most substantial overall net gain of sediment in a reach was between 2011 and 2022 at structure A1700 near Caruthersville, Mo. (site 38). This result was expected because structure A1700 is downstream from the confluences of the Missouri and Ohio Rivers, and therefore subject to the largest streamflows, the largest streamflow fluctuations, and the most substantial sediment flux, as has historically been observed at this site.

The presence of riprap blankets, pier size and nose shape, and alignment to flow had a substantial effect on the size of the scour hole observed for a given pier. Piers that were surrounded by riprap blankets had scour holes that were substantially smaller (to nonexistent) compared to piers at which no rock or riprap were present. New riprap blankets were surveyed at pier 3 of structure L0098 at Brownville, Nebraska, and at piers 15–18 of structure A1700 near Caruthersville, Mo., that effectively mitigated the scour holes historically observed at these piers. Narrow piers having round or sharp noses that were aligned with flow often had scour holes that were difficult to discern from nearby bed features, whereas piers having wide or blunt noses resulted in larger, deeper scour holes. Several of the structures had piers that were skewed to primary approach flow. Scour holes near these piers consistently displayed greater depth on the side of the pier with impinging flow and deposition on the leeward side of the pier.

Introduction

Scour in alluvial channels is the removal of channel-bed and bank material by flowing water and is the leading cause of bridge failures in the United States (Arneson and others, 2012). Scour at a bridge site is caused by short- and long-term geomorphic processes and the local effects from elements of the structure in or next to the waterway (Huizinga and Rydlund, 2004; Arneson and others, 2012). Because the effects of scour can be severe and dangerous, bridges and other structures over waterways are routinely assessed and inspected. High-flow conditions attributed to higher velocity and depth from increased streamflow can exacerbate scour processes.

The Missouri Department of Transportation (MoDOT) manages most of the transportation infrastructure within Missouri. A part of their responsibility is to periodically inspect highway structures, including bridges that span waterways. All or most of these structures can be inspected from land or personnel lift trucks deployed from the roadway of the structure; however, for structures over primary waterways, such as the Missouri and Mississippi Rivers, inspecting the submerged part of the bridge requires a different approach.

The U.S. Geological Survey (USGS), in cooperation with MoDOT, began assessing scour at selected waterway crossings in Missouri in 1988 (Becker, 1994) and throughout the State in 1991 (Huizinga and Rydlund, 2004). In 2007, the USGS, in cooperation with MoDOT, began monitoring scour at bridges using single-beam echosounders (Rydlund, 2009) and surveying channel bathymetry using a multibeam echosounder mapping system (MBMS; Huizinga and others, 2010; Huizinga, 2012, 2013; also refer to report references listed in table 1). The MBMS is a useful tool not only for surveying channel bathymetry but also for providing a medium- to high-resolution representation of submerged, structural elements of the bridge. In 2010, the first round of periodic surveys at waterway crossings across the Missouri and Mississippi Rivers throughout Missouri began with bridges in the Kansas City, Missouri, area and were followed by bridges in the St. Louis, Mo., area, bridges on the Missouri River between Kansas City and St. Louis, and those on the periphery of Missouri (table 1). During high-flow conditions in June–August 2011, many of the highway bridges and several of the railroad bridges along the length of the Missouri River downstream from Montana were assessed (Densmore and others, 2013; Dietsch and others, 2014), including the 37 highway bridges (at 28 crossings) over the Missouri River in and into Missouri (Huizinga, 2012). Starting with the 2011 surveys, an acoustic Doppler current profiler (ADCP) has also been used to collect velocity and streamflow information along transects near the bridges. These surveys help MoDOT fulfill the need for underwater inspection of bridges over the Missouri and Mississippi Rivers and provide a valuable snapshot in time of the channel-bed elevations and velocities in the area near the bridge crossings. These snapshots of the channel bed can be used for developing or modifying tools for predicting bridge scour and other geomorphologic processes.

The study detailed in this report covers the surveys at the highway bridges across the Missouri and Mississippi Rivers on the periphery of Missouri (fig. 1), except for the new bridge over the Mississippi River at Louisiana, Mo. (fig. 1),

Table 1. Routine periodic surveys of bridges crossing the Missouri and Mississippi Rivers in and into Missouri (modified from Huizinga, 2024).

Dates of routine surveys	Report references	Data references	Special notes
		Kansas City area	
March 2010	Huizinga (2010)	Huizinga (2020b)	Excluded L0734, A7650 not yet built.
June 2015	Huizinga (2016)	Huizinga (2020b)	Excluded K0456/A0450.
August 2019	Huizinga (2022a)	Huizinga (2021)	None.
		St. Louis area	
October 2010	Huizinga (2011)	Huizinga (2017b)	A6500 not yet built.
May 2016	Huizinga (2017a)	Huizinga (2017b)	None.
August 2020	Huizinga (2023)	Huizinga (2022b)	Included new bridges A8141 at Washington and A8504 at Louisiana, Mo.
		Mid-Missouri	
April–May 2013	Huizinga (2014)	Huizinga (2020c)	None.
May 2017	Huizinga (2020a)	Huizinga (2020c)	Excluded K0969, included A8340 in Kansas City.
May 2021	Huizinga and Rivers (2023a)	Huizinga (2024)	Excluded K0969/A8141 at Washington
		Periphery of Missouri	
June 2014	Huizinga (2015)	Huizinga (2020d)	None.
July–August 2018	Huizinga (2020e)	Huizinga (2020d)	Excluded K0932.

which was under construction at the time of the previous surveys in that area (July–August 2018) and was surveyed with the St. Louis area bridges in August 2020 (tables 1 and 2). Therefore, this study details surveys at seven bridges at six crossings (table 2).

Purpose and Scope

The purpose of this report is to describe the equipment and methods used and to document results of bathymetric and velocimetric surveys completed on June 13–22, 2022, of the Missouri and Mississippi River channel near seven highway bridges at six crossings on the periphery of Missouri (fig. 1; table 2). The results obtained from the bathymetric and velocimetric surveys of the channels document the channel-bed geometry and water velocity distribution at the time of the surveys and provide characteristics of scour holes that may be useful in developing or modifying predictive guidelines or equations for computing potential scour depth. These data also may be used by MoDOT as a minor flood-flow comparison to help assess the bridges for stability and integrity issues with respect to bridge scour. Results are also compared to previous surveys at the sites (Huizinga, 2012, 2015, 2020e). Although it is beyond the scope of the current (2022) study to examine all the antecedent conditions that created the observed channel-bed configuration in these surveys, the comparisons with previous surveys under different streamflow conditions nevertheless contribute to understanding the many complexities of sediment transport and resulting channel-bed net conditions.

Description of Study Area

The generalized study area for this report covers the Missouri River where it forms the northwestern border of Missouri, and the Mississippi River along the eastern border of Missouri (fig. 1). The study area excludes the greater St. Louis, Mo., area and the new bridge at Louisiana, Mo., surveyed in 2020 (Huizinga 2023; fig. 1). On the Missouri River, the highway crossings at Brownville, Nebraska, and St. Joseph, Mo., were examined as part of this study (fig. 1; table 2). On the Mississippi River, the highway crossings at Hannibal, Mo.; at Chester, Illinois; at Cape Girardeau, Mo.; and near Caruthersville, Mo., were examined (fig. 1; table 2). The site numbering sequence used in previous studies on the Missouri and Mississippi Rivers (Huizinga, 2012, 2015) is used in this report for consistency and comparability.

Description of Streamflow Conditions

Data from selected stage gages and streamgages on the Missouri and Mississippi Rivers were used to determine the flow conditions during the surveys. Upstream from Kansas City, Mo., the Missouri River at Brownville, Nebr., streamgage (USGS station 06810070; USGS, 2023a; fig. 1), and Missouri River at St. Joseph, Mo., streamgage (USGS station 06818000; USGS, 2023a; fig. 1; hereafter referred to as the "St. Joseph streamgage"), indicate the Missouri River was between minor flood rises when these sites were surveyed on June 22, 2022 (fig. 2*A*). During the survey, streamflow estimated from velocity data on the Missouri River on June 22, 2022, was measured at about 38,700 cubic feet per second (ft^3/s) with an ADCP at the U.S. Highway 36 crossing at St. Joseph (site 2, fig. 1; table 3), which is slightly less than the rated streamflow (obtained from the rating curve) of 41,900 ft^3/s for the St. Joseph streamgage (USGS, 2023a; fig. 1). This measured streamflow has a daily exceedance probability of about 50 percent (the probability that the indicated streamflow value would be equaled or exceeded on any given day at that streamgage; USGS, 2023b) and is about 45 percent less than the 90-percent annual exceedance probability (AEP; the probability that the indicated streamflow value would be equaled or exceeded within a period of 1 year; also known as the 1-year recurrence interval) flood discharge of 70,600 ft^3/s (U.S. Army Corps of Engineers [USACE], 2004a, plate E–20). Daily exceedance probabilities for the St. Joseph streamgage were computed using daily streamflow from 1957 to 2022 (USGS, 2023b).

The Mississippi River was receding from a minor flood peak in early June (flood stage is 17 feet (ft) at Hannibal, Mo. [USACE stage gage HNNM7; National Weather Service, 2024; figs. 1–2], and is 27 ft at Chester, Ill. [USGS station 07020500; USGS, 2023a; figs. 1–2]). Structure A5054 on Interstate 72 at Hannibal, Mo. (site 31, fig. 1), was surveyed on June 13, and streamflow on the Mississippi River was about 156,000 ft^3/s as measured during the survey (table 3), which is less than the 50-percent AEP (2-year recurrence interval) regulated flood flow of 209,000 ft^3/s at Hannibal (table C–M–2 in USACE, 2004b). Daily flow statistics were not computed for the stage gage at Hannibal (USACE stage gage HNNM7). Structure L0135 on State Highway 51 at Chester, Ill. (site 36, fig. 1), was surveyed on June 14, and streamflow on the Mississippi River was measured at about 339,000 ft^3/s during the survey (table 3), which is slightly less than the rated discharge of 345,000 ft^3/s for the Mississippi River at Chester, Ill., streamgage (USGS station 07020500; USGS, 2023c; fig. 1). This measured streamflow has a daily exceedance of about 17 percent (computed using daily streamflow from 1942 to 2022; USGS, 2023c), which indicates higher flow conditions, but is less than the 50-percent AEP (2-year recurrence interval) regulated flood flow of 480,000 ft^3/s at Chester (table D–28 in USACE, 2004c). Structure A5076 on State Highway 34 at Cape Girardeau, Mo. (site 37, fig. 1), also was surveyed on June 14, and streamflow on the Mississippi River was about 335,000 ft^3/s as measured during the survey (table 3), which also is less than the 50-percent annual exceedance probability (2-year recurrence interval) regulated flood flow of 483,000 ft^3/s at the Mississippi River at Cape Girardeau, Mo., streamgage (USGS station 07020850; table D–28 in USACE, 2004c). Although daily flow statistics and exceedance

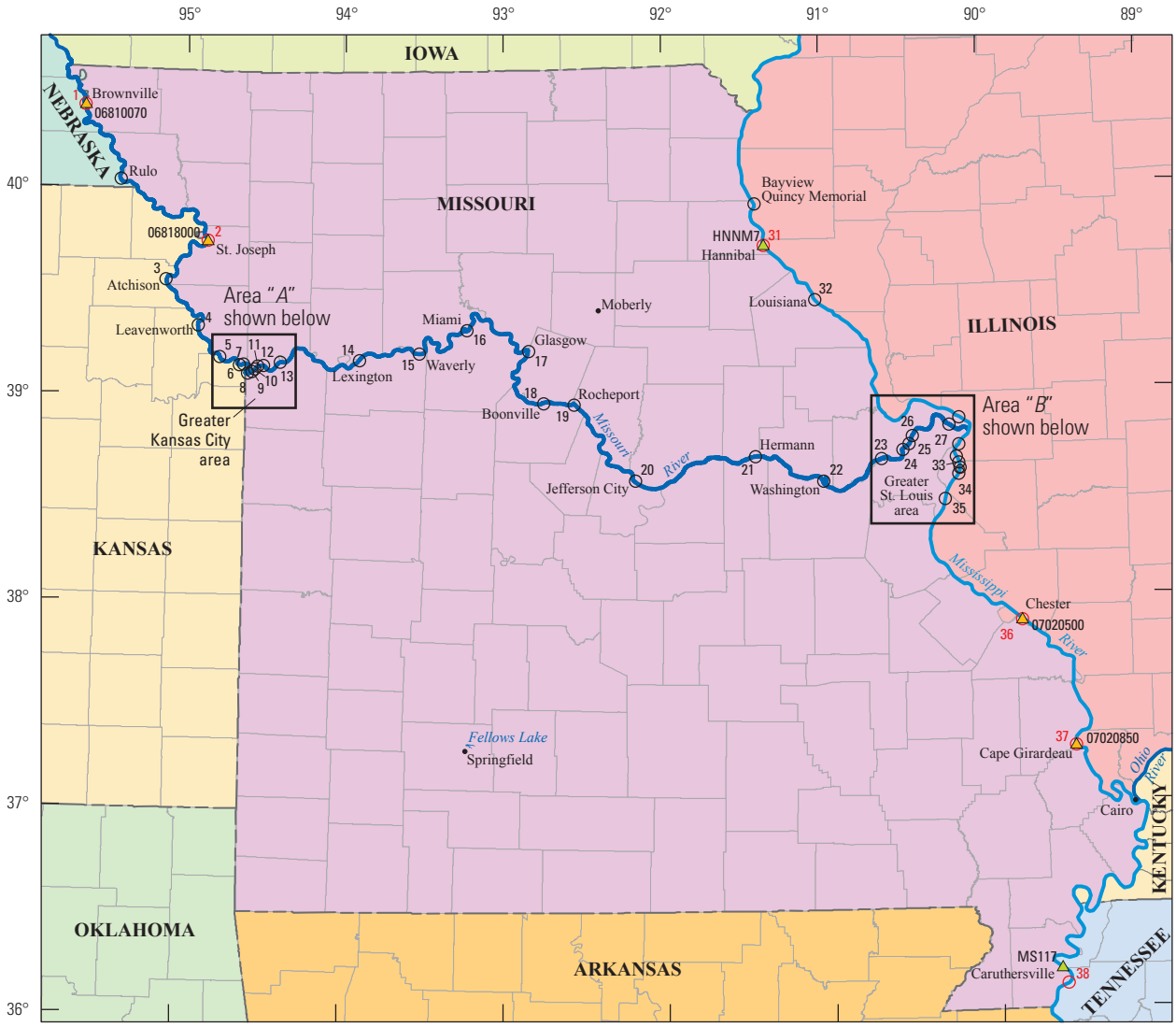

Figure 1. Location of highway bridges crossing the Missouri and Mississippi Rivers in and into Missouri, and bathymetric surveys of the Missouri and Mississippi River channels from June 13 to 22, 2022.

Table 2. Highway bridges crossing the Missouri and Mississippi Rivers on the periphery of Missouri.

[Bridges are listed in downstream order. US, U.S. highway; --, not applicable; W, westbound; E, eastbound; IS, interstate highway; MO, Missouri State highway]

Site number (fig. 1)	Structure number	Local name	River	County, State	Route	River mile[a]	Surveyed as part of this study	Remarks	Figures
1	L0098	Brownville	Missouri	Atchison, Mo.	US 136	535.3	Yes	--	1, 6, 7, 8, 9, 10, 11, 12, 1.1
2	A3664 W	St. Joseph	Missouri	Buchanan, Mo.	US 36 W	447.9	Yes	Dual bridge crossing	1, 13, 14, 15, 16, 17, 18, 19, 1.2
	A3664 E			Doniphan, Kans.	US 36 E		Yes	Dual bridge crossing	
31	A5054	Hannibal	Mississippi	Marion, Mo.	IS 72	309.5	Yes	--	1, 20, 21, 22, 23, 24, 25, 1.3, 1.4
32	A8504	Louisiana	Mississippi	Pike, Mo.	US 54	283.2	No	Replaced K0932 in 2019, surveyed in 2020	1
36	L0135	Chester	Mississippi	Perry, Ill.	MO 51	109.9	Yes	--	1, 26, 27, 28, 29, 30, 31, 1.5
37	A5076	Bill Emerson Memorial	Mississippi	Cape Girardeau, Mo.	MO 34	51.5	Yes	--	1, 32, 33, 34, 35, 36, 37, 1.6
38	A1700	Caruthersville	Mississippi	Pemiscot, Mo.	IS 155	838.9	Yes	--	1, 38, 39, 40, 41, 42, 43, 44, 45, 1.7, 1.8

[a]River mile for sites 1 and 2 is the distance upstream from the confluence of the Missouri River with the Mississippi River at St. Louis, Mo. (fig. 1). For sites 31 through 37, river mile is the distance upstream on the Upper Mississippi River, starting at the confluence with the Ohio River at Cairo, Ill. (fig. 1), at river mile 953.5 of the Lower Mississippi River. For site 38, river mile is the distance upstream on the Lower Mississippi River, starting at the mouth of the Mississippi River at the Gulf of Mexico.

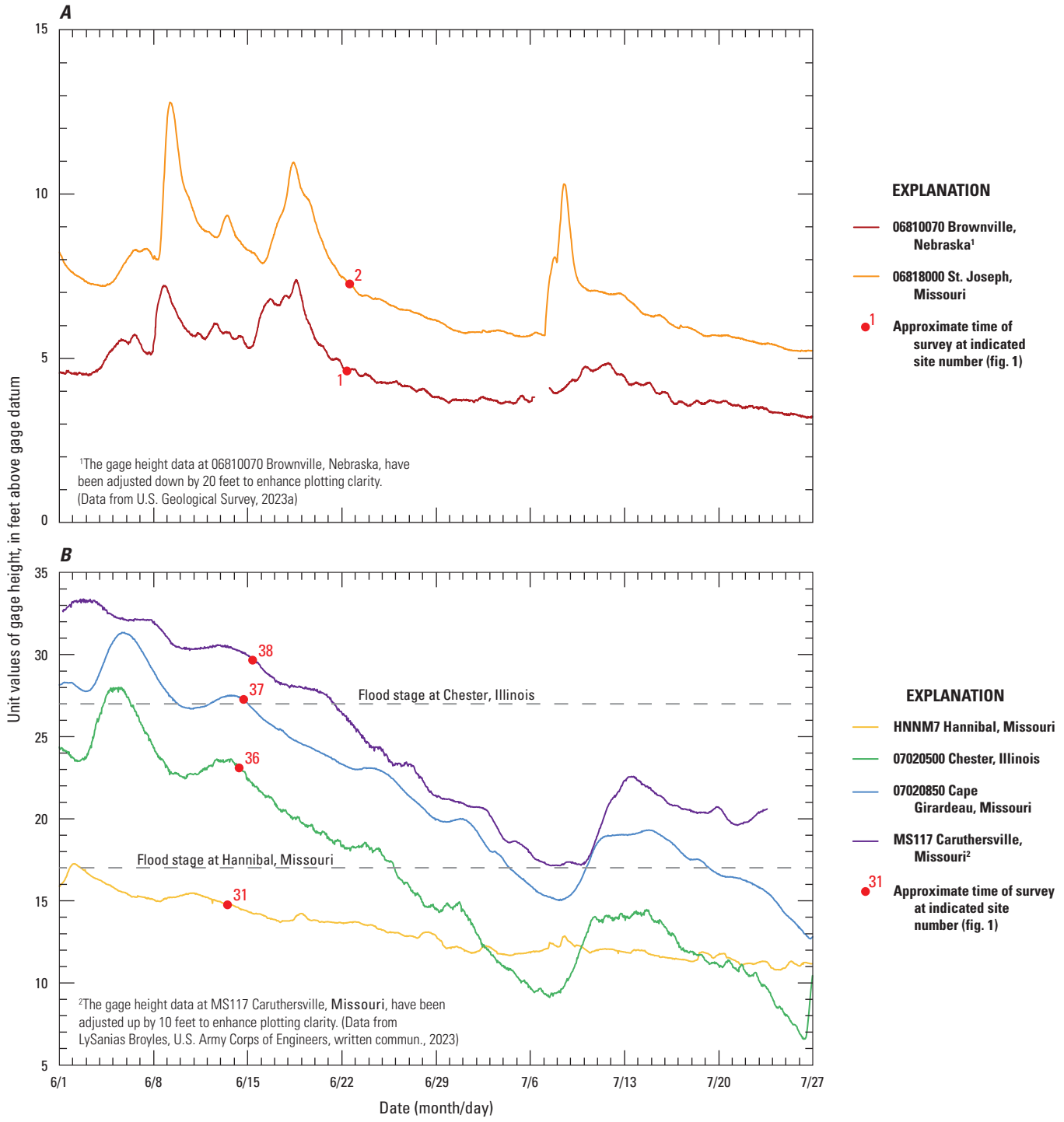

Figure 2. Hourly values of streamgage height at selected stage- and streamflow-gaging stations in the study area from June 1 to July 27, 2022. *A*, Missouri River upstream from Kansas City. *B*, Mississippi River along the eastern border of Missouri (U.S Geological Survey, 2023a; LySanias Broyles, U.S. Army Corps of Engineers, written commun., 2023).

Table 3. Bridge and survey information and selected channel-bed elevations from surveys on the Missouri and Mississippi Rivers on the periphery of Missouri, June 13–22, 2022.

[Data are summarized from Huizinga and Rivers (2023b). Sites are shown on figure 1. Dates are given in month/day/year. All elevations are in feet above the North American Vertical Datum of 1988. ADCP, acoustic Doppler current profiler; US, U.S. highway; IS, Interstate highway; MO, State highway]

Site number (fig. 1)	Structure number	Survey date	Route	River mile[a]	Streamflow estimated from ADCP measurements,[b] in cubic feet per second	Average water-surface elevation near the bridge, in feet	Average channel-bed elevation,[c] in feet	Approximate elevation of the indicated percentile of the bathymetric data, in feet		Approximate local minimum channel elevation,[d] in feet
								5th percentile	95th percentile	
1	L0098	06/22/22	US 136	535.3	37,300	884.3	868.5	864.5	875.5	845
2	A3664 E & W	06/22/22	US 36	447.9	38,700	796.1	779.6	770.3	789.2	755
31	A5054	06/13/22	IS 72	309.5	156,000	463.3	437.3	428.2	446.8	422
36	L0135	06/14/22	MO 51	109.9	339,000	363.3	329.9	316.5	346.8	309[e]
37	A5076	06/14/22	MO 34	51.5	335,000	331.1	291.9	275.6	317.6	264[e]
38	A1700	06/15/22	IS 155	838.9	468,000	250.3	199.4	175.8	224.0	158

[a]River mile for sites 1 and 2 is the distance upstream from the confluence of the Missouri River with the Mississippi River at St. Louis, Mo. (fig. 1). For sites 31 through 37, river mile is the distance upstream on the Upper Mississippi River, starting at the confluence with the Ohio River at Cairo, Ill. (fig. 1), at river mile 953.5 of the Lower Mississippi River. For site 38, river mile is the distance upstream on the Lower Mississippi River, starting at the mouth of the Mississippi River at the Gulf of Mexico.

[b]The average streamflow obtained while making the various velocity transects. The reported value is the streamflow computed using Global Navigation Satellite System (GNSS) essential fix data string as the reference, as described in the "Surveying Methods" section of the text.

[c]The statistical average of the gridded raster surface of channel-bed elevations.

[d]The minimum channel-bed elevation of the gridded raster surface, not necessarily in any scour holes near the bridge.

[e]The minimum channel-bed elevation is in a scour hole near a substructural element at this site.

probability data are not readily available for structure A1700 on Interstate 155 near Caruthersville, Mo. (site 38, fig. 1), it is assumed that the measured streamflow of 468,000 ft^3/s follows the same trend as the upstream stations and is near or slightly less than the 50-percent AEP at Caruthersville (USACE stage gage MS117).

Streamflow conditions in these daily and annual exceedance ranges are in the minor flood-flow regime. In an analysis of real-time scour monitoring data at Jefferson City, Mo., Huizinga (2014) noted that substantial pier scour generally begins soon after the onset of hydrograph rise (substantial rise of 8 ft or more at that site), although the scour often does not reach maximum depth until the peak stage is reached or sometime thereafter (refer to fig. 35 in Huizinga, 2014). Although peak streamflow conditions were not happening during this study, streamflow was substantially higher than base flow based on the daily exceedance values. Although the scour conditions captured at the sites in this study may not represent the maximum scour potential at the sites, the cumulative information gathered during multiple surveys from 2008 to 2022 at these sites remains useful for determining scour for a variety of flow conditions, particularly when combined with, or compared to, a scour scenario captured at high flood-flow conditions.

Description of Equipment and Basic Processing

The bathymetry of the Missouri and Mississippi River at each of the bridges was determined using a high-resolution MBMS. The various components of the MBMS used for this study are described in previous studies on the Missouri and Mississippi Rivers in Missouri (refer to report references listed in table 1) and on the Missouri and Yellowstone Rivers in North Dakota (Densmore and others, 2013). MBMS survey methods and data quality checks were similar to these previous studies. A brief description of the equipment follows, and a more-complete description of the various system components and methods used in this study are available in previous reports by Huizinga (2010), Huizinga and others (2010), and Densmore and others (2013).

An MBMS is an integration of several individual components: the multibeam echosounder (MBES), a sound-velocity probe, an inertial navigation system (INS), and a data-collection and data-processing computer. The MBES used in this study is the Norbit iWBMSh (fig. 3), operated at a frequency of 400 kilohertz (kHz). The iWBMSh is similar in operation to the MBES systems used in other previous studies on the periphery of Missouri and is the same system used in the previous surveys in 2018 (Huizinga, 2020e), with a curved piezoceramic receiver array that enables bathymetric data to be collected throughout a swath range of 210 degrees. Optimum data usually are collected in a swath of less than 160 degrees (80 degrees on each side of nadir, or directly below the MBES); nevertheless, the swath can be electronically rotated to either side of nadir, enabling data collection along sloping banks up to a depth just below the water surface. The sound-velocity probe provides real-time measurements of the speed of sound at the MBES to accurately determine the depth readings of the MBES (Hughes Clarke and others, 1996). The river environment tends to be well mixed, such that the sound velocity at the MBES is sufficiently representative of a sound-velocity profile of the full water column. The Norbit iWBMSh uses the Applanix Position Orientation Solution for Marine Vessels (POS MV) OceanMaster INS system, consisting of an inertial measurement unit (IMU) attached directly to the MBES mount in a "tightly coupled" configuration (fig. 3*A*) and two Global Navigation Satellite System (GNSS) antennae. The INS provides position in three-dimensional space and measures the attitude of the vessel (pitch, roll, yaw, and heading) to accurately position the data received by the MBES. Real-time kinematic (RTK) differential corrections for the INS came from cellular communication with the MoDOT GNSS real-time network for the navigation and tide solution during the 2022 surveys.

Like in all previous surveys after 2010 (refer to report references listed in table 1), the navigation information from the 2022 surveys was postprocessed using the POSPac Mobile Mapping Suite (MMS) software (version 8.7; Applanix Corporation, 2021) to mitigate the effects of degraded positional accuracy of the vessel while near or under a bridge resulting from GNSS outages. The POSPac MMS software provides tools to identify and compensate for sensor and environmental errors to compute an optimally blended navigation solution from the GNSS and raw IMU data. The blended navigation solution (called a "smoothed best estimate of trajectory" or "SBET" file) generated by postprocessing the navigation data was applied to the survey at a given bridge to minimize the effects of the GNSS outages. Because of advances in technology, surveys before 2010 do not have an SBET file and are more likely to have artifacts resulting from minor positional variations between surveys.

Data from the MBES and INS components were processed and integrated into a cohesive dataset for cleanup and visualization. A computer onboard the survey vessel ran the HYPACK/HYSWEEP data acquisition software (version 2022; HYPACK, Inc., 2020) that was used to prepare for and perform bathymetric surveys. After completing the surveys, the acquired depth data were further processed to remove data spikes and other spurious points in the multibeam swath trace, georeferenced using the navigation and position solution data from the SBET file and visualized in HYPACK/HYSWEEP as a gridded bathymetric surface or a point cloud.

Information about the velocity of the river at various points throughout each study reach was collected using an ADCP, similar to previous studies since 2011 by Huizinga (for example, refer to Huizinga, 2012, 2022a). A Teledyne RD Instruments RiverPro ADCP operating at 1,200 kHz was used to obtain velocities at depth-dependent variable-height increments, or "bins," throughout the water column. The RiverPro

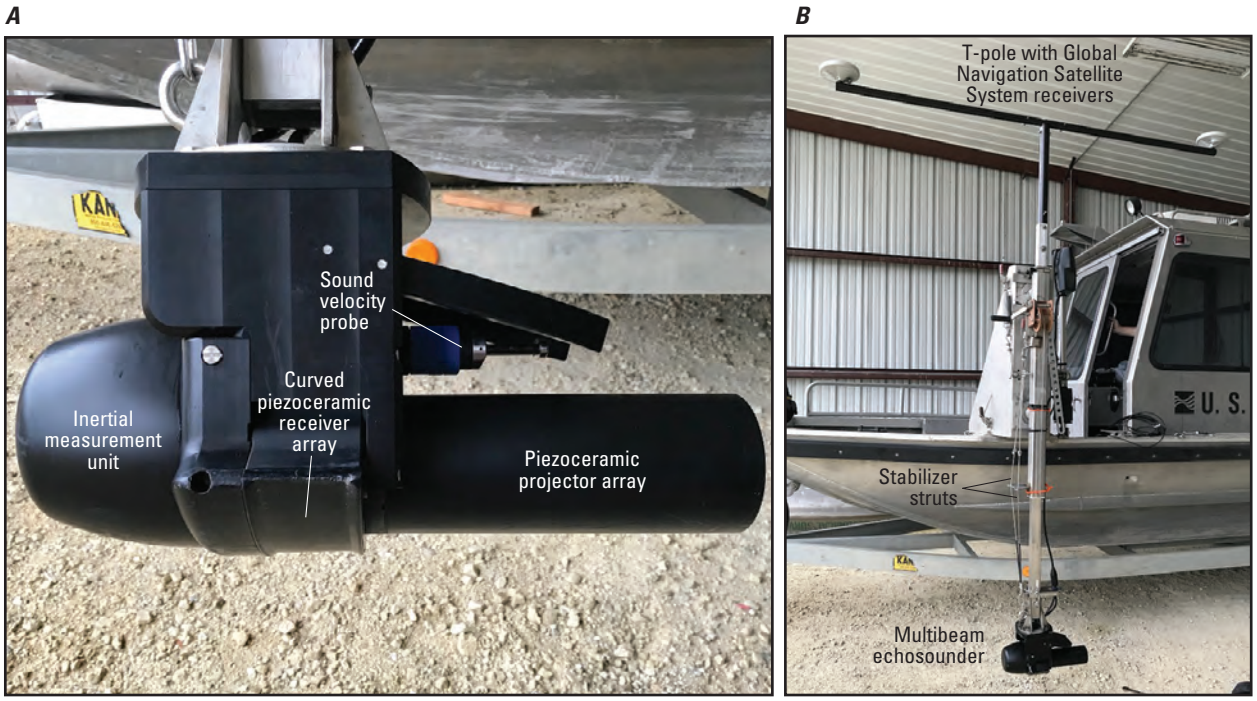

Figure 3. The multibeam echosounder. Photographs by Richard J. Huizinga, U.S. Geological Survey (USGS). *A*, Viewed from the side. *B*, Mounted on the port side of the USGS boat.

ADCP operates in depths from about 0.5 to 100 ft to determine the velocity of water by measuring the Doppler shift of an acoustic signal reflected from various particles suspended in the water (Mueller and others, 2013). By measuring the Doppler shift in four different beam directions, the velocity of the water in each bin can be determined in three dimensions. The depth-averaged velocities from the two traverses of a given section line were computed using averaging algorithms from the Velocity Mapping Toolbox (version 4.09; Parsons and others, 2013).

Basic Description of Methods

The methods used to acquire and ensure the collection of quality data were the same as those used in previous studies using the MBES (methods are detailed in Huizinga and others, 2010; Huizinga, 2010, 2012). A brief summary of—and any differences from—these methods are highlighted below.

Surveying Methods

Generally, the surveyed area extended across the active channel from bank to bank, just like the previous studies on the Missouri and Mississippi Rivers (Huizinga and others, 2010; Huizinga, 2012, 2013; also refer to references listed in table 1). The surveyed reaches were about 1,640 ft long in the direction of flow, positioned so that the surveyed highway bridges were about one-third to one-half of the total length from the upstream boundary, generally using the same upstream and downstream boundaries as were used in the 2011 flood study on the Missouri River (Huizinga, 2012) and in the earliest Mississippi River surveys (Huizinga, 2015). The upstream and downstream boundaries of the surveyed areas were assumed to capture all the substantial hydraulic effects (wake vortices and shear flow) of the bridge structures.

Like in previous studies, bathymetric data were obtained along longitudinal transect lines, and each survey was designed such that the survey swaths overlapped to ensure complete coverage of the channel bed and minimize sonic "shadows" (Huizinga and others, 2010). Many of the surveyed swaths had substantial overlap (ranging from 25 to 50 percent), except in shallow areas near the channel banks or spur dikes and near in-flow structures or debris rafts (overlap ranging from 0 to 10 percent). Areas near bridge piers and along the banks also were surveyed in an upstream direction with the MBES swath electronically tilted to port or starboard to increase the acquisition of bathymetric data higher on the banks and sides of the piers. The electronically tilted swath generally was 120 to 160 degrees wide, extending from 10 degrees above horizontal on the bank-ward or pier-ward side of the survey vessel, and 20 to 60 degrees past nadir below the vessel.

After completing the bathymetric survey at a given site, velocity data were obtained with the ADCP on seven transections spanning the channel within the study area. The position

and speed of the boat was determined using a differential GNSS receiver mounted on a pole directly above the ADCP. The bottom-track reference method for determining boat speed was anticipated to be unusable because of moving channel-bed material, so the boat velocity was determined using the GNSS essential fix data from the differential GNSS receiver (the NMEA–0183 GGA string [shorthand for the $GPGGA standard output format for GNSS essential fix data defined by the National Marine Electronics Association 0183 standard that includes information on the three-dimensional location and accuracy of the GNSS receiver; National Marine Electronics Association, 2002]). The distance between the velocity section lines generally was about 260 ft. Three sections were upstream, and four sections were downstream from the bridge being surveyed. Each section line was traversed in each direction across the river, and the reported velocity values were the average from the two traverses of a given section line. Streamflow for a site was computed as the average of the streamflow measurements from the reciprocal pairs (two transects per section line) at all the various sections in the reach. Generally, measured streamflow for any individual transect was within 5 percent of the average.

Survey Quality-Assurance Measures

For the MBMS, the principal quality-assurance measures were assessed in real time during the survey. The MBMS operator assessed the quality of the collected data in real time by making visual observations of cross-track swath shape (such as convex, concave, or skewed bed returns in flat, smooth bottoms), noting data-quality flags and alarms from the MBES and the INS, and noting comparisons between adjacent overlapping swaths.

In addition to the real-time quality-assurance assessments, beam angle checks and a suite of patch tests were done to ensure quality data were acquired from the MBMS for the 2022 surveys. Patch tests are a series of dynamic calibration tests that are used to check for subtle variations in the orientation and timing of the MBES with respect to the INS and real-world coordinates (Huizinga, 2023), and primarily are used to determine angular offsets to roll, pitch, and yaw caused by the alignment of the transducer head relative to the INS (fig. 4). These offsets have been observed to be essentially constant for a given equipment configuration and survey season, barring an event that causes the mount to change such

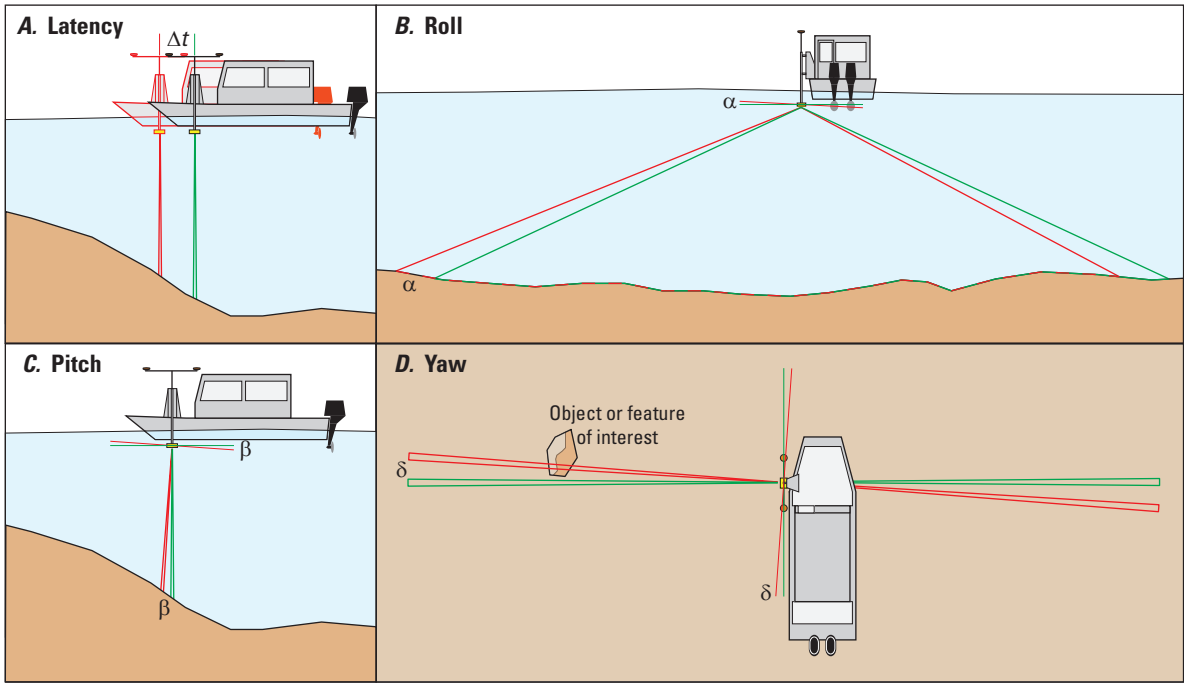

Figure 4. Generalized effects on data from a multibeam echosounder. *A*, Timing offset for latency. *B*, Angular offset for roll. *C*, Angular offset for pitch. *D*, Angular offset for yaw (from Huizinga, 2022a).

as striking a floating or submerged object (refer to report references listed in table 1; Huizinga and others, 2023; Rivers and others, 2023).

The beam angle check and an initial patch test were completed on April 13, 2022, at Fellows Lake near Springfield, Mo. (fig. 1). An additional patch test was completed during surveying of the Calumet Sag channel in Chicago, Ill. (not shown on fig. 1), on August 3, 2022. The results of the beam angle check (table 4) were within the recommended performance standards used by the U.S. Army Corps of Engineers for hydrographic surveys for all the representative angles below 75 degrees (U.S. Army Corps of Engineers, 2013). Points acquired outside of the central 100–110 degrees of the swath generally had overlap with adjacent swaths, which increases the quality of the survey in the overlapped areas because of duplication.

Although the MBES had several minor strikes of floating or submerged debris at various times during the 2022 survey season, no changes to the roll or pitch angles were apparent from the beginning to the end of the river surveys in May (table 5). The tightly coupled configuration of the Norbit iWBMSh, wherein the IMU of the INS is mounted on the same mounting bracket as the MBES (fig. 3*A*) results in no measured timing offset and no measured angular offset for pitch (table 5). The yaw is a measure of the alignment of the GNSS receivers relative to the IMU of the INS on the echosounder head, and no offset for yaw was measured in either patch test (table 5). The measured angular offset for roll remained a constant −0.10 (table 5), which is consistent with results for this equipment configuration in other recent surveys (Huizinga, 2023; Rivers and others, 2023). It was noted in the earliest work with the MBMS in Missouri (Huizinga, 2010) that a sensitivity analysis of the four offsets indicated that the ultimate position of surveyed points in three-dimensional space was least sensitive to the angular offset for yaw, whereas it was most sensitive to the angular offset for roll. Processing all the data for the bridge surveys detailed in this report with an angular offset of roll of –0.10 degree and no angular offset for pitch or yaw generally yielded good results with no noticeable artifacts caused by incorrect offsets.

Angular offsets were applied to the bathymetric data before removing data spikes and other spurious points in the multibeam swaths using automatic filters and manual editing. The bathymetric data were then projected to a three-dimensional grid at a resolution of 1.64 ft using the Combined Uncertainty and Bathymetry Estimator (CUBE) method (Calder and Mayer, 2003), as implemented in the MBMax processing package of the HYPACK/HYSWEEP software (HYPACK, Inc., 2020) and used to generate a gridded raster surface of the channel bed (and associated uncertainty) near each bridge (hereinafter referred to as a "bathymetric surface") using ArcMap (version 10.8.1; Esri, 2023).

A quality-assurance plan has been established for streamflow and velocity measurements using ADCPs that includes several instrument diagnostics checks and calibrations. These standard operating procedures were followed when acquiring the velocity profile data for these surveys. For a detailed description of these procedures, refer to Mueller and others (2013).

Uncertainty Estimation

Similar to recent bathymetry studies in Missouri (refer to report references listed in table 1; Huizinga and others, 2023; Rivers and others, 2023), uncertainty in each survey was estimated by computing the uncertainty for each survey-grid cell in the bathymetric surface of the survey area using the CUBE method (Calder and Mayer, 2003). The gridded uncertainty is a measure of the variability of the individual points in the cell used to determine the CUBE-derived elevation for the cell. Statistics of gridded uncertainty for each of the survey areas are shown in table 6. An example of the spatial distribution of gridded uncertainty typically observed in the survey data at structure A1700 on Interstate 155 is shown in figure 5. The uncertainty data were output and combined with the three-dimensional bathymetry data and are included with metadata in the USGS data release associated with this study (Huizinga and Rivers, 2023b).

More than 90 percent of the uncertainty values at all the sites were less than 0.50 ft (table 6), which is within the specifications for a "Special Order" survey, the second-most-stringent survey standard of the International Hydrographic Organization (IHO; International Hydrographic Organization, 2020). For all but structure A1700 (site 38), more than 75 percent of the uncertainty values were less than 0.25 ft (table 6). The tops of bridge substructural elements (pier footings and seal courses) typically had uncertainty values of less than 0.25 ft. Like noted in previous surveys with this type of equipment (for example, Huizinga, 2012, 2016), the uncertainty values were larger near moderate-relief features (banks, spur dikes, rock riprap and outcrops, and scour holes near piers). The largest uncertainty in this group of surveys was 6.56 ft (table 6); however, as noted in previous studies, uncertainty values of this magnitude typically happened near high-relief features, such as the front or side of a pier footing. Occasionally, the uncertainty values also were larger (1.00 ft or greater) in the outermost beams of the multibeam swath where overlap occurred with an adjacent swath, particularly when the MBES head was electronically tilted for the survey lines along the banks. Overlapping adjacent swaths in the channel thalweg (the line of maximum depth in the channel) also can display larger uncertainty values because substantial bed movement can happen between survey passes (fig. 5).

The uncertainty of the gridded data computed using the CUBE method has been decreasing with time compared to previous surveys (refer to table 4 in previous studies of the periphery of Missouri area; Huizinga, 2012, 2015, 2020e). The decrease in uncertainty primarily is the result of improvements in data-collection equipment and methods. The tightly coupled configuration of the Norbit iWBMSh used in these surveys decreases some of the uncertainty by substantially reducing the lever arm length (and therefore the potential movement)

Table 4. Results of a beam angle check from two check lines over a reference surface at Fellows Lake near Springfield, Missouri, on April 13, 2022.

[<, less than; --, no data]

Beam angle limit, in degrees	Maximum outlier, in feet	Mean difference, in feet	Standard deviation, in feet	95-percent confidence, in feet
0	0.26	0.00	0.07	0.13
5	0.23	0.00	0.07	0.10
10	0.26	0.00	0.07	0.13
15	0.33	0.00	0.07	0.13
20	0.36	0.00	0.07	0.16
25	0.33	0.00	0.10	0.20
30	0.36	0.00	0.10	0.20
35	0.46	0.03	0.10	0.16
40	0.46	0.03	0.10	0.16
45	0.43	0.10	0.07	0.16
50	0.36	0.07	0.07	0.16
55	0.39	0.07	0.10	0.20
60	0.49	0.03	0.16	0.30
65	0.79	0.03	0.20	0.39
70	0.82	0.13	0.20	0.39
75	0.66	0.07	0.20	0.36
		Performance standards[1]		
Threshold	1.00	<0.20	--	<0.80
Result	Met	Met	--	Met

[1]Performance standard check values are from table 3-1 in U.S. Army Corps of Engineers (2013) for soft sand/silt bottoms.

Table 5. Patch test results for various multibeam projects in 2022.

Date of test	Timing offset, inseconds	Angular offset for roll, indegrees	Angular offset for pitch, in degrees	Angular offset for yaw, in degrees	Location
04/13/2022	0	−0.10	0.00	0.00	Fellows Lake near Springfield, Missouri (fig. 1)
08/03/2022	0	−0.10	0.00	0.00	Calumet Sag channel in Chicago, Illinois (not shown on fig. 1)

Table 6. Total gridded uncertainty results for bathymetric data at a 1.64-foot grid spacing from surveys on the Missouri and Mississippi Rivers on the periphery of Missouri, June 13–22, 2022.

[Data are summarized from Huizinga and Rivers (2023b)]

Site number (fig. 1)	Structure number	Uncertainty, in feet				Percentage of bathymetry points with uncertainty value less than a given threshold			
		Maximum	Mean	Median	Standard deviation	1.00 foot	0.50 foot	0.25 foot	0.10 foot
1	L0098	6.50	0.07	0.07	0.09	99.8	99.3	97.6	93.5
2	A3664 E & W	6.43	0.08	0.07	0.13	99.7	98.7	95.8	88.2
31	A5054	6.56	0.09	0.10	0.07	100.0	99.8	98.8	74.9
36	L0135	6.56	0.16	0.13	0.11	99.9	99.1	84.5	38.2
37	A5076	6.43	0.20	0.16	0.14	99.7	97.5	75.7	20.9
38	A1700	6.56	0.29	0.26	0.17	99.7	90.1	48.5	10.7

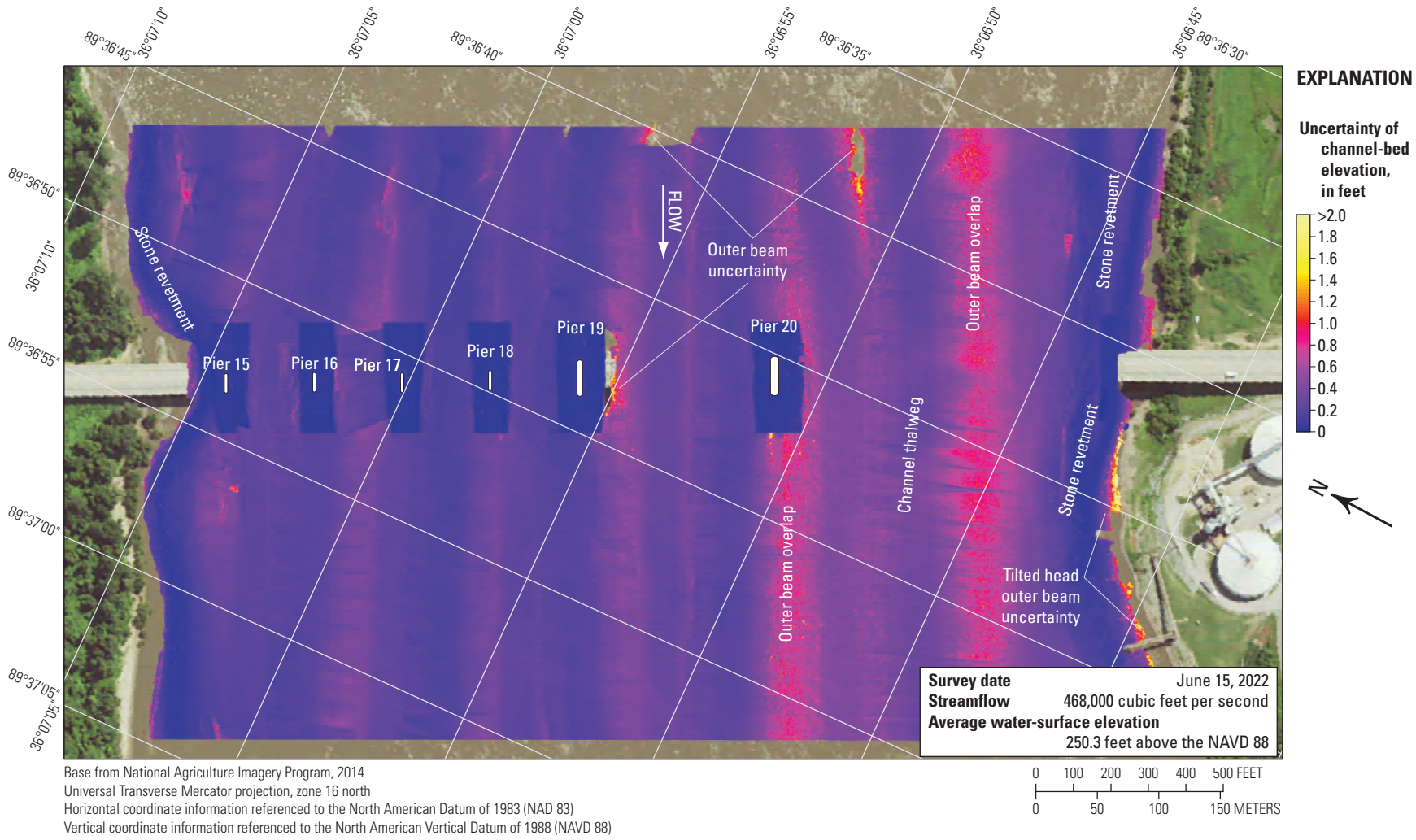

Figure 5. Uncertainty of gridded bathymetric data from the Mississippi River channel near structure A1700 on Interstate 155 near Caruthersville, Missouri.

between the MBES and IMU. The ability to electronically tilt the swath substantially reduces the time between when unrotated, down-looking data and rotated, side-looking data are collected, which reduces the uncertainty of the data in the swath overlap zone that might otherwise experience more substantial bed movement.

The survey at structure A1700 on Interstate 155 near Caruthersville had one of the highest maximum values (6.56 ft) and the highest median value (0.26 ft) of gridded uncertainty, as well as a lower percentage of bathymetry points with a gridded uncertainty of less than the various thresholds (table 6). The survey at this site was obtained with relatively smooth longitudinal swaths (fig. 5), which was the case at nearly all the sites surveyed in this study. The primary anomalies at this site were observed near the outermost beams of adjacent swaths and along the banks and near the piers, where the MBES was used in an electronically tilted configuration to extend the potential coverage in these areas, resulting in higher uncertainty values. Generally, the magnitude and distribution of uncertainty observed at this site are representative of those observed at all the sites.

Results of Bathymetric and Velocimetric Surveys

The site-specific results for each bridge are discussed in the following sections grouped by river, starting with the upstream-most bridge site and progressing downstream. The range of bed elevations, described as "the channel-bed elevations," for each survey was based on statistical analyses of the bathymetric surface at each site and covers the 5th to 95th percentile range of the data. Because the surveys generally were limited to the active channel from bank-to-bank excluding overbank areas, this percentile range generally covered the channel bed but excluded the banks and localized high or low spots, such as spur dikes or scour holes near piers or spur dikes. All elevation data were referenced to the North American Vertical Datum of 1988 (NAVD 88) using the geoid model GEOID18.

For consistency with earlier studies, dune sizes are described in general terms for each of the bridge sites using the categories set by Huizinga (2012) for the discussion of bathymetry during the 2011 flood. In this report, small dunes and ripples are those that are less than 5 ft high from crest to trough, medium dunes are those that are 5 to 10 ft high, large dunes are those that are 10 to 15 ft high, and very large dunes are those that are 15 ft or more in height.

The bathymetry data from previous surveys (Huizinga, 2012, 2015, 2020e) for all six crossings from the bridge sites in this study are included with metadata in Huizinga (2020d). A map showing the difference in channel-bed elevation for the area common to the comparison surveys is included for each site, and data from previous surveys are included in the cross-section plot for that bridge. The difference maps were created using the Geomorphic Change Detection (GCD; version 7) add-in tool for ArcGIS available through the Riverscapes Consortium (2022). GCD computes elevation difference and volumetric change in storage between two gridded raster surfaces (each as a digital elevation model [DEM] of the surface) derived from repeat topographic or bathymetric surveys. The GCD program provides a suite of tools to associate the uncertainties for points in the various surveys (using the uncertainty values associated with each gridded point, or an average uncertainty of the survey when point-specific uncertainty data were not available [survey data from 2011 or before]) and propagates those uncertainties through the DEM of difference (DoD) map. The GCD program also provides a way to segregate the best estimates of change using threshold masks. A threshold mask of 95-percent confidence was used for comparisons in the current study, and summary statistics (maximum, minimum, and average) of the DoD maps were determined. Sediment volumes for cut (scour) and fill (deposition) between the 2022 survey and any previous surveys between 2008 and 2018 also were determined. The surveys are loosely compared to previous surveys based simply on timing and the streamflow at the time of the surveys. Additionally, shaded triangulated irregular network (TIN) images of the channel and side of pier were prepared for each surveyed pier. These visualizations are shown in figures 1.1 to 1.8.

In the DoD maps presented and discussed in the sections that follow, only the area common to both surveys is analyzed. A polygon generally covered by the 2022 survey is used as a white backdrop to enhance the visibility of the color scale used in the DoD map. As a result, areas with differences less than the propagated uncertainties of the compared surveys are shown as white areas between scour and deposition, generally in the range of –1 to +1 ft difference. In the site-specific discussions that follow, these areas are equivocal and within the 95-percent confidence bounds of uncertainty of detectable change (hereinafter referred to as "within the bounds of uncertainty"). As mentioned in the "Uncertainty Estimation" section, the gridded uncertainty has been decreasing with time through improvements in data-collection equipment and methods; therefore, the equivocal areas generally are narrower in comparisons with more recent surveys, and wider in comparisons with older surveys. Small areas not surveyed in one or the other of the surveys being compared also are displayed as white areas; however, these often are "embedded" in an area of scour or deposition, and generally not on the boundary between scour and deposition. Furthermore, occasionally large areas (usually around the perimeter of the surveyed area) that were not covered in the earlier survey of the comparison also are displayed as white areas. These unsurveyed areas are noted on the DoD maps and usually resulted in a distinct break from an area of scour or deposition to an area of no data. Equivocal areas that coincide with revetment or a rock outcrop are highlighted in the discussion.

When calculating difference between two surveys near sloped or vertical features, small horizontal positional variations between the surveys can result in substantial calculated elevation differences. A schematic of this phenomenon is shown in figure 6, where a position offset of one grid spacing (0.25 m) resulted in apparent deposition or scour on the opposing faces of a spur dike or the opposing sides of a pier. When deposition and scour are apparent on opposing faces of a feature in the following site-specific discussions and maps, the likely cause is a minor horizontal positional variance between the surveys.

Although the configuration of the channel bed and the underlying sediment transport conditions at a site are associated with an instantaneous streamflow in the discussions that follow, a given bathymetric surface reflects more than those instantaneous transport conditions. A wide variety of factors affect the channel-bed configuration of a reach for a specific streamflow, including magnitude of flow velocities and velocity distribution; the number, size, and timing of previous flood rises; whether the stage currently is rising or falling; and other local hydraulic conditions (Gilbert and Murphy, 1914; Simons and Richardson, 1966). Furthermore, the channel-bed configuration at a site is affected by upstream and local sediment conditions

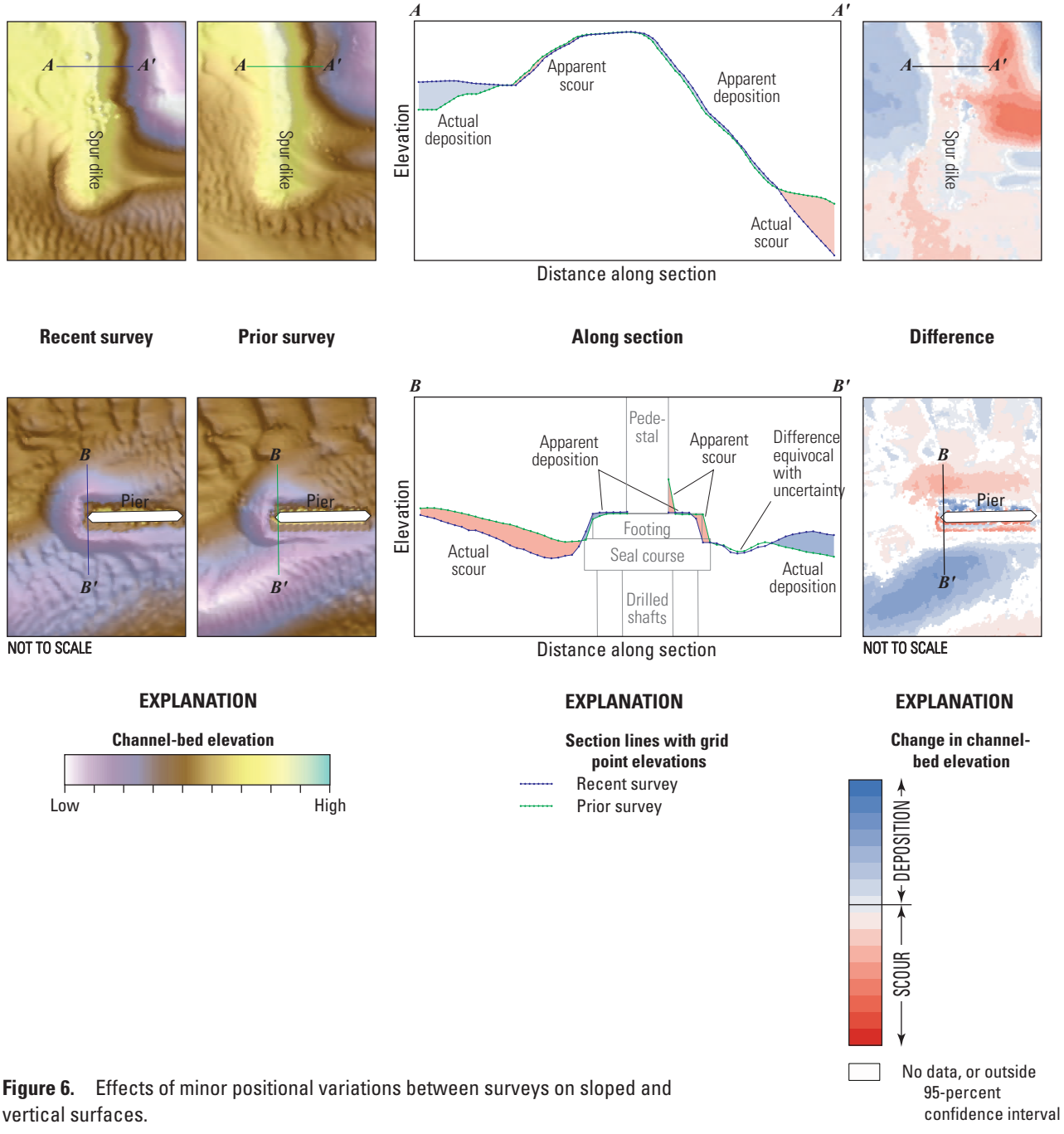

Figure 6. Effects of minor positional variations between surveys on sloped and vertical surfaces.

(size and spatial distribution) and contributions, as well as water temperature and other seasonal variations (Simon, Li and Associates, 1985). Because of the myriad number and interactions between factors affecting sediment transport conditions and the resulting bed conditions, it was assumed that the configuration and size of bed forms observed during the current (2022) surveys in the mid-Missouri area depended on more than the instantaneous streamflow at a given site. Although it is beyond the scope of the current (2022) study to examine all the antecedent conditions that created the observed channel-bed configuration, the comparisons with previous surveys under different streamflow conditions nevertheless contribute to understanding the many complexities of sediment transport and resulting channel-bed net conditions.

As in recent previous studies (refer to report references listed in table 1), when discussing the vertically averaged velocity values obtained during the surveys in the sections that follow, neighboring vectors having random variations in direction and magnitude were assumed to indicate nonuniform flow in the section resulting from shear and wake vortices. Conversely, neighboring vectors having gradual and systematic variations were assumed to indicate uniform flow in the section. The Missouri River is highly turbulent even in the absence of structures that generate strong shear or wakes, but in the interest of conciseness, nonuniform flow is loosely described as "turbulent" in the following sections.

Structure A5054 on Interstate 72 at Hannibal, Missouri.

Surveys on the Missouri River

There are five unique highway crossings of the Missouri River upstream from Kansas City to the Missouri–Iowa State line (fig. 1). Two of the crossings are maintained by MoDOT and were surveyed as part of this study. Bathymetry and velocity data from these two surveys are included with metadata in Huizinga and Rivers (2023b).

Structure L0098 on U.S. Highway 136 at Brownville, Nebraska

Structure L0098 (site 1; table 2) on U.S. Highway 136 crosses the Missouri River at river mile (RM) 535.3 at Brownville, Nebr., in the northwestern corner of Missouri (fig. 1). The site was surveyed on June 22, 2022, and the average water-surface elevation of the river in the survey area, determined by the RTK GNSS tide solution, was 884.3 ft (table 3; fig. 7). Streamflow on the Missouri River was about 37,300 ft^3/s during the survey (table 3).

The survey area was about 1,640 ft long and about 740 ft wide, extending across the active channel from bank to bank, except for a shallow area between the spur dikes on the left (eastern) bank (fig. 7). The survey area extended about 740 ft upstream from the centerline of structure L0098. The channel-bed elevations ranged from about 864 to 876 ft for most of the surveyed area (5th to 95th percentile range of the bathymetric data; fig. 8), on the downstream sides of the various spur dikes on the left (east) bank (fig. 7; table 3). The channel bed was covered with small to medium dunes and ripples. As in previous surveys (Huizinga, 2012, 2015, 2020e), a rock outcrop was present on the right (west) bank upstream from the bridge, and a stone revetment was present on the right bank downstream from the bridge (fig. 7).

The scour hole that historically had been observed near pier 3 in previous surveys (refer to fig. 6 in Huizinga [2020e]) was conspicuously absent in the 2022 survey, having been mitigated by the apparent installation of a riprap blanket scour countermeasure around the pier sometime since the most-recent previous survey in 2018 (figs. 7, 1.1*A*, 1.1*B*). Information from bridge plans indicates that pier 3 is founded on sheet piling caissons on bedrock, with about 51 ft of bed material between the bottom of the scour hole and bedrock at the upstream face of the pier (fig. 9; difference between "Approximate minimum elevation in scour hole near pier/bent" and "Approximate elevation of bedrock near pier/bent" in table 7). The unique configuration of the sheet pile caissons and ice breaker of the pier are clearly seen in the shaded TIN images for pier 3 (fig. 1.1). The surveyed bed generally was similar to the most-recent previous multibeam surveys in 2014 and 2018, except near pier 3 where the riprap blanket scour countermeasures now exist (fig. 9).

The computed difference between the survey DEMs with a probabilistic threshold mask of 95-percent confidence based on uncertainty (hereinafter, referred to simply as "the difference") from the survey on June 22, 2022, and the previous survey on August 13, 2018 (fig. 10), indicated about 93 percent of the joint area of interest had change greater than the 95-percent confidence interval of uncertainty (hereinafter referred to as "detectable change"), which means only about 7 percent of the differences in the joint area of interest were equivocal and within the bounds of uncertainty (table 8). Bed variation seemed about equal between scour and deposition from 2018 to 2022 in the DoD (fig. 10); however, erosion was dominant in the upstream part of the reach and along the tips of the spur dikes on the left (east) bank throughout the reach, whereas substantial deposition was apparent near the pier, in the wake vortex area downstream, and between the spur dikes on the left side of the channel near the left (east) bank (fig. 10). The average difference between the bathymetric surfaces (the statistical mean value of the gridded raster surface [fig. 10] created from the thresholded difference between the 2022 and 2018 gridded raster bathymetric surfaces) was +0.41 ft (table 8), indicating minor to moderate channel aggradation between the 2018 and 2022 surveys. The net volume of cut in the reach from 2018 to 2022 was about 34,500 cubic yards (yd^3), and the net volume of fill was about 50,100 yd^3, resulting in a net gain of about 15,600 yd^3 of sediment between 2018 and 2022 (table 8). The cross sections from the two surveys along the upstream face of the bridge are not substantially different from one another for most of the cross section, except pier 3 (fig. 9). The frequency distribution of bed elevations in 2022 also was similar to 2018 and 2014 (fig. 8). The stone revetement on the right (west) bank showed areas of minor scour and deposition, and the spur dike on the left (east) bank showed minor erosion on one side and deposition on the other (fig. 10); however, deposition or scour apparent on opposing faces of a feature likely resulted from minor horizontal positional variances between the surveys (fig. 6).

The difference between the survey on June 22, 2022, and the survey on June 3, 2014, (fig. 11), indicates about 57 percent of the joint area of interest had detectable change, which means about 43 percent of the differences in the joint area of interest are equivocal and within the bounds of uncertainty (table 8). Scour and deposition are roughly balanced throughout most of the reach between 2014 and 2022 in the DoD, except along the left (east) bank near the spur dikes, and near pier 3 (fig. 11). The average difference between the bathymetric surfaces was +0.27 ft (table 8), indicating minor overall channel aggradation between the 2014 and 2022 surveys. The net loss of sediment between 2014 and 2022 was about 19,700 yd^3, and the net volume of fill was about 26,000 yd^3, resulting in a net gain of only about 6,300 yd^3 of sediment between 2018 and 2022 (table 8). Streamflow in 2022 was very similar to 2014 (table 8), which may account for the similarity in overall characteristics between the surveys (figs. 9 and 11). The stone revetment and rock outcrop on the right (west) bank has localized areas of deposition (fig. 11). As with the previous DoD, deposition or scour apparent on opposing faces of a feature (such as a pier or spur dike) likely results from minor horizontal positional variances between the surveys (fig. 6).

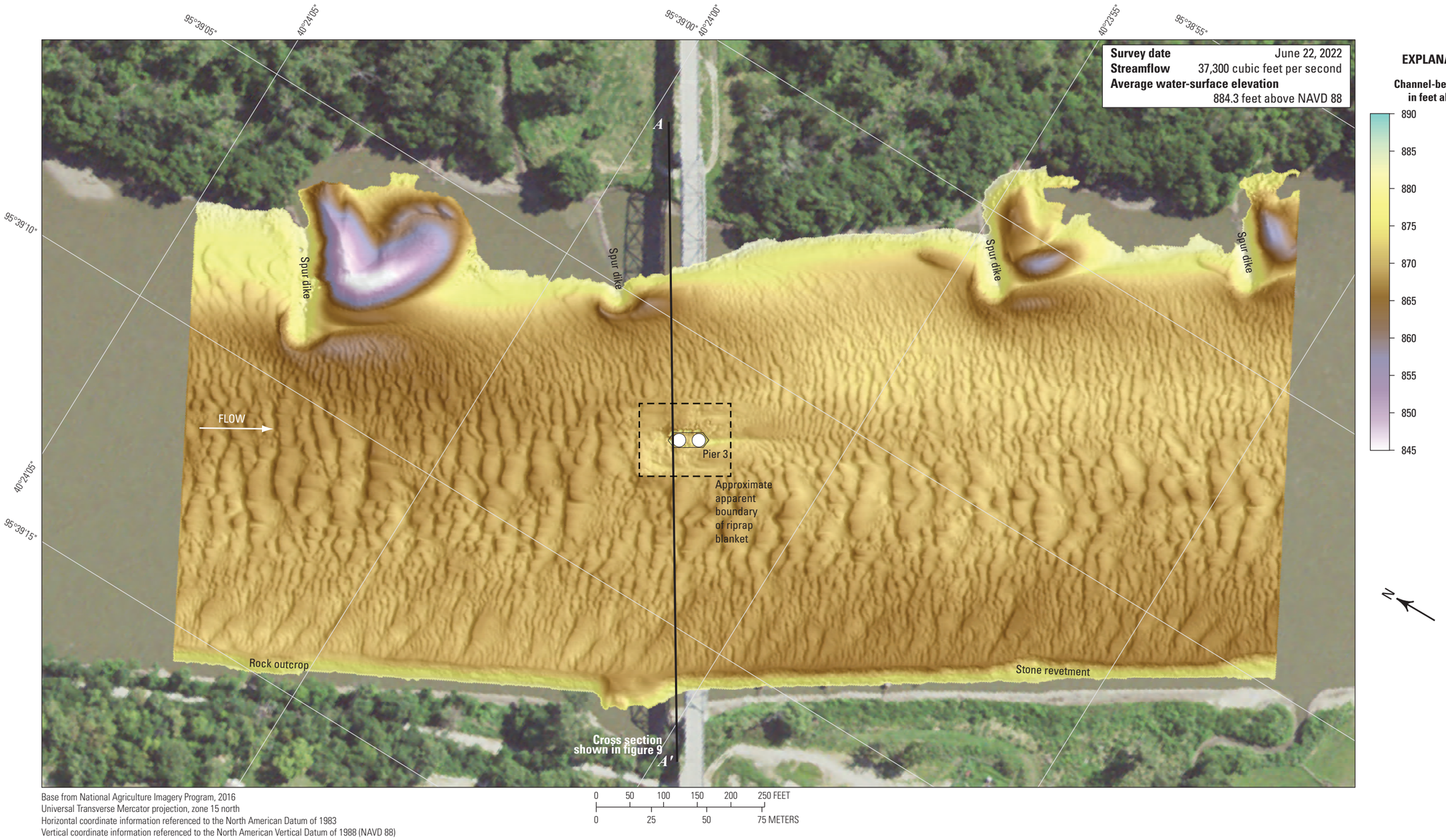

Figure 7. Bathymetric survey of the Missouri River channel near structure L0098 on U.S. Highway 136 at Brownville, Nebraska.

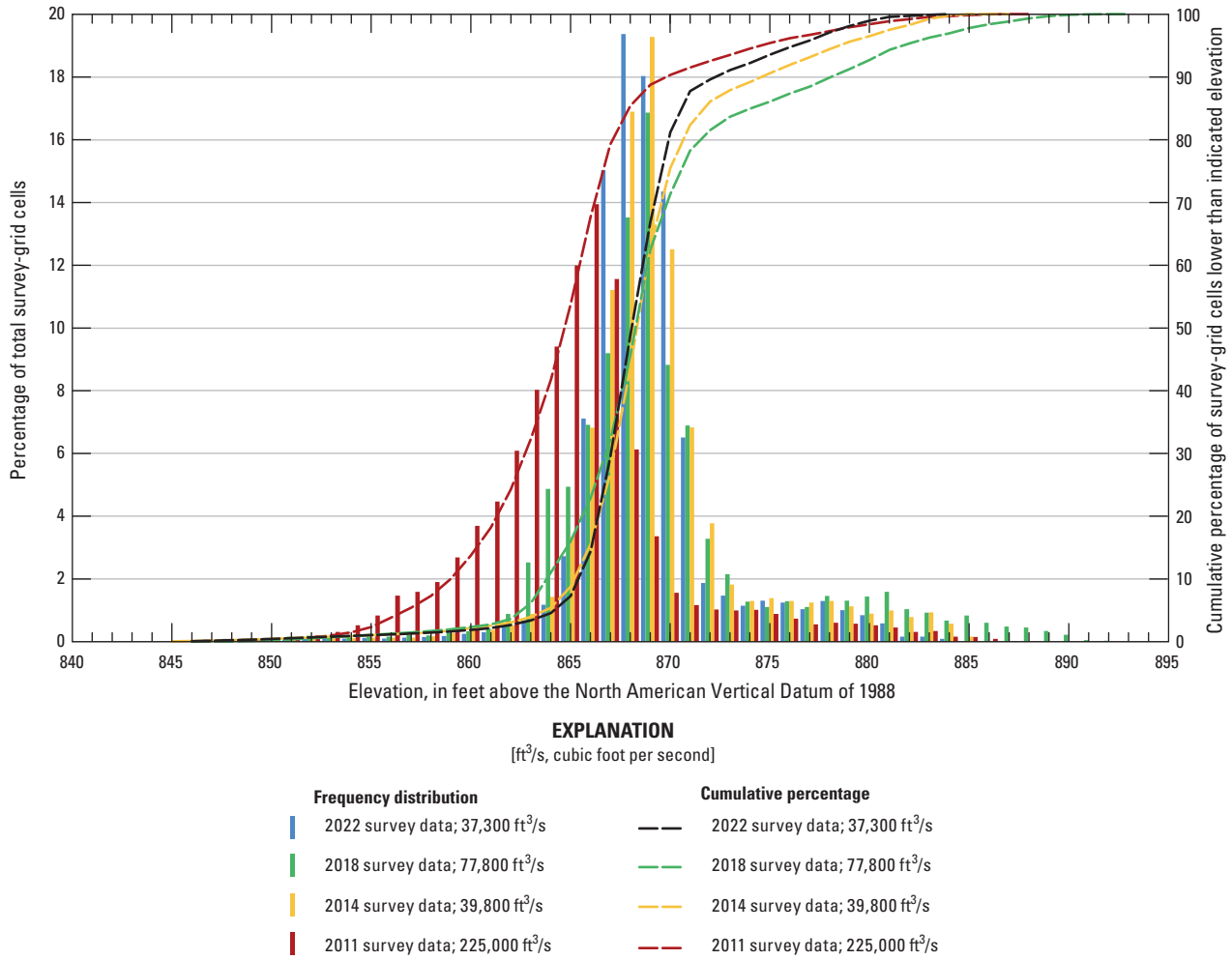

Figure 8. Frequency distribution of bed elevations for bathymetric survey-grid cells in 1-foot elevation bins on the Missouri River near structure L0098 on U.S. Highway 136 at Brownville, Nebraska, on June 22, 2022, compared to previous surveys in 2011, 2014, and 2018 (Huizinga, 2012, 2015, and 2020e, respectively).

The difference between the survey on June 22, 2022, and the earliest survey during flooding on July 13, 2011 (fig. 12), indicates about 92 percent of the joint area of interest had detectable change, which means only about 8 percent of the differences in the joint area of interest are equivocal and within the bounds of uncertainty (table 8). Deposition is dominant throughout most of the reach between 2011 and 2022 in the DoD, except in localized areas near the tips of the spur dikes on the left (east) bank (fig. 12). The average difference between the bathymetric surfaces was +4.43 ft (table 8), indicating substantial channel aggradation between the 2011 and 2022 surveys. The net gain of sediment in the reach between 2011 and 2022 was about 165,100 yd^3, which is by far the largest net gain of the two sites on the Missouri River, as well as the second largest net gain of all the sites surveyed in 2022 (table 8). The cross section from the 2011 survey along the upstream face of the bridge varies from 5 to 15 ft below the other survey sections, with a substantially lower bed near the left (east) bank downstream from the spur dike there (fig. 9). The frequency distribution of bed elevations in 2011 is unique compared to the other distributions at this site, with a substantially higher percentage of cells at channel-bed elevations 8–10 ft lower than the other surveys (fig. 8). The stone revetment on the right (west) bank showed signs of localized substantial deposition, whereas the spur dikes on the left (east) bank showed minor scour (fig. 12). As with the previous DoD, deposition or scour apparent on opposing faces of a feature (such as a pier or spur dike) likely resulted from minor horizontal positional variances between the surveys (fig. 6).

The vertically averaged velocity vectors indicated mostly uniform flow in the middle of the channel, with velocities ranging from about 4 to 7 feet per second (ft/s) except near the spur dikes on the left (east) bank where local lower velocities and turbulence were observed (fig. 13). The wake vortices downstream from the main channel pier were not pronounced and seemed to be no greater than the general nonuniformity of flow observed in the channel (fig. 13). Minor localized turbulence was present in all the sections (fig. 13).

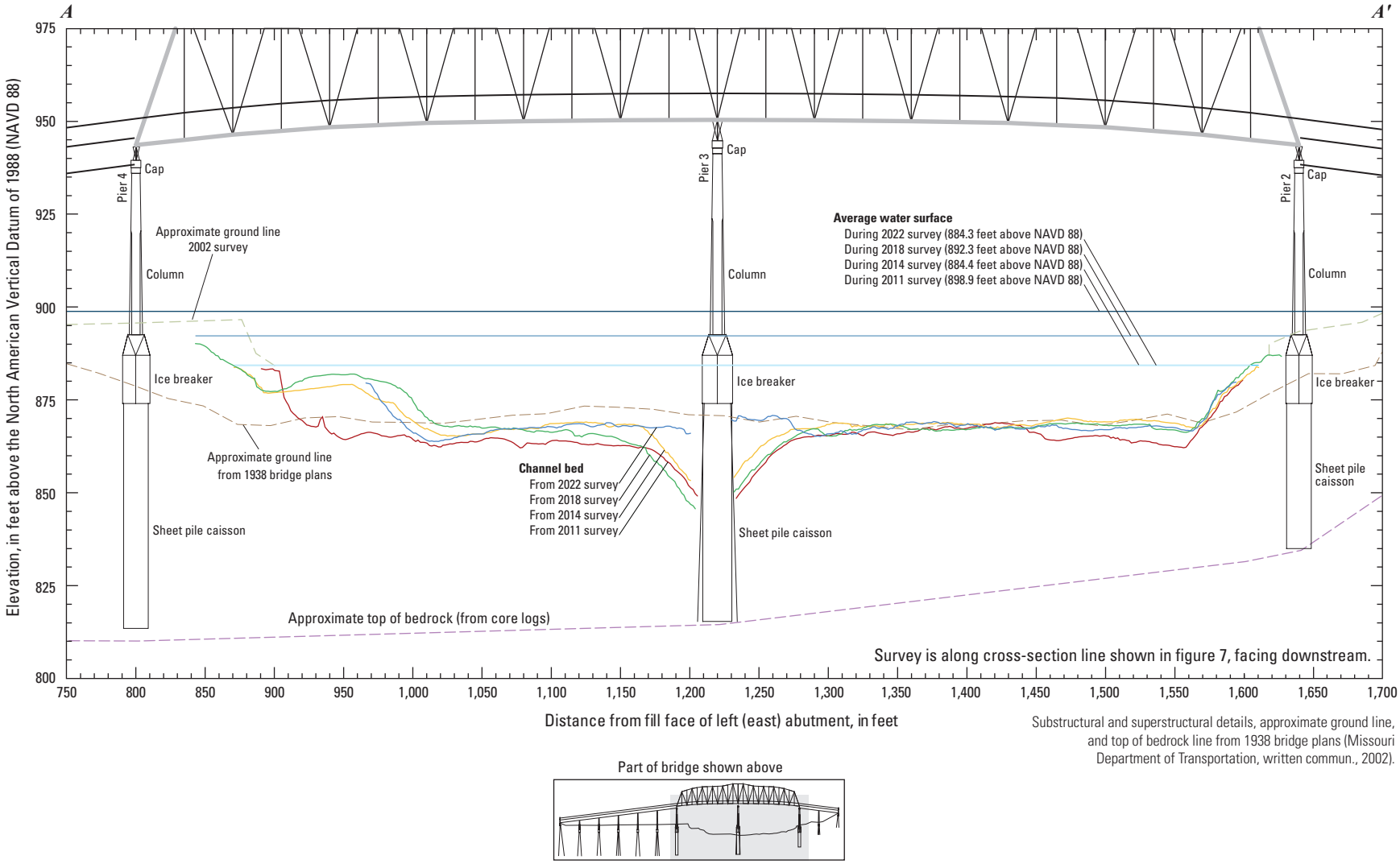

Substructural and superstructural details, approximate ground line, and top of bedrock line from 1938 bridge plans (Missouri Department of Transportation, written commun., 2002).

Figure 9. Key features, substructural and superstructural details, and surveyed channel bed of structure L0098 on U.S. Highway 136 crossing the Missouri River at Brownville, Nebraska.

Table 7. Results near piers and bents from surveys on the Missouri and Mississippi Rivers on the periphery of Missouri, June 13–22, 2022.

[Data are summarized from Huizinga and Rivers (2023b). Sites are shown on figure 1. All elevations are in feet above the North American Vertical Datum of 1988. MoDOT, Missouri Department of Transportation; --, not known/applicable]

Site number (fig. 1)	Structure number	MoDOT pier/bent number	Foundation information				Approximate flow angle of attack near pier/bent, in degrees	Approximate minimum elevation in scour hole near pier/bent,[a] in feet	Approximate elevation of scour hole at upstream pier/bent face, in feet	Approximate elevation of bedrock near pier/bent, in feet	Approximate distance between bottom of scour hole and bedrock, in feet	Depth of scour hole from average upstream channel bed, in feet
			Type	Width, in feet	Penetration into bedrock, in feet	Bottom of seal course elevation, in feet						
1	L0098	3	Caisson	21	0	--	0	[b]866	[b]866	815	51[b]	5[b]
2	A3664 E & W	10	Drilled shaft	30	25	758.00	15	762	762	745	18	20
		9	Drilled shaft	24	25	774.00	0	758[c]	769	745	13[c]	22[c]
		8	Pile cap	19.5	1	789.00	10	758[c]	782	745	13[c]	22[c]
31	A5054	11	Pile cap	36	0	419.00	10	433	444	351	82	0
		10	Pile cap	36	0	421.00	15	437	445[b]	357	80	2[b]
		9	Pile cap	35	0	411.00	10	434	439[b]	380	54	3[b]
		8	Drilled shaft	36	15	405.00	10	426	426	394	32	7
		7	Drilled shaft	36	15	402.00	15	423	427	395	28	2
		6	Drilled shaft	35	15	401.00	20	423	424	395	28	6
		5	Drilled shaft	35	28	436.00	10	448[d]	448[d]	435	13	0[d]
36	L0135	13	Footing	15	1	--	0	351[d]	351[d]	345	6	0[d]
		12	Footing	16	3	--	0	321[d]	321[d]	317	2	0[d]
		11	Caisson	24	1	--	5	309	309	266	43	17
		10	Caisson	16	2	--	5	329	329	245	84	8
37	A5076	7	Drilled shaft	32	19	301.00	([e])	([e])	([e])	243	([e])	([e])
		6	Drilled shaft	32	20	292.00	0	312	312	245	67	6
		5	Drilled shaft	32	22	285.00	0	300	300	245	56	4
		4	Caisson	60	1	--	30	270	282[b]	244	26	9[b]
		3	Caisson	67	1	--	30	264	288[b]	250	14	10[b]
		2	Footing	60	1	--	30	([e])	([e])	290	([e])	([e])

Table 7. Results near piers and bents from surveys on the Missouri and Mississippi Rivers on the periphery of Missouri, June 13–22, 2022.—Continued

[Data are summarized from Huizinga and Rivers (2023b). Sites are shown on figure 1. All elevations are in feet above the North American Vertical Datum of 1988. MoDOT, Missouri Department of Transportation; --, not known/applicable]

Site number (fig. 1)	Structure number	MoDOT pier/bent number	Foundation information				Approximate flow angle of attack near pier/bent, in degrees	Approximate minimum elevation in scour hole near pier/bent,[a] in feet	Approximate elevation of scour hole at upstream pier/bent face, in feet	Approximate elevation of bedrock near pier/bent, in feet	Approximate distance between bottom of scour hole and bedrock, in feet	Depth of scour hole from average upstream channel bed, in feet
			Type	Width, in feet	Penetration into bedrock, in feet	Bottom of seal course elevation, in feet						
38	A1700	21	Caisson	39	0	158.52[f]	30	225[d]	225[d]	--	--	[d]0
		20	Caisson	66	0	119.20[f]	30	189	189[b]	--	--	[b]8
		19	Caisson	29	0	139.35[f]	10	208	208[b]	--	--	[b]6
		18	Pile cap	50.8	0	188.00	0	215	217[b]	--	--	0[b]
		17	Pile cap	39.7	0	196.50	0	223	223[b]	--	--	0[b]
		16	Pile cap	42	0	196.50	20	220	220[b]	--	--	0[b]
		15	Pile cap	39.7	0	196.92	15	[b,d]221	221[b,d]	--	--	0[b,d]
		14	Pile cap	18	0	240.00	([e])	([e])	([e])	--	--	([e])

[a]The point of lowest elevation in the scour hole near the bridge pier/bent, not necessarily at the upstream face.

[b]Pier appears to be partially or totally surrounded with a riprap blanket.

[c]Scour hole at this pier was substantially affected by adjacent spur dike.

[d]Scour hole at this pier is substantially affected by stone revetment or bedrock.

[e]Unable to obtain data because pier was in very shallow water.

[f]Elevation of bottom of caisson is shown because it is not founded on bedrock.

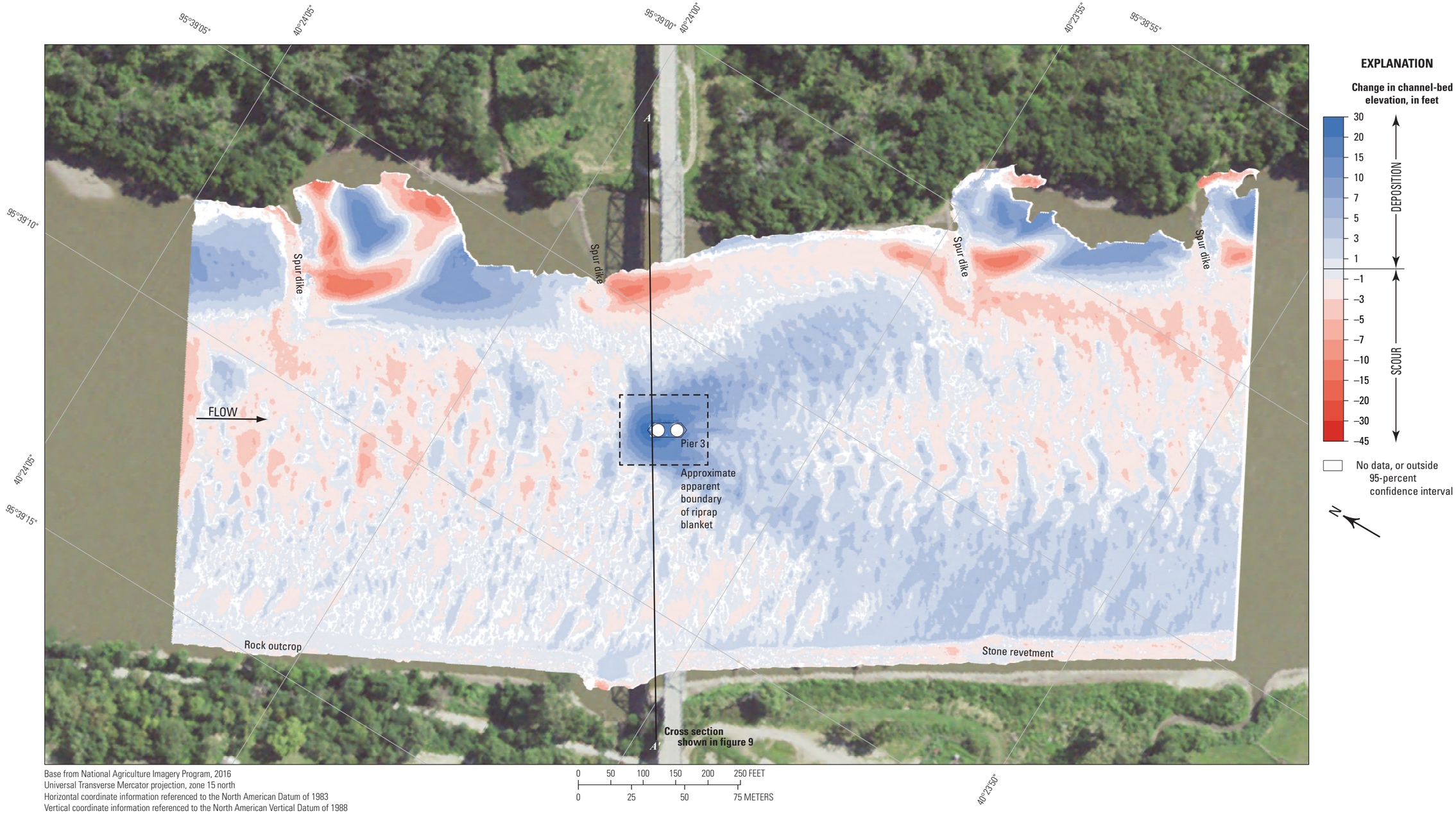

Figure 10. Difference between surfaces created from bathymetric surveys of the Missouri River channel near structure L0098 on U.S. Highway 136 at Brownville, Nebraska, on June 22, 2022, and August 13, 2018, with probabilistic thresholding.

Table 8. Summary information and bathymetric surface difference statistics from surveys on the Missouri and Mississippi Rivers on the periphery of Missouri, from June 13–22, 2022, and previous surveys (Huizinga, 2012, 2015, 2020e).

[Dates are shown as month/day/year. All elevations are referenced to the North American Vertical Datum of 1988. MoDOT, Missouri Department of Transportation; Min, minimum; Max, maximum; A, Huizinga (2012); B, Huizinga (2015); C, Huizinga (2020e)]

Site number (fig. 1)	MoDOT structure number	Previous survey					Difference between 2022 survey and previous survey[a]				
		Source of data	Date	Streamflow, in cubic feet per second	Surveyed area, in 1×10^6 square feet	Average water-surface elevation, in feet	Stream-flow, in cubic feet per second	Stream-flow, in percent	Surveyed area, in 1×10^6 square feet	Surveyed area, in percent	Average water-surface elevation, in feet
1	L0098	A	07/13/11	225,000	1.159	898.9	−187,700	−503	−0.047	−4.2	−14.6
		B	06/03/14	39,800	1.195	884.4	−2,500	−6.7	−0.083	−7.5	−0.1
		C	08/13/18	77,800	1.228	892.3	−40,500	−109	−0.116	−10.5	−7.9
2	A3664 E&W	A	07/14/11	218,000	1.440	817.2	−179,300	−463	−0.092	−6.8	−21.1
		B	06/04/14	66,100	1.045	799.8	−27,400	−70.8	[e]0.303	22.5	−3.7
		C	07/16/18	96,100	1.457	805.8	−57,400	−148	−0.109	−8.1	−9.7
31	A5054	B	06/05/14	198,000	3.033	464.6	−42,000	−26.9	0.010	0.3	−1.3
		C	07/18/18	173,000	3.039	464.0	−17,000	−10.9	0.004	0.1	−0.7
36	L0135	B	06/09/14	363,000	3.041	363.9	−24,000	−7.1	0.024	0.8	−0.6
		C	07/24/18	290,000	3.078	360.4	49,000	14.5	−0.013	−0.4	3.0
37	A5076	B	06/10/14	377,000	3.224	331.7	−42,000	−12.5	0.089	2.7	−0.6
		C	07/25/18	282,000	3.163	328.2	53,000	15.8	0.150	4.5	3.0
38	A1700	B	12/10/08	156,000	3.510	228.4	312,000	66.7	[f]0.798	18.5	21.9
		B	05/05/11	2,040,000	4.281	277.4	−1,572,000	−336	0.027	0.6	−27.1
		B	06/11/14	629,000	4.418	251.8	−161,000	−34.4	−0.109	−2.5	−1.5
		C	07/26/18	420,000	4.316	245.9	48,000	10.3	−0.007	−0.2	4.4

Table 8. Summary information and bathymetric surface difference statistics from surveys on the Missouri and Mississippi Rivers on the periphery of Missouri, from June 13–22, 2022, and previous surveys (Huizinga, 2012, 2015, 2020e). —Continued

[Dates are shown as month/day/year. All elevations are referenced to the North American Vertical Datum of 1988. MoDOT, Missouri Department of Transportation; Min, minimum; Max, maximum; A, Huizinga (2012); B, Huizinga (2015); C, Huizinga (2020e)]

Site number (fig. 1)	Statistics of differences between 2022 and previous bathymetric survey surfaces, in feet				Max-difference near upstream pier face(s),[c,d] in feet	Joint area of interest with detectable change, in percent	Net volume of cut, in cubic yards	Net volume of fill, in cubic yards	Net change in sediment volume, in cubic yards
	Min[b,c]	Max[b,c]	Average[c]	Standard deviation					
1	−15.5	34.9	4.43	3.90	15.3	92	8,000	173,100	165,100
	−13.0	33.2	0.27	2.54	12.6	57	19,700	26,000	6,300
	−14.8	33.2	0.41	3.09	19.5	93	34,500	50,100	15,600
2	−25.1	23.9	−1.34	5.91	−15.6	85	129,300	73,500	−55,800
	−18.7	16.0	1.02	2.37	−7.4	60	12,500	35,400	22,900
	−22.2	19.9	−1.83	4.47	−19.9	98	134,200	46,400	−87,800
31	−33.2	25.5	−0.30	3.24	13.2	71	112,500	89,000	−23,500
	−32.5	27.2	−1.86	2.49	−5.1	86	205,500	26,700	−178,800
36	−40.7	37.1	0.35	2.31	6.6	70	63,000	90,300	27,300
	−35.0	41.2	−0.52	1.86	5.6	81	92,600	46,100	−46,500
37	−45.0	34.4	−1.71	3.98	−10.2	71	221,500	78,600	−142,900
	−34.8	35.2	−1.79	2.87	−12.4	83	215,200	42,300	−172,900
38	−40.5	50.8	−5.47	12.16	30.0	91	936,800	300,500	−636,300
	−54.4	50.0	5.83	7.99	32.7	89	143,100	888,100	745,000
	−61.6	49.3	−4.69	9.83	33.6	86	896,500	260,100	−636,400
	−43.6	49.2	−0.71	6.21	31.1	90	405,600	305,600	−100,000

[a]A positive value of difference means the 2022 value was larger than the previous value, whereas a negative value means the 2022 value was smaller than the previous value.

[b]The maximum or minimum value of change likely is near a vertical pier face and affected by minor positional variances (fig. 6).

[c]A positive value represents deposition, a negative value represents scour.

[d]The maximum difference near the upstream pier face was from near the location of the "approximate elevation of scour hole at upstream pier face" in table 7.

[e]The surveyed reach in 2014 was substantially narrower because of a wide band of floating debris along the right bank.

[f]The surveyed reach in 2008 was narrower and shorter in length because of lower flow conditions and not surveying as high on the banks.

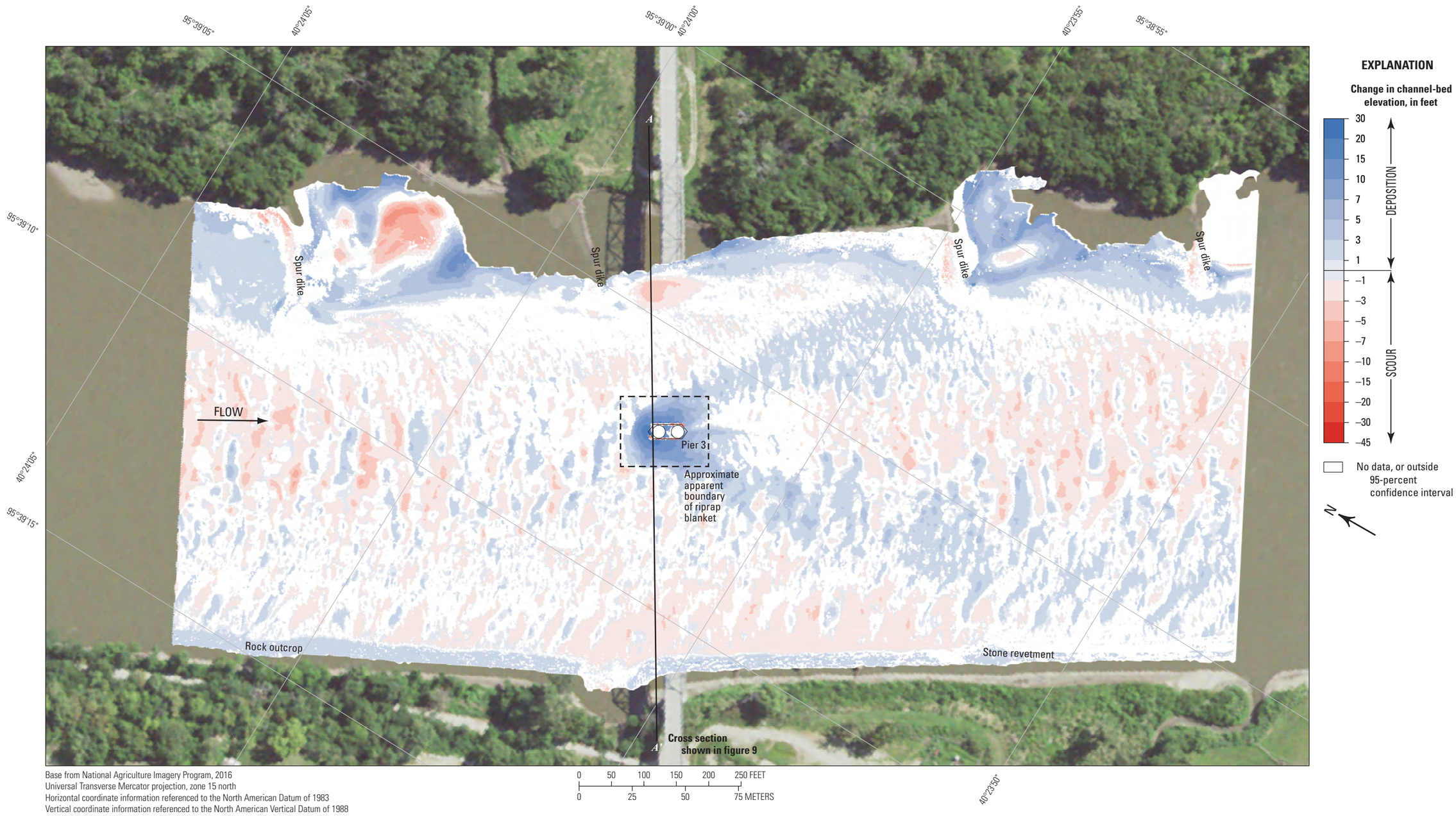

Base from National Agriculture Imagery Program, 2016
Universal Transverse Mercator projection, zone 15 north
Horizontal coordinate information referenced to the North American Datum of 1983
Vertical coordinate information referenced to the North American Vertical Datum of 1988

Figure 11. Difference between surfaces created from bathymetric surveys of the Missouri River channel near structure L0098 on U.S. Highway 136 at Brownville, Nebraska, on June 22, 2022, and June 3, 2014, with probabilistic thresholding.

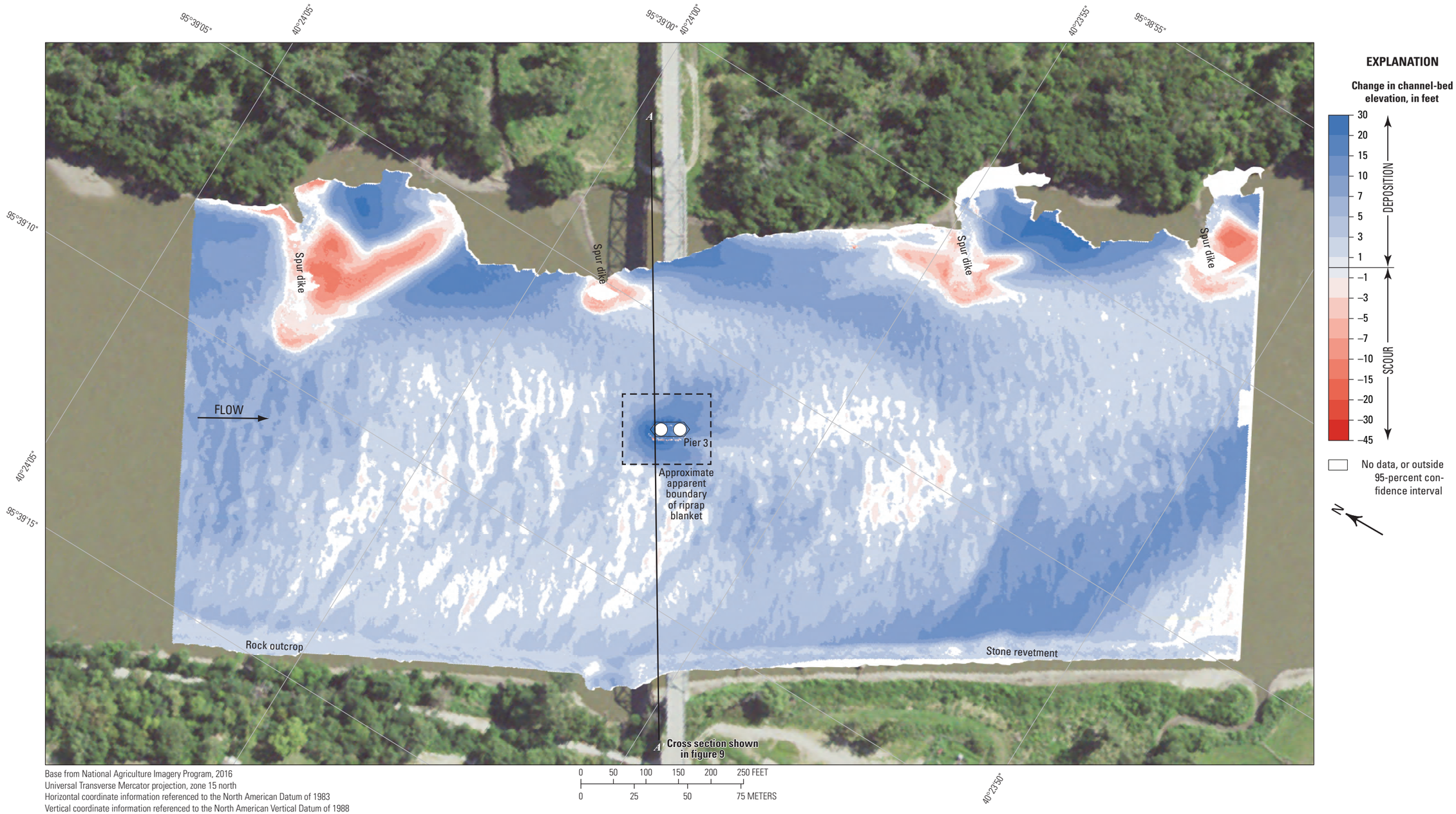

Base from National Agriculture Imagery Program, 2016
Universal Transverse Mercator projection, zone 15 north
Horizontal coordinate information referenced to the North American Datum of 1983
Vertical coordinate information referenced to the North American Vertical Datum of 1988

Figure 12. Difference between surfaces created from bathymetric surveys of the Missouri River channel near structure L0098 on U.S. Highway 136 at Brownville, Nebraska, on June 22, 2022, and July 13, 2011, with probabilistic thresholding.

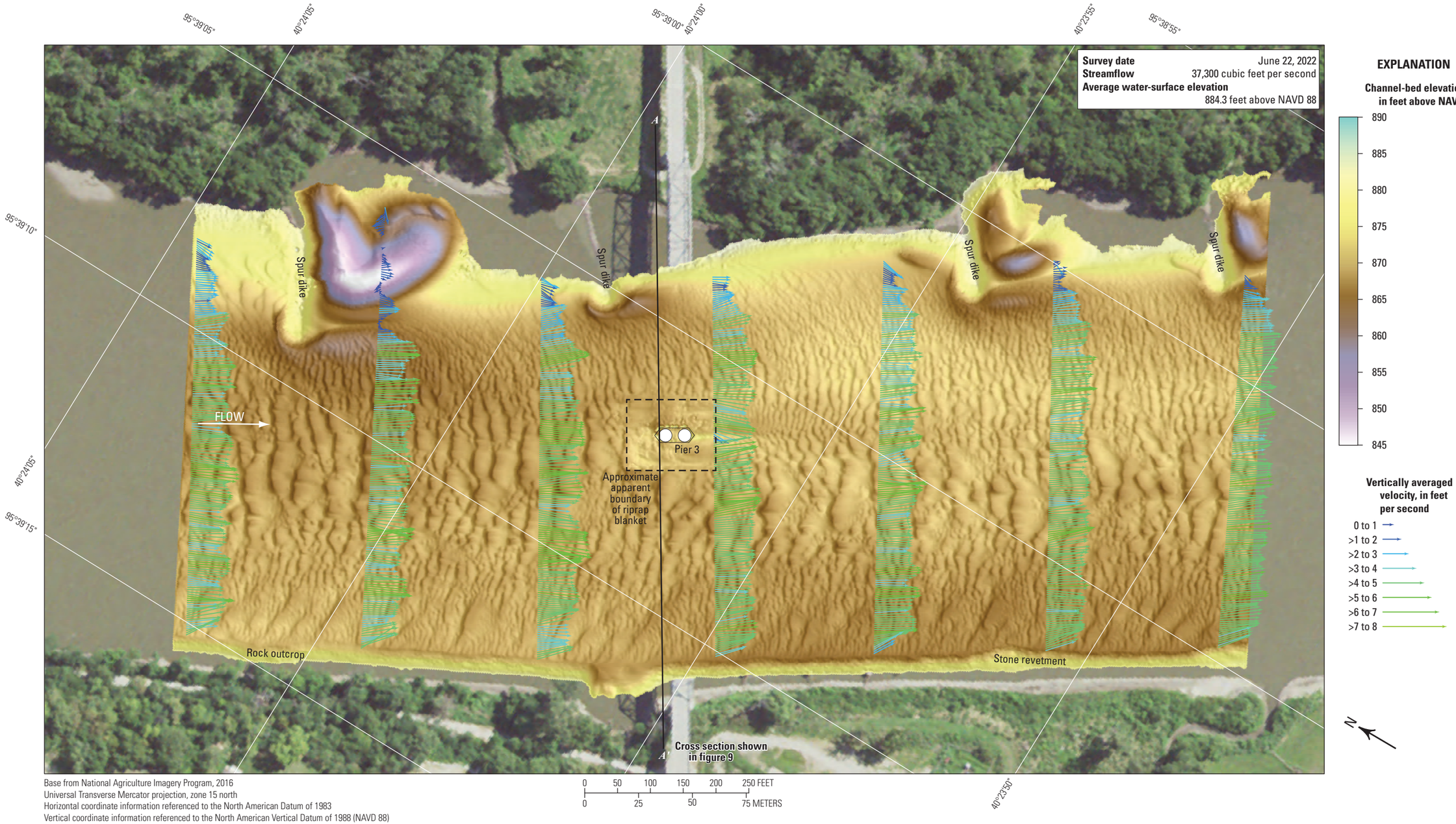

Base from National Agriculture Imagery Program, 2016
Universal Transverse Mercator projection, zone 15 north
Horizontal coordinate information referenced to the North American Datum of 1983
Vertical coordinate information referenced to the North American Vertical Datum of 1988 (NAVD 88)

Figure 13. Bathymetry and vertically averaged velocities of the Missouri River channel near structure L0098 on U.S. Highway 136 at Brownville, Nebraska.

Dual Bridge Structure A3664 on U.S. Highway 36 at St. Joseph, Missouri

Structure A3664 (site 2; table 2) consists of twin bridges on U.S. Highway 36 crossing the Missouri River at RM 447.9 at St. Joseph, Mo., on the western side of Missouri north of Kansas City, Mo. (fig. 1). The site was surveyed on June 22, 2022, and the average water-surface elevation of the river in the survey area, determined by the RTK GNSS tide solution, was 796.1 ft (table 3; fig. 14) and streamflow was about 38,700 ft^3/s during the survey (table 3).

The survey area was about 1,640 ft long and about 885 ft wide, extending from bank to bank in the main channel (fig. 14). The survey area extended about 655 ft upstream from the centerline of structure A3664 (fig. 14). The channel-bed elevations ranged from about 770 to 789 ft throughout the survey area (5th to 95th percentile range of the bathymetric data; fig. 15), except near the spur dikes on the right (west) bank (fig. 14; table 3). The channel bed between the left (east) bank and the spur dikes was filled with small dunes and ripples (fig. 14). Substantial scour holes were present downstream from the spur dikes on the right (west) side (fig. 14). Stone revetment was present on the left (east) bank throughout the reach (fig. 12). A localized deep scour hole downstream from the downstream spur dike on the right bank had a minimum channel-bed elevation of about 755 ft (table 3; fig. 14). As in previous surveys (Huizinga, 2012, 2015, 2020e), stone revetment was present on the left (east) bank throughout the reach (fig. 14).

The scour hole near pier 10 (figs. 14 and 1.2) had a minimum channel-bed elevation of 762 ft, about 4 ft above the bottom of the seal course elevation of 758 ft (table 7). The footing and seal course were evident at the upstream end of pier 9 in the map and shaded pier TIN images (figs. 14 and 1.2*A–B*). The cross section along the upstream bridge face indicates the channel bed is lower than the seal course at pier 9 (fig. 16; table 7), and a hazy area under the upstream end of the seal course in the shaded pier TIN of the right side (fig. 1.2*D*) further implies the seal course was undermined. The pile cap footing of upstream pier 8 also appears to be partly undermined in the cross section along the upstream bridge face (fig. 16; table 7), but the point data were too thin in this area to create a meaningful shaded pier TIN of the area. Information from bridge plans indicates that piers 9 and 10 are founded on shafts drilled into bedrock, with about 13 ft of bed material between bedrock near pier 9 and the bottom of the scour hole caused by the spur dike (figs. 14 and 16; table 7). Pier 8 is founded on steel H-piles driven to refusal on bedrock, also with about 13 ft of bed material between bedrock near pier 8 and the bottom of the scour hole caused by the spur dike (figs. 14 and 16; table 7). In modern construction, bridge substructural elements usually are pinned or socketed to bedrock (Brown and others, 2018; American Association of State Highway Transportation Officials, 2020), but exposure of usually buried substructural elements warrants special consideration and observation. Along the upstream bridge face, the surveyed bed from 2022 generally falls within the fluctuating range of elevations observed in previous multibeam surveys, except near pier 10 where the 2022 cross section most closely mimics the 2014 survey (fig. 16).

The difference between the survey on June 22, 2022, and the previous survey on July 16, 2018 (fig. 17), indicates about 98 percent of the joint area of interest had detectable change, which means only about 2 percent of the differences in the joint area of interest are equivocal and within the bounds of uncertainty (table 8). Erosion appears dominant throughout the reach between 2018 and 2022 in the DoD, except localized areas of substantial deposition downstream from the spur dikes on the right (west) bank and minor to moderate deposition in the middle of the upstream channel (fig. 17). The average difference between the bathymetric surfaces was –1.83 ft (table 8), indicating moderate channel degradation between the 2018 and 2022 surveys. The net volume of cut in the reach from 2018 to 2022 was about 134,200 yd^3, and the net volume of fill was about 46,400 yd^3, resulting in a net loss of about 87,800 yd^3 of sediment between 2018 and 2022 (table 8). The bed surface in the cross section from the 2022 survey along the upstream face of the bridge was below the 2018 survey section, except near pier 9 (fig. 16). The water-surface elevation in 2022 also was substantially lower than in 2018 (table 8; fig. 16). The frequency distribution of bed elevations in 2022 is similar in shape to the 2018 distribution, but with a higher percentage of cells at channel-bed elevations about 4–5 ft lower than 2018 (fig. 15). The area downstream from the spur dike on the upstream right bank showed substantial erosion of as much as 30 ft and deposition of as much as 20 ft (fig. 17), and the erosion likely affected the scour observed near pier 10 (figs. 16 and 17). The stone revetment on the left (east) bank showed localized signs of minor erosion and deposition, and the various spur dikes throughout the channel showed minor scour on one face and deposition on the other (fig. 17). As with previous DoDs, deposition or scour apparent on opposing faces of a feature likely results from minor horizontal positional variances between the surveys (fig. 6). The areas of apparent erosion of the stone revetment tend to be near the upper edges of the banks and may be the result of larger uncertainty in the outer beams in the 2022 survey, particularly near the water surface (fig. 5).

The difference between the survey on June 22, 2022, and the survey on June 4, 2014 (fig. 18), indicates about 60 percent of the joint area of interest had detectable change, which means about 40 percent of the differences in the joint area of interest are equivocal and within the bounds of uncertainty (table 8). Minor erosion and deposition appear nearly balanced throughout the reach between 2014 and 2022 in the DoD, with deposition slightly more dominant and with localized substantial erosion and deposition near the ends and downstream from the spur dikes (fig. 18). However, the average difference between the bathymetric surfaces was +1.02 ft (table 8), indicating moderate channel aggradation between the 2014 and 2022 surveys, and the net gain of sediment between 2014 and 2024 was about 22,900 yd^3 (table 8). The cross section from the 2022 survey along the upstream face of the bridge is most like the 2014 survey section, varying 5 to 10 ft above and below the 2014

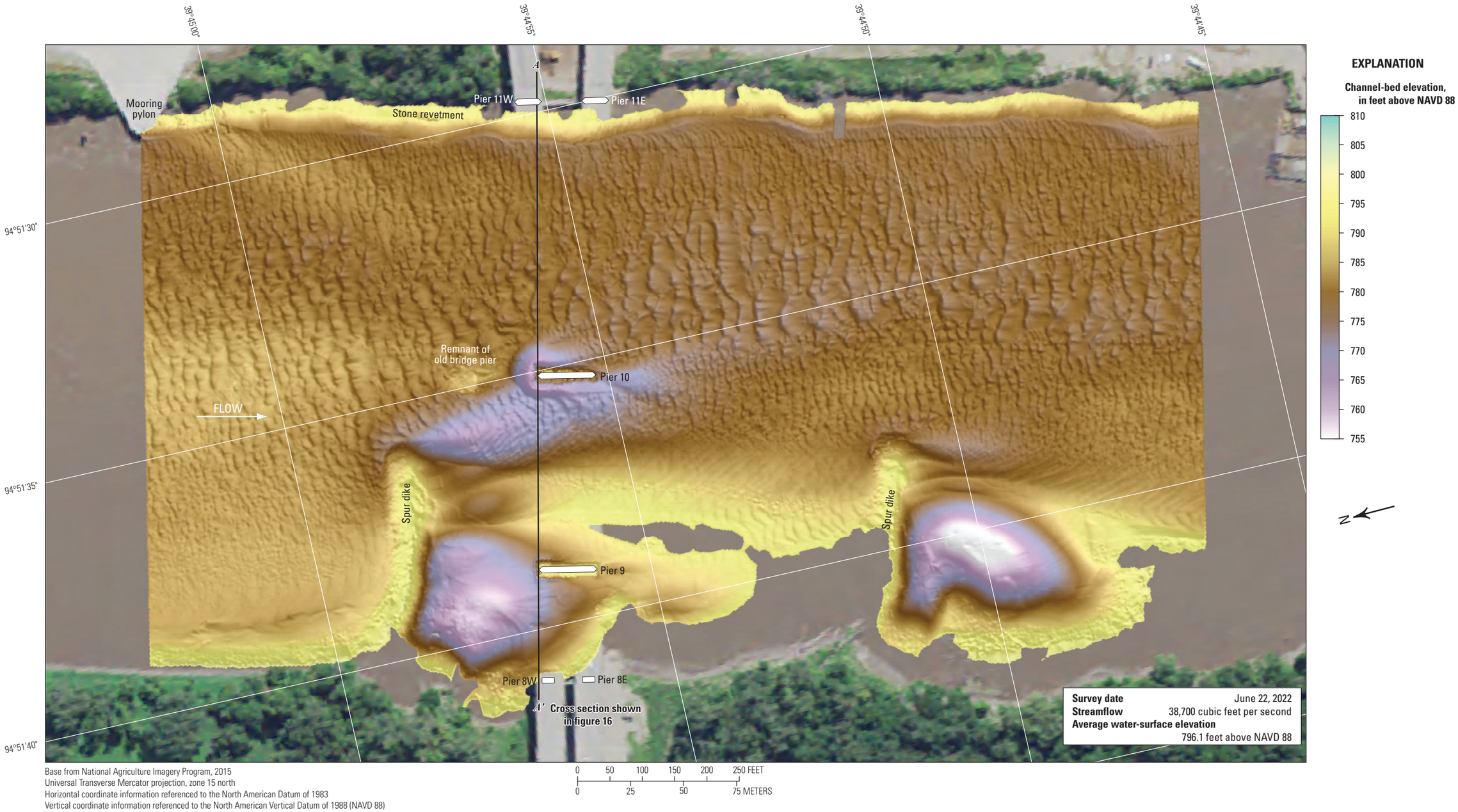

Figure 14. Bathymetric survey of the Missouri River channel near dual bridge structure A3664 on U.S. Highway 36 at St. Joseph, Missouri.

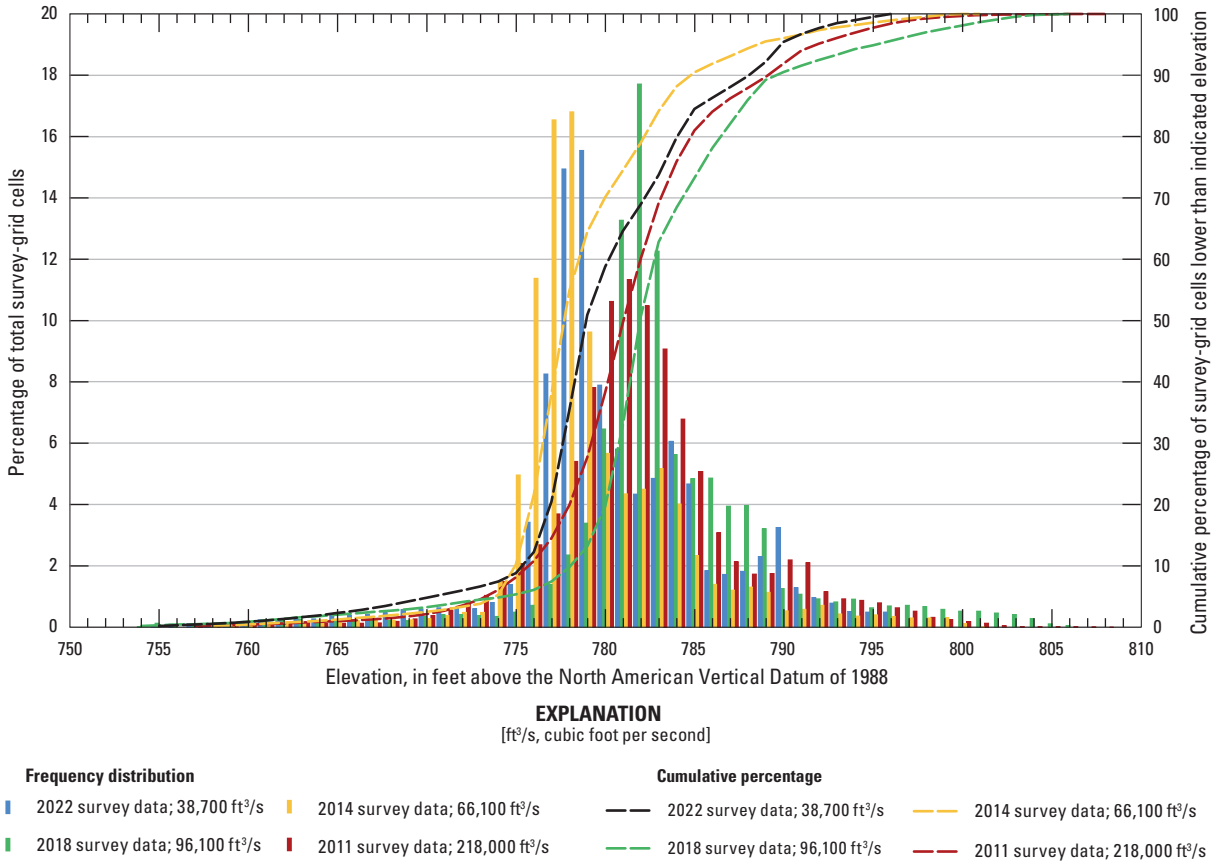

Figure 15. Frequency distribution of bed elevations for bathymetric survey-grid cells in 1-foot elevation bins on the Missouri River near structure A3664 on U.S. Highway 36 at St. Joseph, Missouri, on June 22, 2022, compared to previous surveys in 2011, 2014, and 2018 (Huizinga, 2012, 2015, and 2020e, respectively).

section (fig. 16). The frequency distribution of bed elevations in 2022 appeared similar in shape to 2014 but shifted about 1–2 ft higher in channel-bed elevations than 2014 (fig. 15). Streamflow in 2022 was most similar to 2014 (table 8), which may account for the similarity in overall characteristics between the surveys (figs. 16 and 18). The stone revetment on the left (east) banks shows a similar area of erosion to the 2018 comparison, again indicating possibly higher uncertainties of the outer beams in the 2022 survey, but most of the left bank is within the bounds of uncertainty (fig. 18). A substantial part of the channel on the right (west) side was not surveyed in 2014 because of substantial floating debris (table 8). As with previous DoDs, deposition or scour apparent on opposing faces of pier 10 likely resulted from minor horizontal positional variances between the surveys (fig. 6).

The difference between the survey on June 22, 2022, and the earliest survey during flooding on July 14, 2011 (fig. 19), indicates about 85 percent of the joint area of interest had detectable change, which means about 15 percent of the differences in the joint area of interest are equivocal and within the bounds of uncertainty (table 8). Erosion appears dominant between 2011 and 2022 in the DoD, with substantial erosion balanced with moderate to substantial deposition in the upstream channel and downstream from the spur dikes (fig. 19). The average difference between the bathymetric surfaces was –1.34 ft (table 8), indicating moderate degradation between the 2011 and 2022 surveys, with a net loss of sediment of about 55,800 yd³ (table 8). The frequency distribution of bed elevations in 2011 was very similar to 2022 (and the other surveys) but shifted about 2–3 ft higher in channel-bed elevations than 2022 (fig. 15). The stone revetment on the left (east) bank showed localized signs of minor scour and deposition, with the same area of moderate erosion as the other DoDs for this site (fig. 19). The piers and various spur dikes throughout the channel showed minor scour on one face and deposition on the other (fig. 19). As with previous DoDs, deposition or scour apparent on opposing faces of a feature likely resulted from minor horizontal positional variances between the surveys (fig. 6).

The vertically averaged velocity vectors indicate mostly uniform flow in the middle of the channel, with velocities ranging from about 3 to 8 ft/s (fig. 20). Local lower velocities and turbulence were observed downstream from the various spur dikes on the right (west) bank (fig. 20). Wake vortices were evident downstream from main channel pier 10 but were not pronounced and seemed to be no greater than the general nonuniformity of flow observed in the channel (fig. 20). Although aligned with primary flow in the channel, pier 10 is slightly skewed to approach flow because of the spur dike on the right (west) bank upstream, causing minor wake vortices and a defined deposition ridge downstream (fig. 20). Minor localized turbulence was present in all the sections (fig. 20).

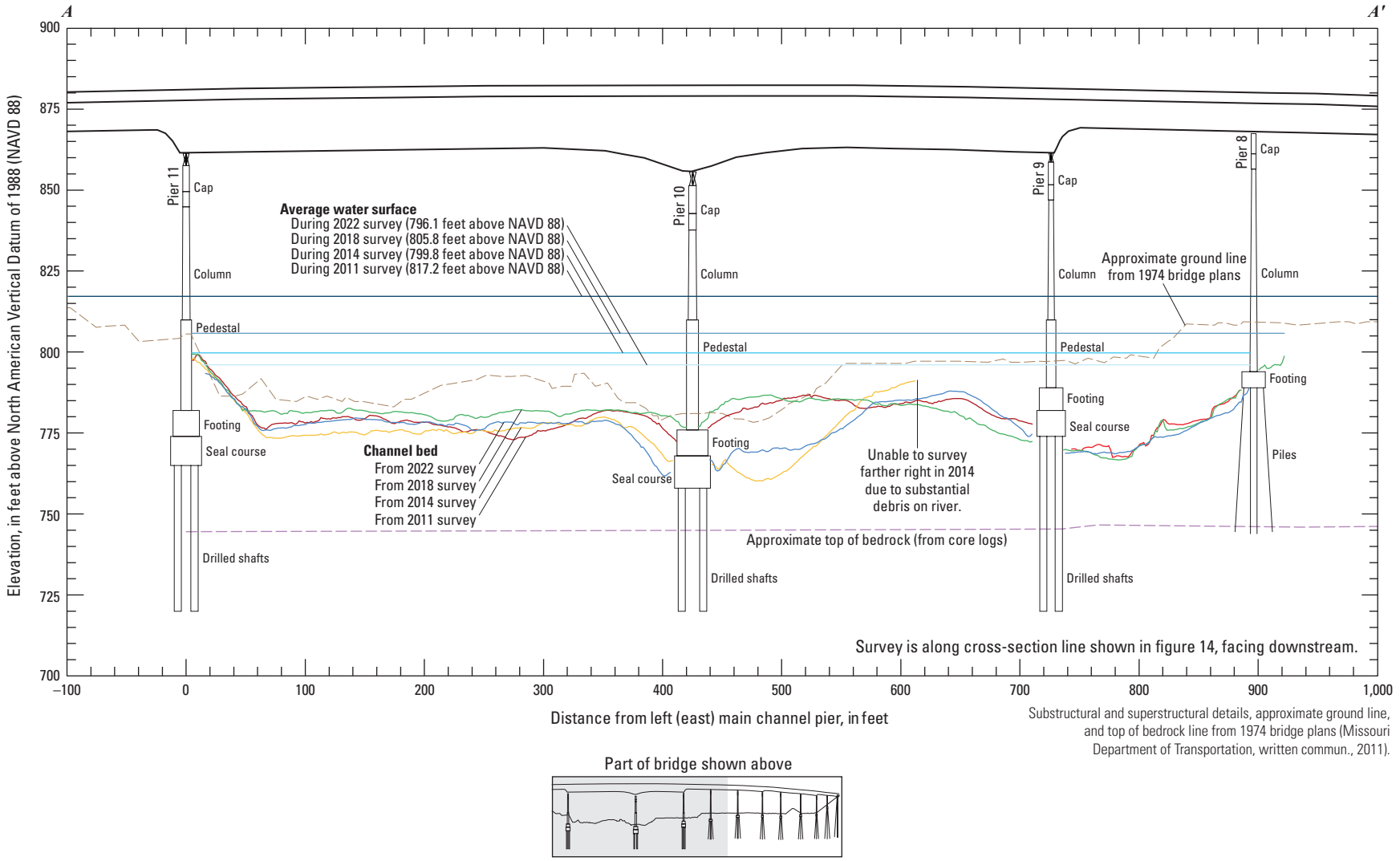

Figure 16. Key features, substructural and superstructural details, and surveyed channel bed of dual bridge structure A3664 on U.S. Highway 36 crossing the Missouri River at St. Joseph, Missouri.

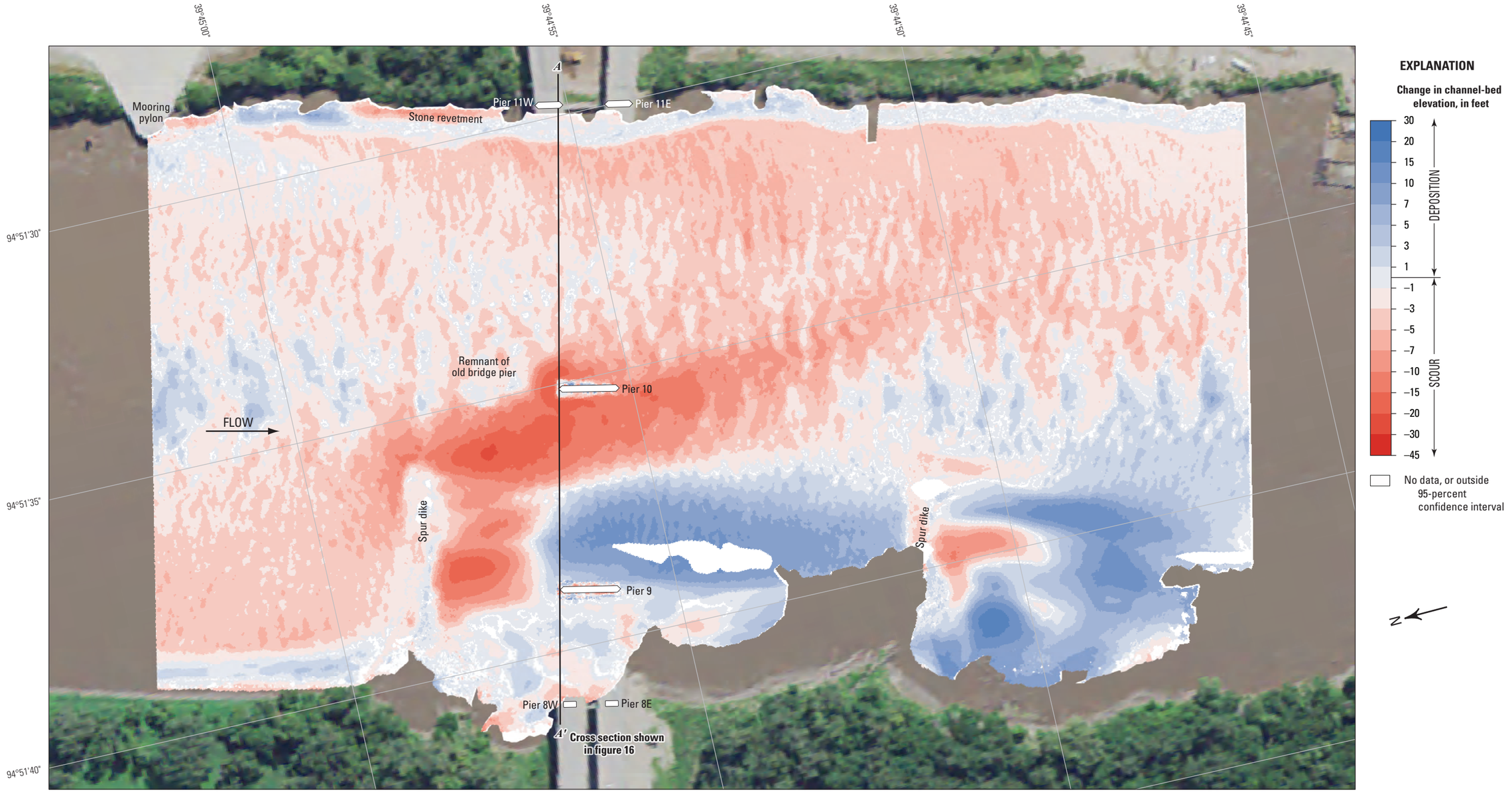

Figure 17. Difference between surfaces created from bathymetric surveys of the Missouri River channel near dual bridge structure A3664 on U.S. Highway 36 at St. Joseph, Missouri, on June 22, 2022, and July 16, 2018, with probabilistic thresholding.

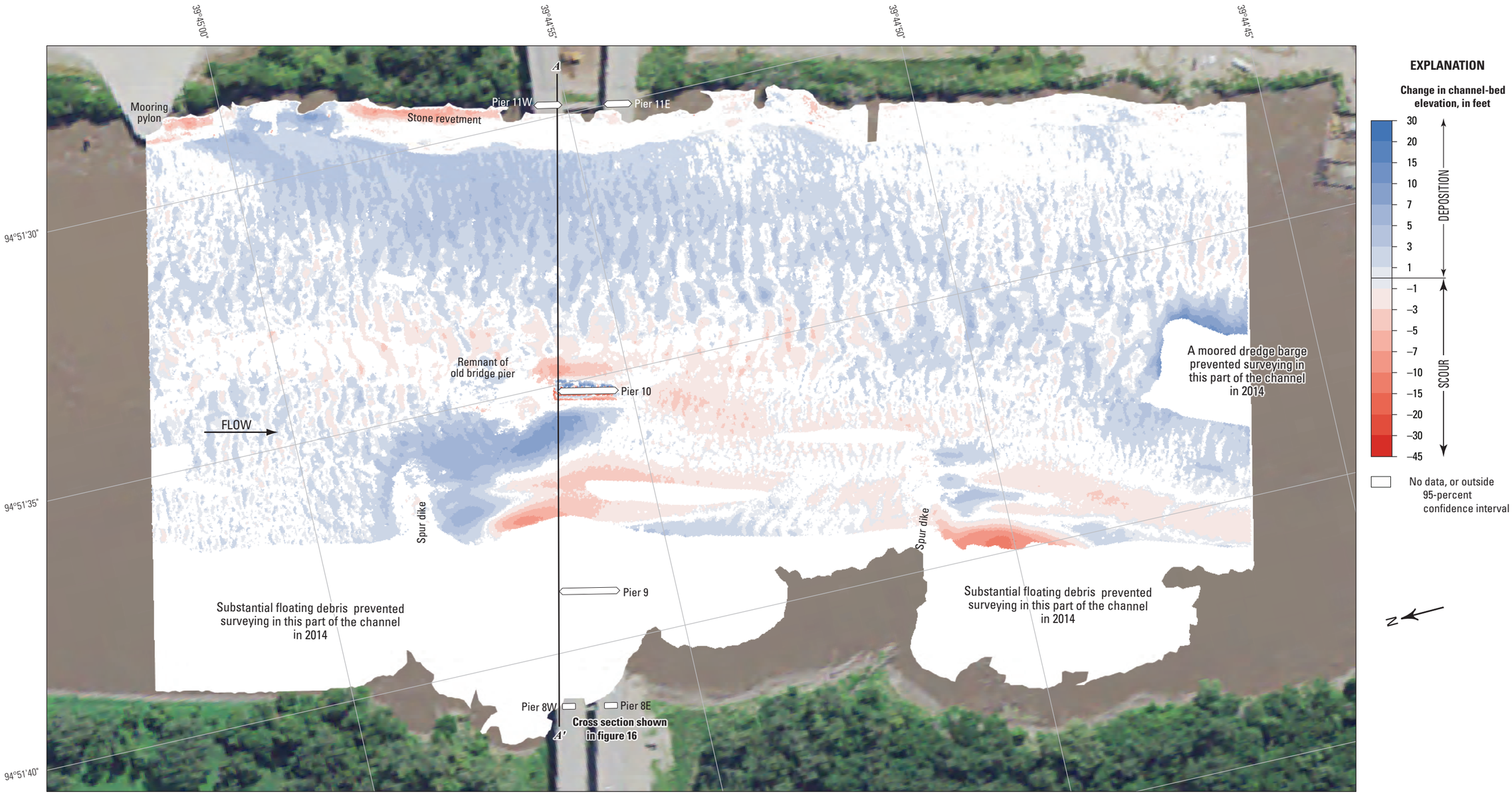

Base from National Agriculture Imagery Program, 2015
Universal Transverse Mercator projection, zone 15 north
Horizontal coordinate information referenced to the North American Datum of 1983
Vertical coordinate information referenced to the North American Vertical Datum of 1988

Figure 18. Difference between surfaces created from bathymetric surveys of the Missouri River channel near dual bridge structure A3664 on U.S. Highway 36 at St. Joseph, Missouri, on June 22, 2022, and June 4, 2014, with probabilistic thresholding.

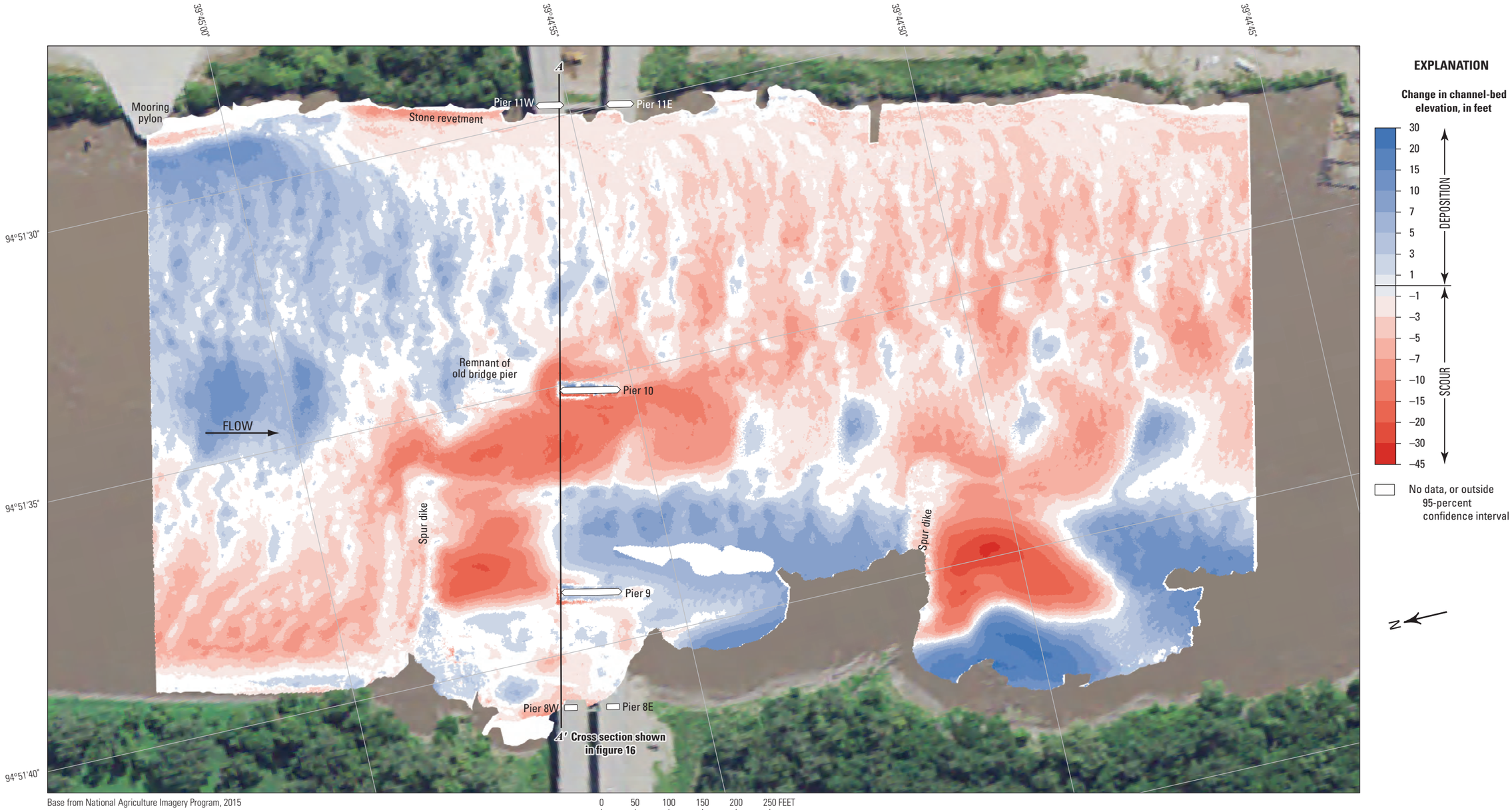

Figure 19. Difference between surfaces created from bathymetric surveys of the Missouri River channel near dual bridge structure A3664 on U.S. Highway 36 at St. Joseph, Missouri, on June 22, 2022, and July 14, 2011, with probabilistic thresholding.

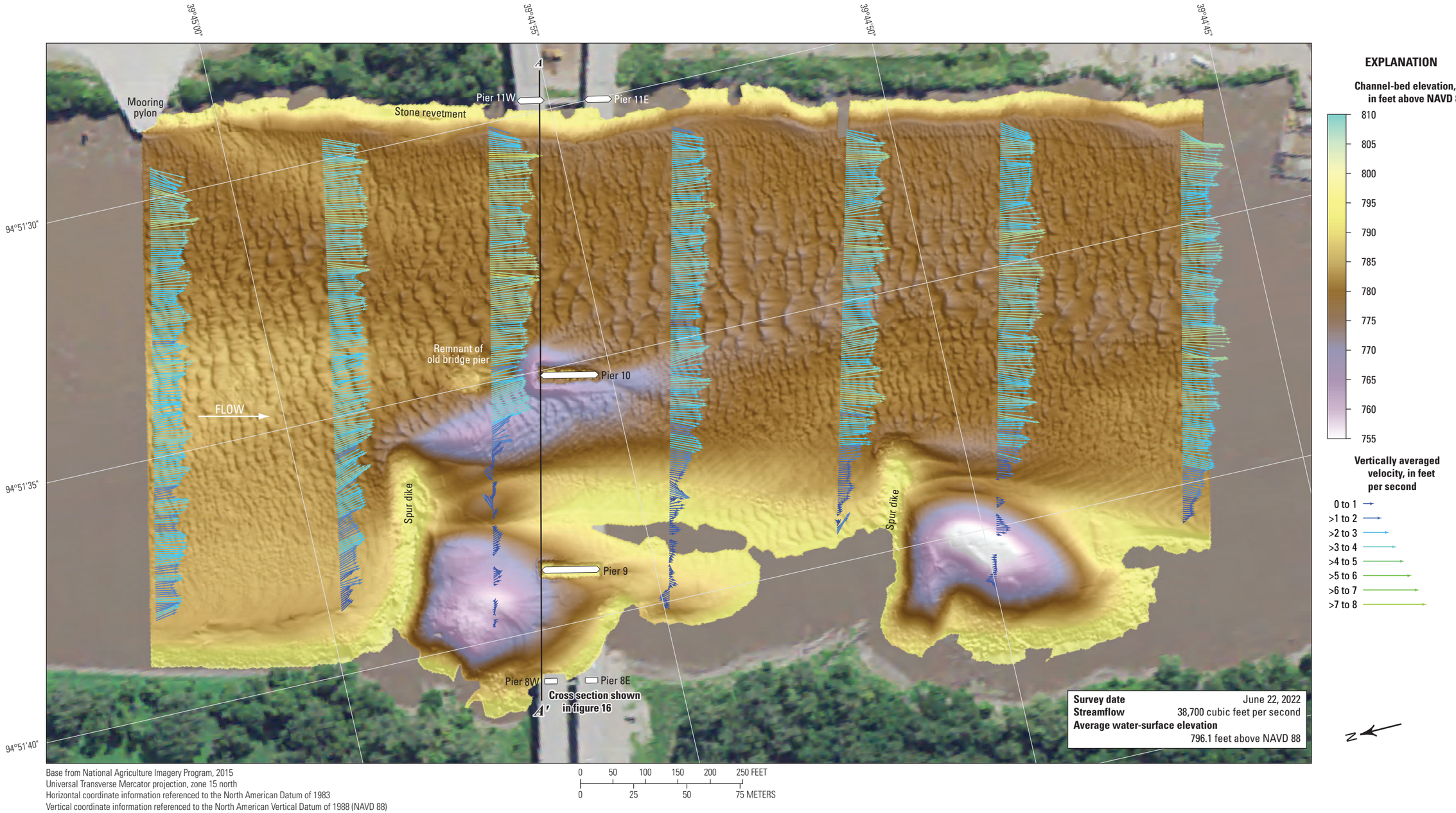

Base from National Agriculture Imagery Program, 2015
Universal Transverse Mercator projection, zone 15 north
Horizontal coordinate information referenced to the North American Datum of 1983
Vertical coordinate information referenced to the North American Vertical Datum of 1988 (NAVD 88)

Figure 20. Bathymetry and vertically averaged velocities of the Missouri River channel near dual bridge structure A3664 on U.S. Highway 36 at St. Joseph, Missouri.

Surveys on the Mississippi River

There are four unique highway crossings of the Mississippi River upstream from St. Louis, and five unique highway crossings of the Mississippi River downstream from St. Louis (fig. 1). Five of these Mississippi River crossings are maintained by MoDOT, and four were surveyed as part of this study. Structure K093 at site 32 on U.S. Highway 54 at Louisiana was replaced by structure A8504 in 2019, and the site was surveyed with the St. Louis area bridges in 2020 (Huizinga, 2023; table 1). Bathymetry and velocity data from the four surveys from the current (2022) study are included with metadata in Huizinga and Rivers (2023b).

Structure A5054 on Interstate 72 at Hannibal, Missouri

Structure A5054 (site 31; table 2) on Interstate 72 crosses the Mississippi River at R M 309.5 at Hannibal, Mo., north of St. Louis, Mo., and south of Quincy, Ill. (fig. 1). The site was surveyed on June 13, 2022, when the average water-surface elevation near the bridge, determined by the RTK GNSS tide solution, was 463.3 ft (table 3; fig. 21), and streamflow on the Mississippi River was measured at about 156,000 ft^3/s during the survey (table 3).

The survey area was about 1,640 ft long and about 1,870 ft wide, extending from bank to bank in the main channel (fig. 21). The survey area extended about 700 ft upstream from the centerline of structure A5054 (fig. 21). The approximate channel-bed elevations ranged from about 428 to 447 ft for most of the surveyed area (5th to 95th percentile range of the bathymetric data; table 3; fig. 22), except near piers 6 through 8 and the thalweg of the channel along the base of the right (southwest) bank (fig. 21; table 3). The left side of the channel between the left (northeast) bank and the channel thalweg was filled with small and medium dune features with superimposed ripples. A spur dike on the left side downstream from the bridge was barely visible above the average bed nearby. As in previous surveys (Huizinga, 2015, 2020e), the right bank consisted of smooth rock or hardpan clay throughout the reach, with no discernable dune features (fig. 21).

The minor scour holes near the upstream end of piers 10 and 11 were difficult to discern from nearby dunes and ripples, and no hole was discernable near pier 5 on the right bank (figs. 21, 1.3*A–D*, 1.4*G*). Alternatively, piers 6 through 8 had well-defined, asymmetric scour holes indicative of being skewed to approach flow. Parts of the footing appear exposed for all the piers in the bathymetric map and in the shaded TIN images (figs. 21, 1.3, 1.4), and piers 6, 7, 9, and 10 seem to be surrounded by partial piles of riprap (figs. 21, 1.3, 1.4). Information from bridge plans indicates that piers 5 through 8 are founded on shafts drilled 15 to 28 ft into bedrock, having about 13 to 32 ft of bed material between the channel bottom and bedrock (table 7; fig. 23). Piers 9 through 11 are founded on steel H-piles driven to refusal on bedrock, having 54 ft of bed material between the channel bottom and bedrock at pier 9, 80 ft of bed material at pier 10, and 82 ft of bed material at pier 11 (fig. 23; table 7). The surveyed bed along the cross section generally was similar to previous multibeam surveys (fig. 23), but as much as 15 ft lower than previous surveys between the left bank and pier 10, and between pier 6 and 8. The cross section along the upstream bridge face indicates partial footing exposure at all the piers (fig. 23), and the exposure is readily apparent in the shaded TIN images of the piers (figs. 1.3, 1.4).

The difference between the survey on June 13, 2022, and the previous survey on July 18, 2018 (fig. 24), indicates about 86 percent of the joint area of interest had detectable change, which means about 14 percent of the differences in the joint area of interest are equivocal and within the bounds of uncertainty (table 8). Erosion appears dominant throughout most of the reach between 2018 and 2022 in the DoD, except for localized areas of moderate deposition in the troughs of the medium dunes in the channel (fig. 24). The average difference between the bathymetric surfaces was –1.86 ft (table 8), indicating moderate channel degradation between the 2018 and 2022 surveys. The net volume of cut in the reach from 2018 to 2022 was about 205,500 yd^3, and the net volume of fill was about 26,700 yd^3, resulting in a net loss of about 178,800 yd^3 of sediment between 2018 and 2022 (table 8). The frequency distribution of bed elevations in 2022 appears similar in shape to 2018, but with a higher percentage of cells at about 2-ft lower channel-bed elevations (fig. 22). The smooth rock or hardpan clay on the right (southwest) bank showed localized signs of minor erosion and deposition, and the left (northeast) bank appears shifted to eastward, resulting in substantial erosion along that bank upstream and downstream from the bridge (fig. 24). This movement of the left (northeast) bank also is evident in recent aerial imagery, which shows 5 to 15 ft of shift in the top of the bank location between 2012 and 2023 (Google Earth, 2012–23; https://earth.google.com/).

The difference between the survey on June 13, 2022, and the earliest survey on June 5, 2014 (fig. 25), indicates about 71 percent of the joint area of interest had detectable change, which means about 29 percent of the differences in the joint area of interest are equivocal and within the bounds of uncertainty (table 8). Scour and deposition appear roughly balanced throughout the reach between 2014 and 2022 in the DoD, with scour and deposition alternating in the troughs of the small to medium dune features in the middle of the channel (fig. 25). The average difference between the bathymetric surfaces was –0.30 ft (table 8), indicating minor channel degradation between the 2014 and 2022 surveys, and the net loss of sediment between 2014 and 2022 was about 23,500 yd^3 (table 8). The frequency distribution of bed elevations in 2022 is similar to 2014, with a slightly higher percentage of cells at channel-bed elevations above 435 ft (fig. 22). The smooth rock hardpan clay on the right (southwest) bank was mostly equivocal with localized signs of very minor deposition, and as noted with the 2018 comparison and confirmed with recent aerial imagery, the left (northeast) bank appears shifted to eastward,

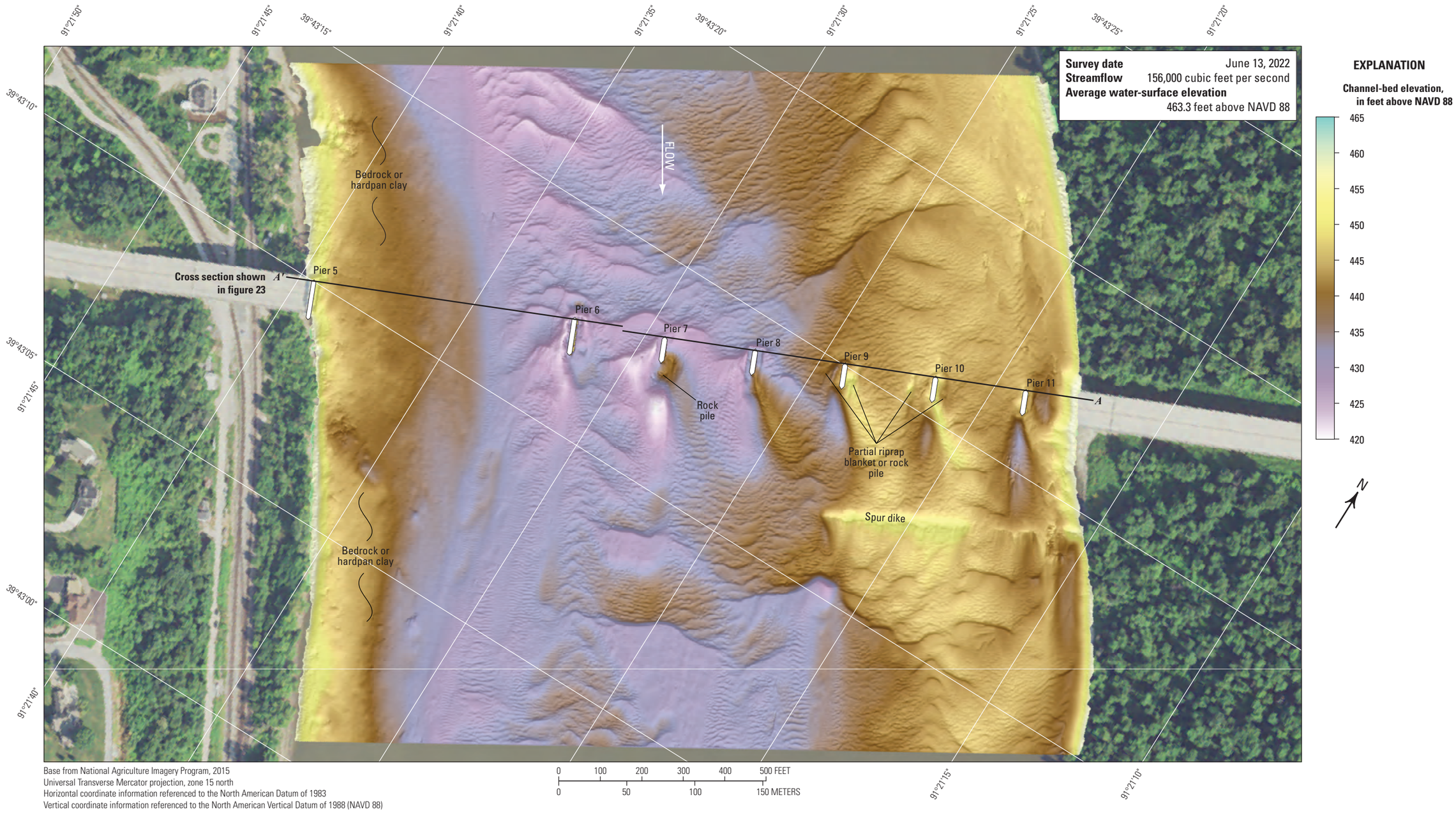

Figure 21. Bathymetric survey of the Mississippi River channel near structure A5054 on Interstate 72 at Hannibal, Missouri.

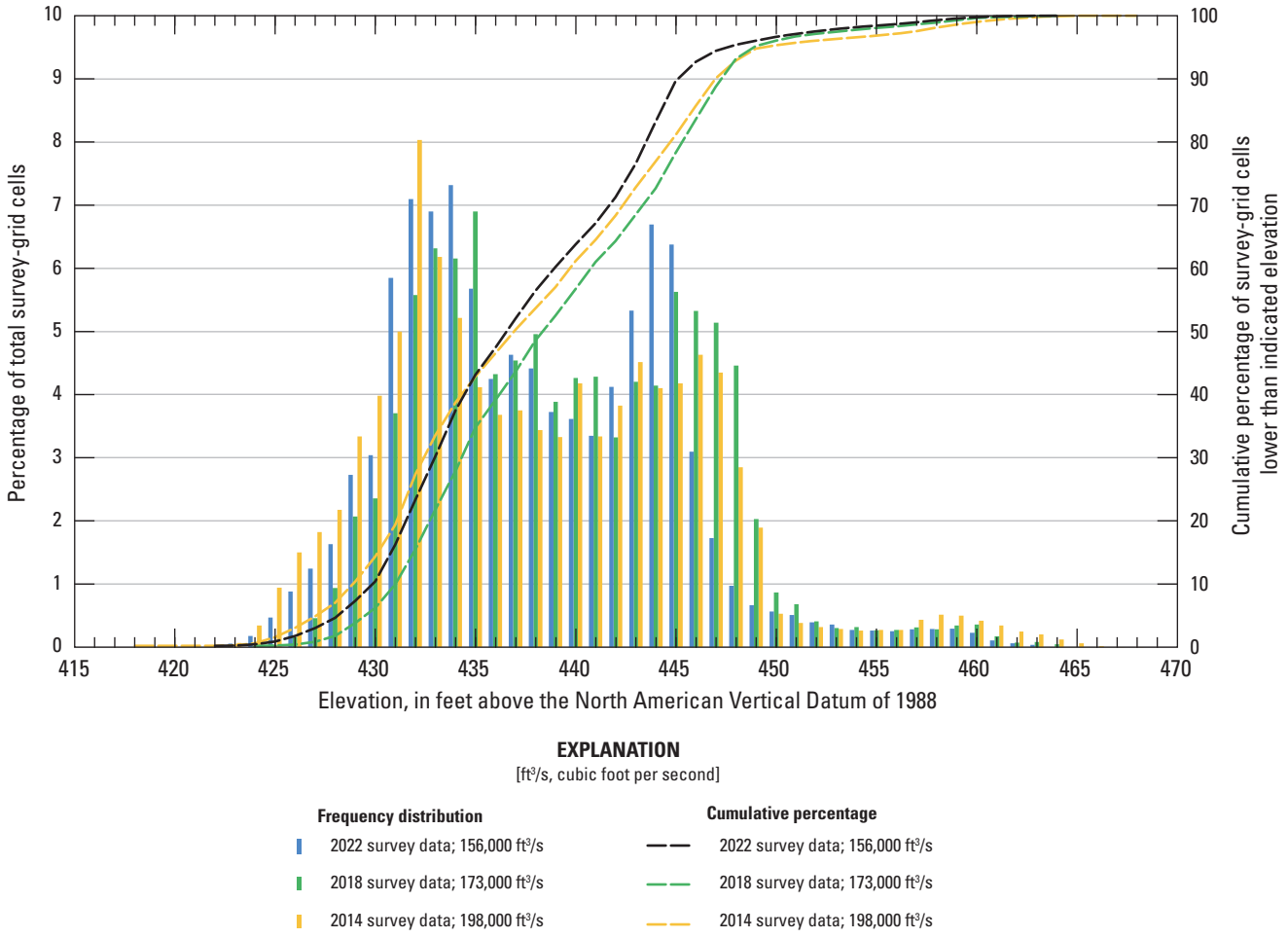

Figure 22. Frequency distribution of bed elevations for bathymetric survey-grid cells in 1-foot elevation bins on the Mississippi River near dual bridge structure A5054 on Interstate 72 at Hannibal, Missouri, on June 13, 2022, compared to previous surveys in 2014 and 2018 (Huizinga, 2015, and 2020e, respectively).

resulting in substantial erosion along that bank upstream and downstream from the bridge (fig. 25). As with previous DoDs, deposition or scour apparent on opposing faces of a feature likely results from minor horizontal positional variances between the surveys (fig. 6).

The vertically averaged velocity vectors indicate mostly uniform flow in the reach, but with localized flow disturbances in direction and magnitude in several of the sections (fig. 26). Velocities ranged from about 2 to 10 ft/s (fig. 26), with lower velocities and turbulence observed downstream from the piers and along the right (southwest) bank (fig. 26). All the piers were skewed to approach flow by 10 to 20 degrees (table 7), causing minor wake vortices and well-defined deposition ridges downstream (fig. 26). Additional flow disturbance may result from upwelling of flow caused by the numerous medium dune features present throughout the channel (Best, 2005; fig. 26).

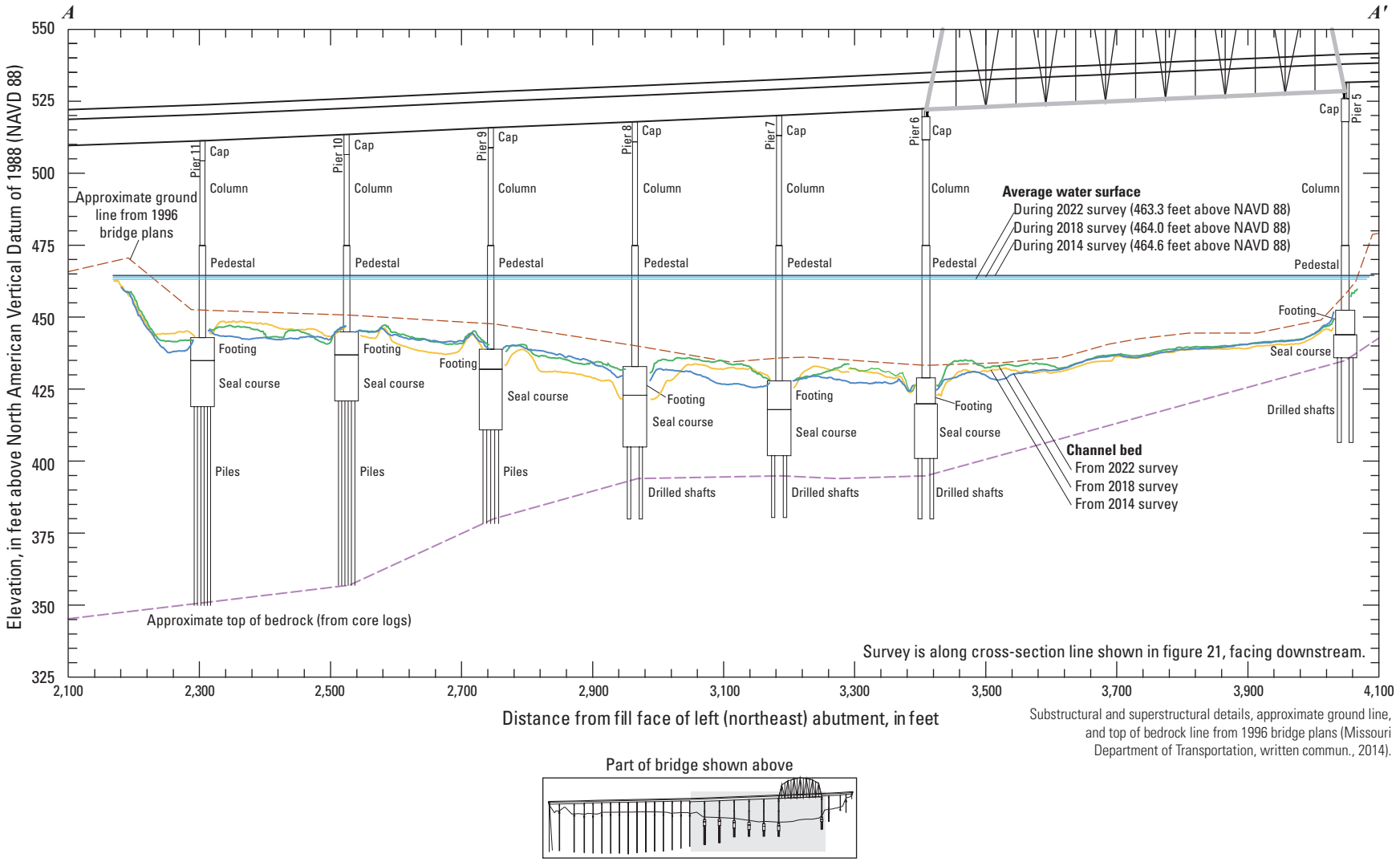

Substructural and superstructural details, approximate ground line, and top of bedrock line from 1996 bridge plans (Missouri Department of Transportation, written commun., 2014).

Figure 23. Key features, substructural and superstructural details, and surveyed channel bed of structure A5054 on Interstate 72 crossing the Mississippi River at Hannibal, Missouri.

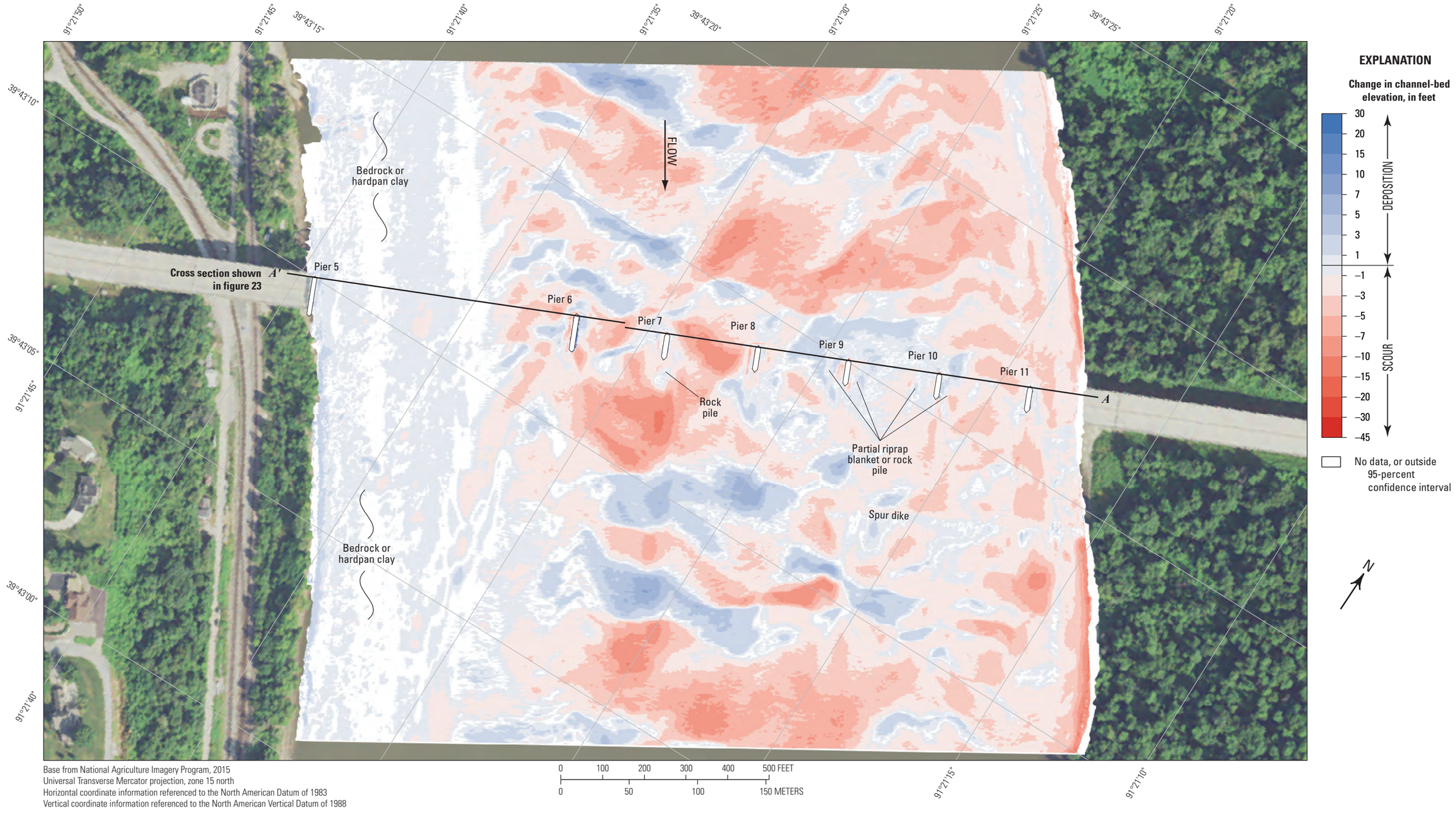

Base from National Agriculture Imagery Program, 2015
Universal Transverse Mercator projection, zone 15 north
Horizontal coordinate information referenced to the North American Datum of 1983
Vertical coordinate information referenced to the North American Vertical Datum of 1988

Figure 24. Difference between surfaces created from bathymetric surveys of the Mississippi River channel near structure A5054 on Interstate 72 at Hannibal, Missouri, on June 13, 2022, and July 18, 2018, with probabilistic thresholding.

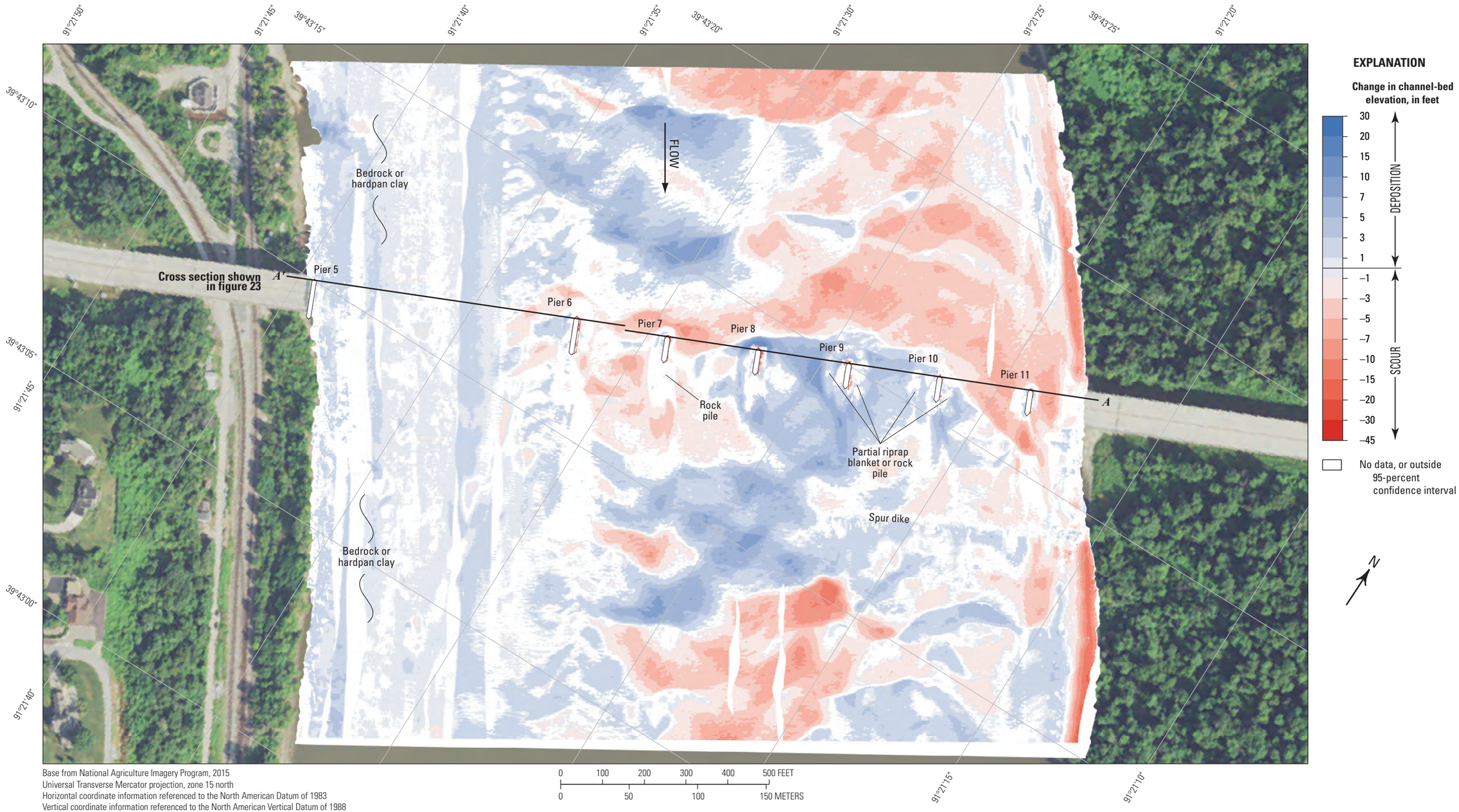

Figure 25. Difference between surfaces created from bathymetric surveys of the Mississippi River channel near structure A5054 on Interstate 72 at Hannibal, Missouri, on June 13, 2022, and June 5, 2014, with probabilistic thresholding.

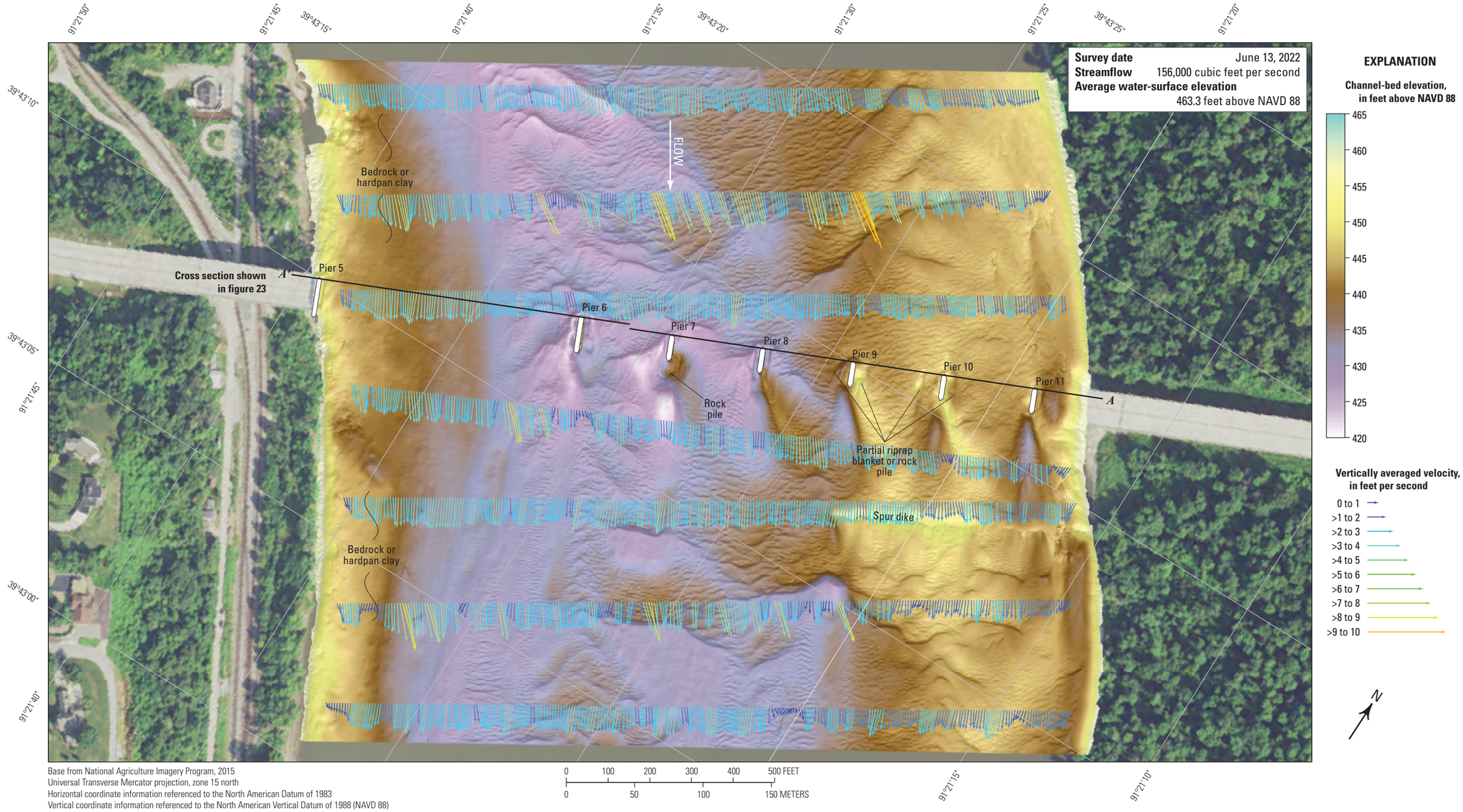

Figure 26. Bathymetry and vertically averaged velocities of the Mississippi River channel near structure A5054 on Interstate 72 at Hannibal, Missouri.

Structure L0135 on State Highway 51 at Chester, Illinois

Structure L0135 (site 36; table 2) on State Highway 51 crosses the Mississippi River at RM 109.9 at Chester, Ill., southeast of and downstream from St. Louis, Mo. (fig. 1). The site was surveyed on June 14, 2022, when the average water-surface elevation of the river in the survey area, determined by the RTK GNSS tide solution, was 363.3 ft (table 3; fig. 27) and streamflow on the Mississippi River was about 339,000 ft^3/s during the survey (table 3).

The survey area was about 1,640 ft and about 1,840 ft wide, extending across the active channel from the left (northeast) bank to the right (southwest) bank in the main channel (fig. 27). The upstream end of the survey area was about 655 ft upstream from the centerline of structure L0135, and piers 10 through 13 were in the water; however, pier 13 was in shallow water on the left bank (fig. 27). The channel-bed elevations ranged from about 316 to 347 ft for most of the surveyed area (5th to 95th percentile range of the bathymetric data; table 3; fig. 28), except near pier 11 and in the thalweg along the left side of the channel (fig. 27; table 3). A well-defined thalweg was present along the left (northeast) bank, about 15 to 20 ft deeper than the channel bed on the right side (fig. 27). A series of medium dunes were present in the channel thalweg and along the right side of the channel throughout the reach, along with numerous small dunes and ripples (fig. 27). As in previous surveys (Huizinga, 2015, 2020e), a bedrock outcrop was present on the left (northeast) bank, and a stone revetement was present on the right (southwest) bank (fig. 27).

Near pier 11, a substantial scour hole had a minimum channel-bed elevation of about 309 ft (table 7), which is about 17 ft below the average channel elevation upstream from the pier (figs. 27, 1.5*D–E*). Information from bridge plans indicates that pier 11 is founded on a caisson on bedrock, having about 43 ft of bed material between the bottom of the scour hole and bedrock (fig. 29; table 7); the top of the caisson is visible in the shaded TIN images (fig. 1.5*D–E*). Near pier 10, a moderate scour hole had a minimum channel-bed elevation of about 329 ft (table 7), which is about 8 ft below the average channel elevation upstream from the pier (figs. 27, 29, 1.5*F–G*). Pier 10 also is founded on a caisson on bedrock, having about 84 ft of bed material between the bottom of the scour hole and bedrock (fig. 29; table 7). Pier 12 is founded on footings on the exposed bedrock on the right bank, with no apparent scour hole nearby (figs. 27, 29, 1.5*B–C*; table 7). Pier 13 also is founded on footings on the exposed bedrock on the right bank and was near the surveyed water surface with no apparent scour hole nearby (figs. 27, 29, 1.5*A*; table 7). In modern construction, bridge substructural elements usually are pinned or socketed to bedrock (Brown and others, 2018; American Association of State Highway Transportation Officials, 2020), but full exposure of usually buried substructural elements warrants special consideration and observation, particularly at an older bridge such as structure L0135 (built in 1940) even when designed to be exposed.

The difference between the survey on June 14, 2022, and the previous survey on July 24, 2018 (fig. 30), indicates about 81 percent of the joint area of interest had detectable change, which means about 19 percent of the differences in the joint area of interest are equivocal and within the bounds of uncertainty (table 8). Scour and deposition appear roughly balanced throughout the reach between 2018 and 2022 in the DoD, with apparent scour and deposition alternating in the troughs of the medium dune features in the thalweg and right side of the channel (fig. 30). The average difference between the bathymetric surfaces was –0.52 ft (table 8), indicating minor degradation of the reach between the 2018 and 2022 surveys. The net volume of cut in the reach from 2018 to 2022 was about 92,600 yd^3, and the net volume of fill was about 46,100 yd^3, resulting in a net loss of about 46,500 yd^3 of sediment between 2018 and 2022 (table 8). The scour holes near piers 10 and 11 are shallower and slightly narrower in 2022 than in 2018 (figs. 29 and 30). The frequency distribution of bed elevations in 2022 appears very similar to 2018, with a slightly higher percentage of cells at the highest elevations than 2018 (fig. 28). The bedrock outcrop along the left (northeast) bank showed localized signs of minor scour, but most of the rock outcrop indicated changes within 1–3 ft of the 2018 elevation, or changes outside the 95-percent confidence interval (fig. 30). As with previous DoDs, deposition or scour apparent on opposing faces of a feature likely results from minor horizontal positional variances between the surveys (fig. 6).

The difference between the survey on June 14, 2022, and the earliest survey on June 9, 2014 (fig. 31), indicates about 70 percent of the joint area of interest had detectable change, which means about 30 percent of the differences in the joint area of interest are equivocal and within the bounds of uncertainty (table 8). Deposition appears dominant throughout most of the reach between 2014 and 2022 in the DoD, with scour and deposition alternating in the troughs of the medium dune features in the thalweg and middle of the channel (fig. 31). The average difference between the bathymetric surfaces was +0.35 ft (table 8), indicating minor channel aggradation between the 2014 and 2022 surveys, and the net gain of sediment between 2014 and 2022 was about 27,300 yd^3 (table 8). The scour holes near piers 10 and 11 are nearly identical in 2014 and 2022 (figs. 29 and 31). As with 2018, the frequency distribution of bed elevations in 2022 is very similar to 2014, with a slightly lower percentage of cells at elevations above 330 ft than in 2014 (fig. 28). Changes to the stone revetment along the right (southwest) bank is mostly equivocal, with localized signs of deposition downstream from the bridge (fig. 31). The bedrock outcrop on the left (northeast) bank showed localized signs of minor to moderate deposition (fig. 31); however, the differences near the rock outcrop would be most affected by minor horizontal positional variances between the surveys. As with previous DoDs, deposition or scour apparent on opposing faces of a feature likely results from minor horizontal positional variances between the surveys (fig. 6).

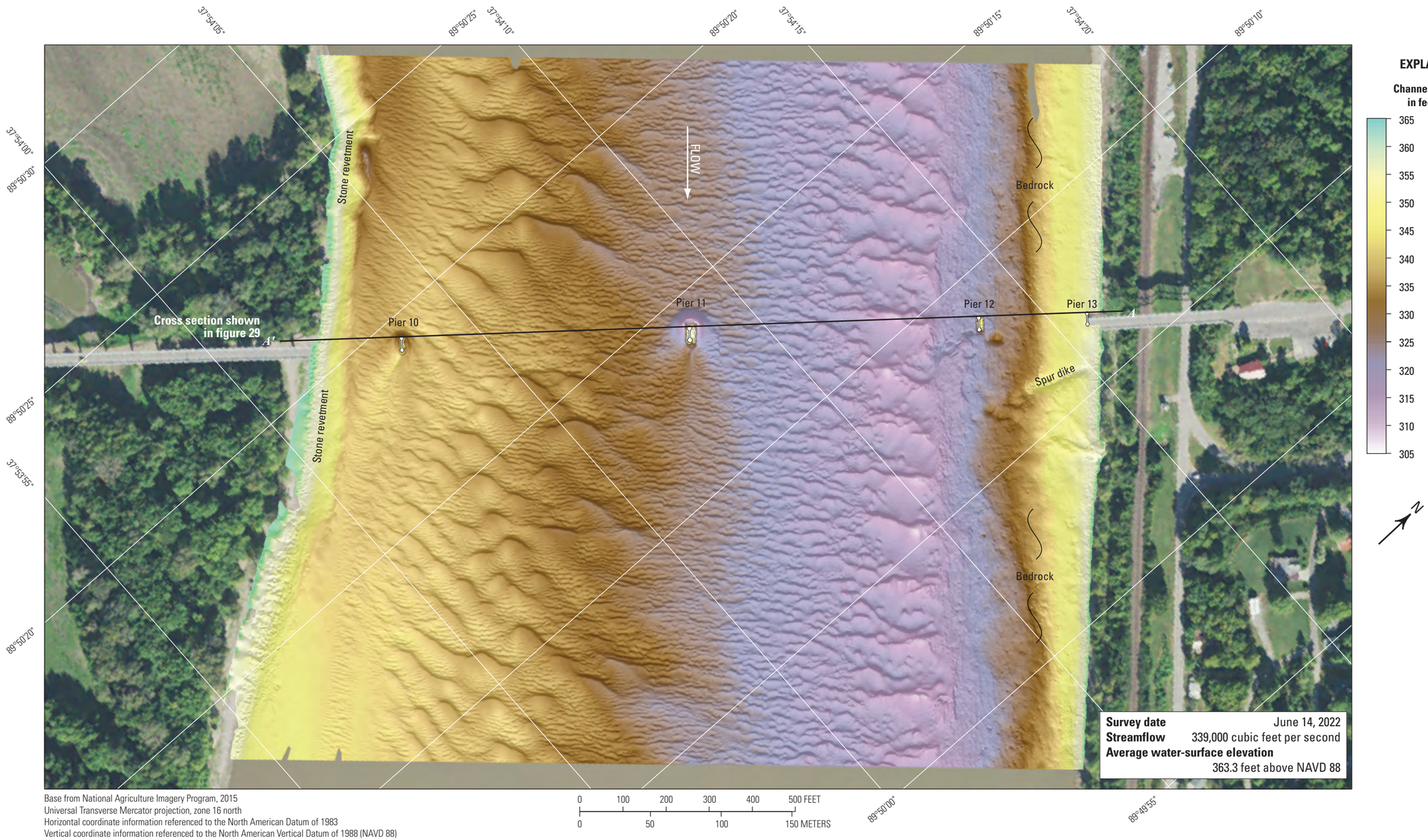

Figure 27. Bathymetric survey of the Mississippi River channel near structure L0135 on State Highway 51 at Chester, Illinois.

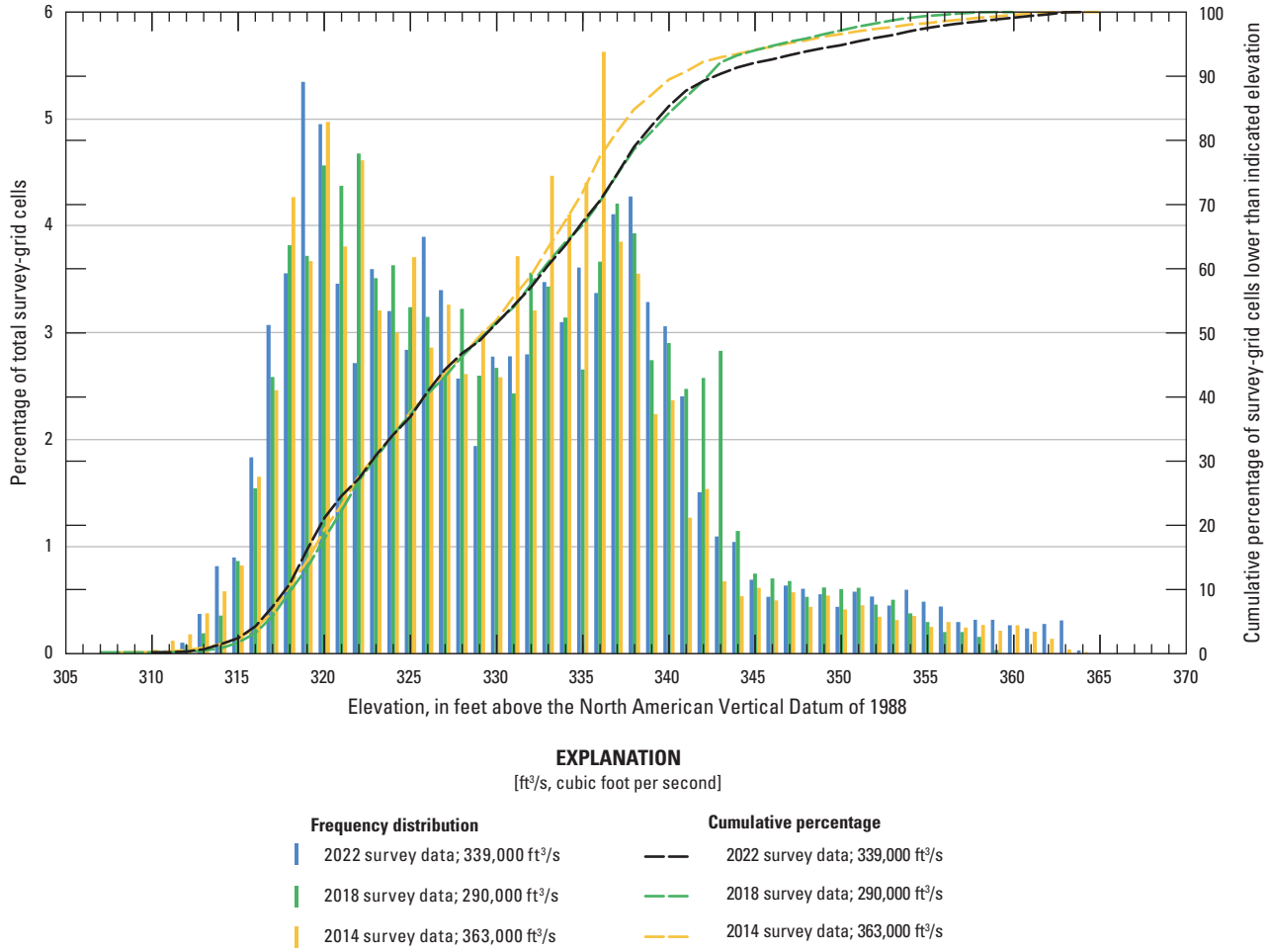

Figure 28. Frequency distribution of bed elevations for bathymetric survey-grid cells in 1-foot elevation bins on the Mississippi River near structure L0135 on State Highway 51 at Chester, Illinois, on June 14, 2022, compared to previous surveys in 2014 and 2018 (Huizinga, 2015, and 2020e, respectively).

The vertically averaged velocity vectors indicate mostly uniform flow in the reach, but with localized flow disturbances in direction and magnitude in several of the sections (fig. 32). Velocities ranged from about 3 to 10 ft/s (fig. 32), with lower velocities and turbulence observed along the right (southwest) bank (fig. 32). Piers 11 and 12 were aligned with flow, as indicated by little to no turbulence observed downstream that can be directly attributed to these piers (fig. 32). Pier 10 had a flow angle of attack of about 5 degrees (table 7), evidenced with turbulence and ridge of sediment deposition downstream (fig. 32). Additional flow disturbance may result from upwelling of flow caused by the numerous medium dune features present throughout the channel (Best, 2005; fig. 32).

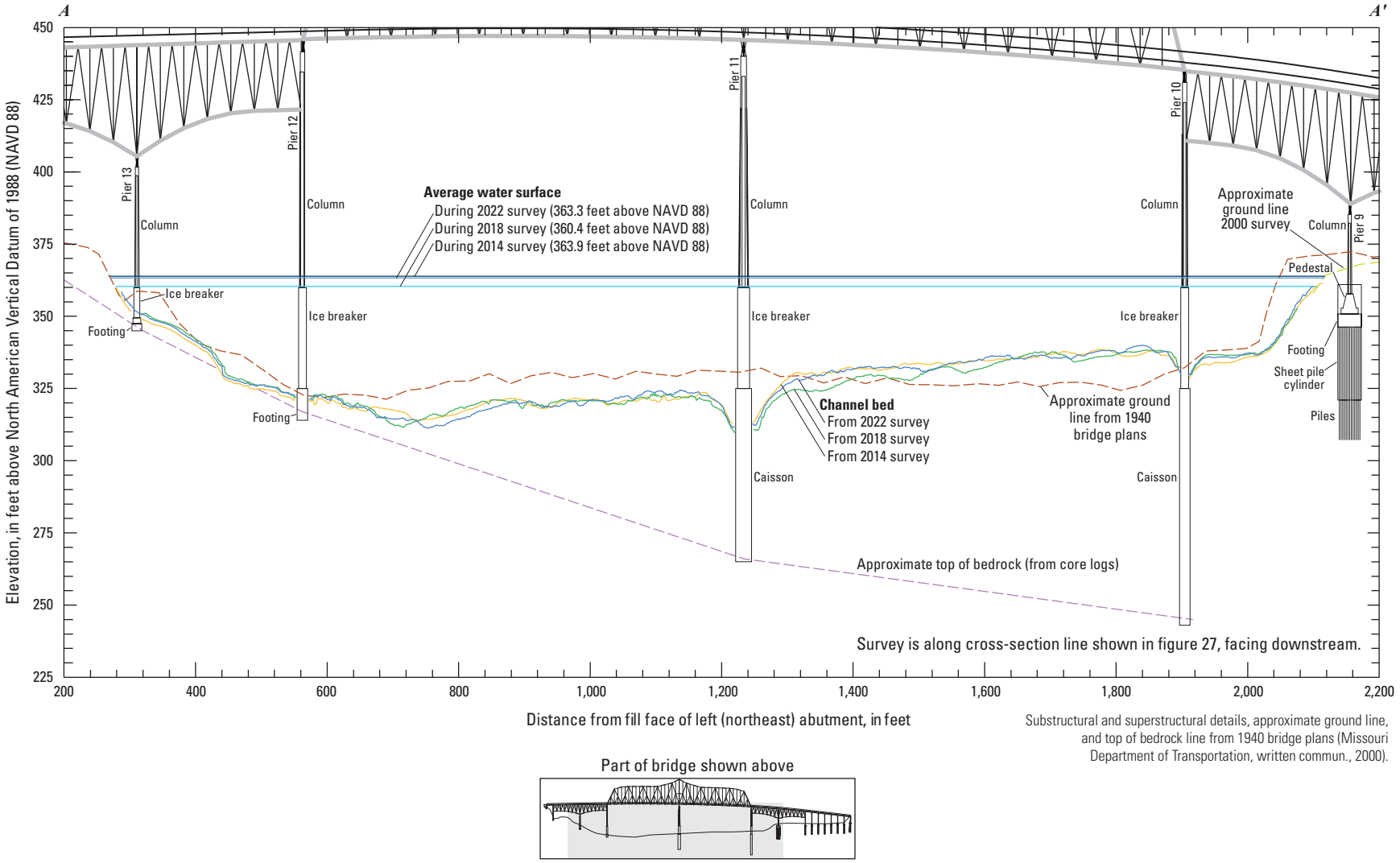

Figure 29. Key features, substructural and superstructural details, and surveyed channel bed of structure L0135 on State Highway 51 crossing the Mississippi River at Chester, Illinois.

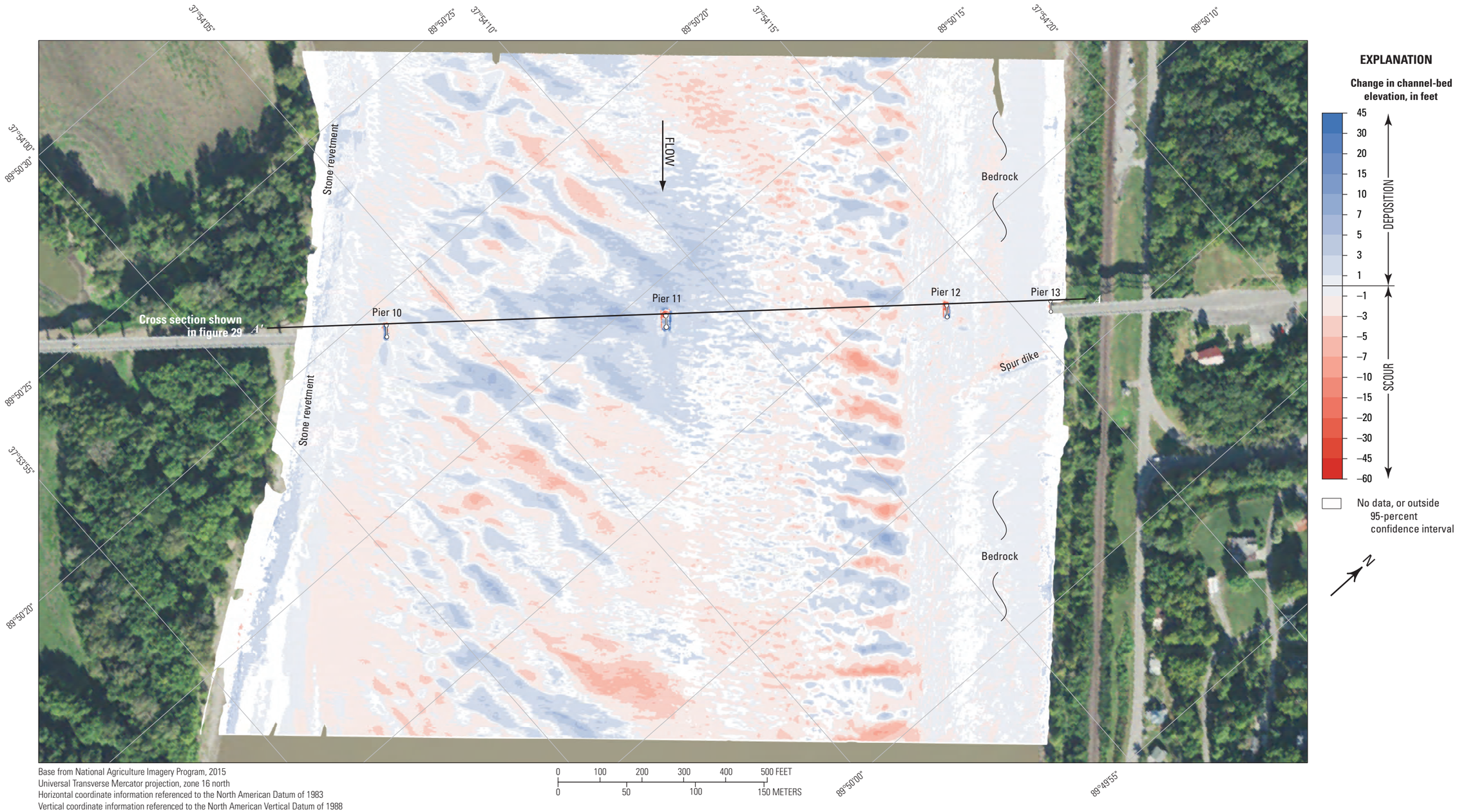

Figure 30. Difference between surfaces created from bathymetric surveys of the Mississippi River channel near structure L0135 on State Highway 51 at Chester, Illinois, on June 14, 2022, and July 24, 2018, with probabilistic thresholding.

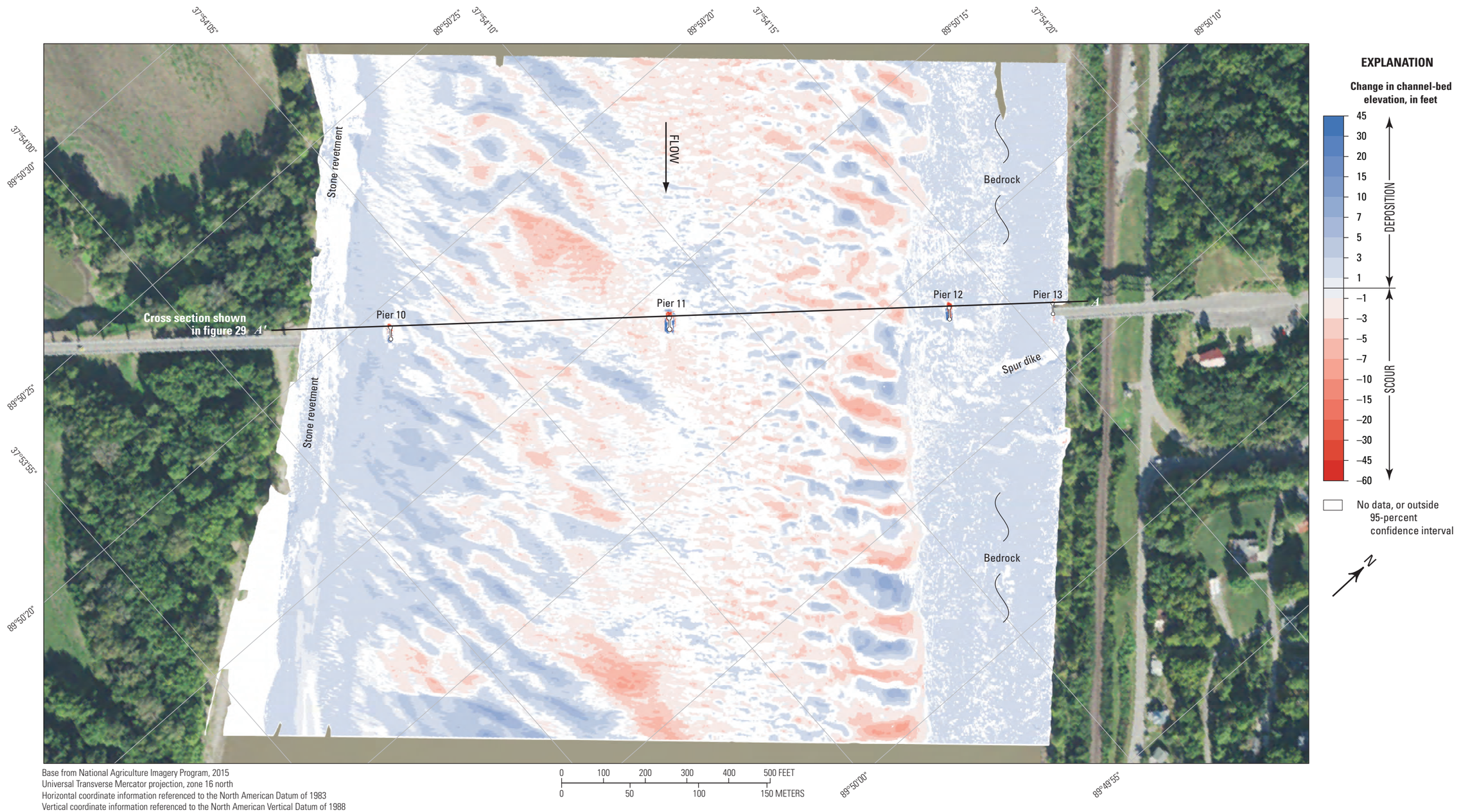

Figure 31. Difference between surfaces created from bathymetric surveys of the Mississippi River channel near structure L0135 on State Highway 51 at Chester, Illinois, on June 14, 2022, and June 9, 2014, with probabilistic thresholding.

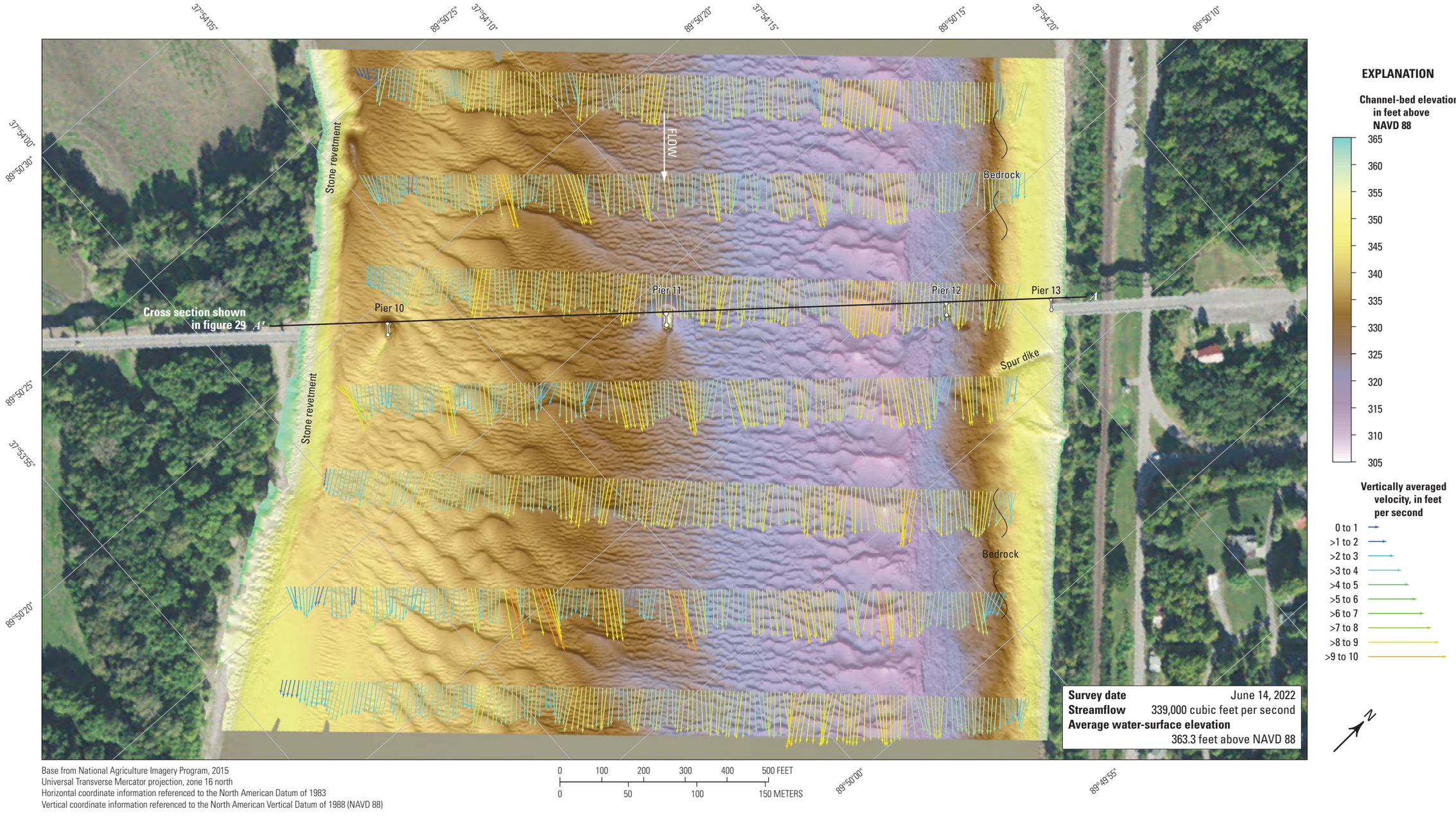

Base from National Agriculture Imagery Program, 2015
Universal Transverse Mercator projection, zone 16 north
Horizontal coordinate information referenced to the North American Datum of 1983
Vertical coordinate information referenced to the North American Vertical Datum of 1988 (NAVD 88)

Figure 32. Bathymetry and vertically averaged velocities of the Mississippi River channel near structure L0135 on State Highway 51 at Chester, Illinois.

Structure A5076 on State Highway 34 at Cape Girardeau, Missouri

Structure A5076 (site 37; table 2) on State Highway 34 crosses the Mississippi River at RM 51.5 at Cape Girardeau, Mo., southeast of and downstream from Chester, Ill., and St. Louis, Mo (fig. 1). The site was surveyed on June 14, 2022, when the average water-surface elevation near the bridge, determined by the RTK GNSS tide solution, was 331.1 ft (table 3; fig. 33) and streamflow on the Mississippi River was about 335,000 ft^3/s during the survey (table 3).

The survey area was about 1,640 ft long and about 1,970 ft wide (perpendicular to flow), extending across the active channel from the left (east) bank to the right (west) bank in the main channel (fig. 33). The upstream end of the survey area was about 730 ft upstream from the centerline of structure A5076 at pier 3, and piers 3 through 6 were in the water. Piers 2 and 7 were in very shallow water on the right and left banks, respectively, and were not surveyed. The channel-bed elevations ranged from about 276 to 318 ft for most of the surveyed area (5th to 95th percentile range of the bathymetric data; table 3; fig. 34), except in the well-defined channel thalweg along the right bank, and downstream from piers 3 and 4 (fig. 33; table 3). Numerous small to medium dunes and ripples were present throughout the channel. The area near the left bank upstream from the bridge was about 20 to 25 ft shallower than in the thalweg on the right side of the channel (fig. 33). As in previous surveys (Huizinga, 2015, 2020e), stone revetment was present on the right (west) bank (fig. 33).

As in previous surveys, piers 3 and 4 seemed to be partially surrounded by piles of riprap or rock (figs. 33, 1.6*E–H*). Scour downstream from the piers in 2022 reached a minimum elevation of 264 ft near pier 3 (table 7; fig. 33) and 270 near pier 4 (fig. 33). A poorly defined, minor scour hole difficult to discern from nearby ripples existed near pier 5 (figs. 33, 1.6*D*), having a minimum channel-bed elevation of about 300 ft (table 7). A minor scour hole also existed near pier 6 (figs. 33, 1.6*A–B)*. The top of the footing was visible at pier 5, and the top of the distribution cap was visible at piers 3 and 4 (figs. 33, 1.6*C–H*). The minimum channel-bed elevation near pier 5 is about 15 ft above the elevation of the bottom of the pier seal course of 285.00 ft, and the minimum channel-bed elevation near pier 6 is about 20 ft above the elevation of the bottom of the pier seal course of 292.00 ft (fig. 35; table 7). Information from bridge plans indicates that piers 3 and 4 are founded on caissons on bedrock, having about 14 ft of bed material between the bottom of the scour hole and bedrock at pier 3, and 38 ft of material at pier 4 (fig. 35; table 7). Piers 5 through 7 are founded on shafts drilled as much as 22 ft into bedrock, having about 56 ft of bed material between the bottom of the scour hole and bedrock at pier 5, and about 67 ft of material at pier 6 (fig. 35; table 7). The exposed tops of the footing and distribution caps at piers 3 through 5 (figs. 33 and 35) might provide some mitigation to the scour holes at these piers as the downward flow of the horseshoe vortex at the pier column face is blunted by the footing (Arneson and others, 2012).

The difference between the survey on June 14, 2022, and the previous survey on July 25, 2018 (fig. 36), indicates about 83 percent of the joint area of interest had detectable change, which means about 17 percent of the differences in the joint area of interest are equivocal and within the bounds of uncertainty (table 8). Erosion appears predominant throughout the reach between 2018 and 2022 in the DoD, except near the left (east) bank where deposition is more dominant (fig. 36). The average difference between the bathymetric surfaces was –1.79 ft (table 8), indicating moderate to substantial channel degradation between the 2018 and 2022 surveys. The net volume of cut in the reach from 2018 to 2022 was about 215,200 yd^3, and the net volume of fill was about 42,300 yd^3, resulting in a net loss of about 172,900 yd^3 of sediment between 2018 and 2022 (table 8). The cross section from the 2022 survey along the upstream face of the bridge generally varies above and below the 2018 survey section (fig. 35). The frequency distribution of bed elevations in 2022 has a slightly wider elevation range than either the surveys in 2018 or 2014 (fig. 34). The stone revetment on the right (west) bank showed localized areas of deposition, but nearly all the indicated changes are within 1 ft of the 2018 elevation, or outside the 95-percent confidence interval (fig. 36). Areas of localized erosion of the stone revetment tend to be near the upper edges of the banks and may be the result of larger uncertainty in the outer beams in the 2022 survey, particularly near the water surface (refer to fig. 5 in "Uncertainty Estimation" section). The scour hole downstream from the spur dike on the left (east) bank has widened to the east since 2018, resulting in substantial erosion there (fig. 36).

The difference between the survey on June 14, 2022, and the earliest survey on June 10, 2014 (fig. 37), indicates about 71 percent of the joint area of interest had detectable change, which means about 29 percent of the differences in the joint area of interest are equivocal and within the bounds of uncertainty (table 8). Erosion again appears predominant throughout the reach between 2014 and 2022 in the DoD, except near the left (east) bank throughout the reach, and localized areas on the right (west) bank downstream from the bridge where deposition is more dominant (fig. 37). The average difference between the bathymetric surfaces was –1.71 ft (table 8), similar to 2018 and again indicating moderate to substantial channel degradation between the 2014 and 2022 surveys. The net loss of sediment between 2014 and 2022 was about 142,900 yd^3, which is less than but consistent with the net loss of sediment between 2018 and 2022 (table 8). As mentioned in the previous paragraph, the frequency distribution of bed elevations in 2022 has a slightly wider elevation range than either the survey in 2018 or 2014 (fig. 34). The stone revetment on the right (west) bank again showed localized areas of deposition (fig. 37); however, nearly all the indicated changes are within 1 ft of the 2014 elevation or are equivocal with uncertainty, and the apparent deposition likely results from

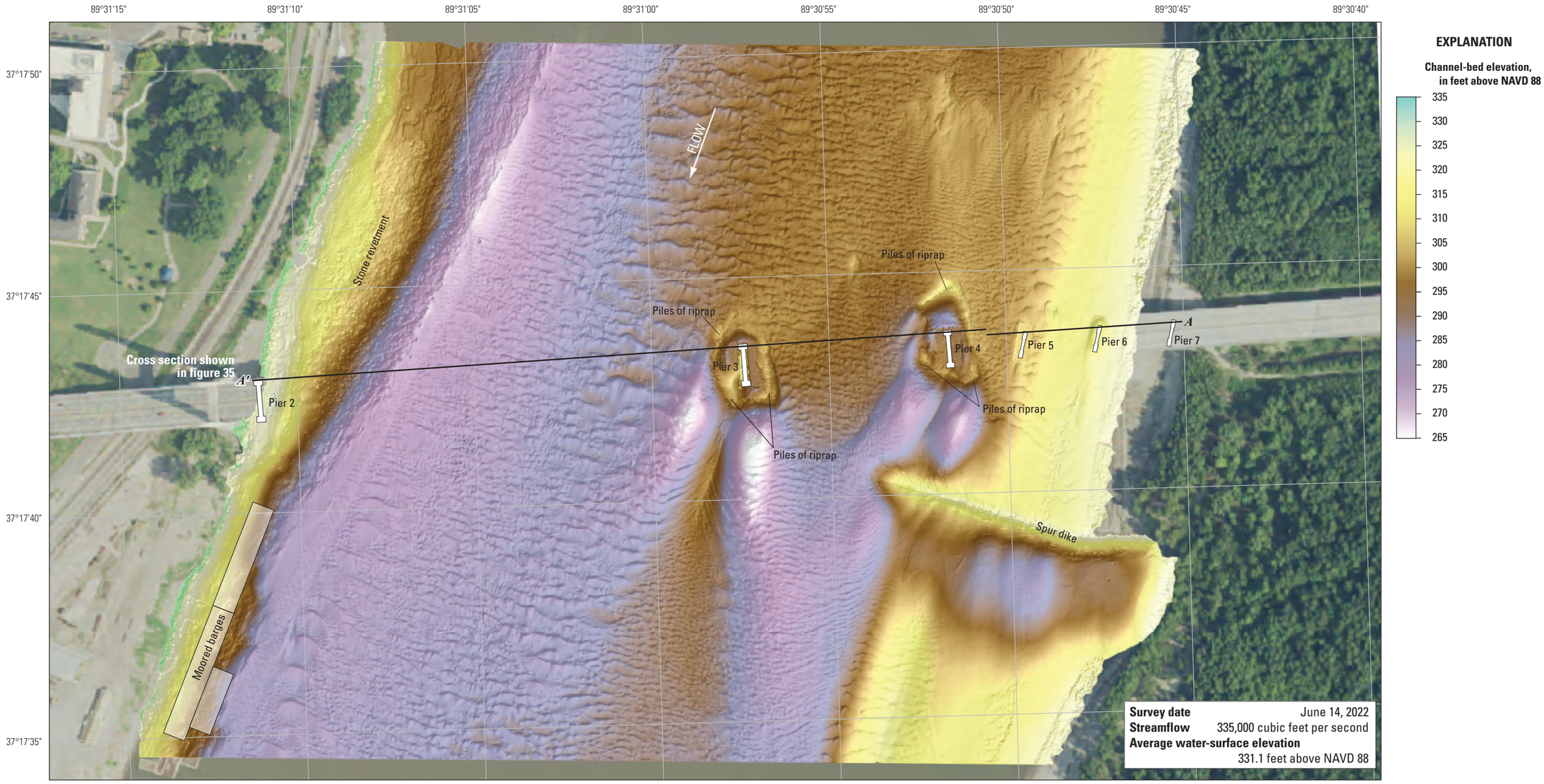

Base from National Agriculture Imagery Program, 2015
Universal Transverse Mercator projection, zone 16 north
Horizontal coordinate information referenced to the North American Datum of 1983
Vertical coordinate information referenced to the North American Vertical Datum of 1988 (NAVD 88)

Figure 33. Bathymetric survey of the Mississippi River channel near structure A5076 on State Highway 34 at Cape Girardeau, Missouri.

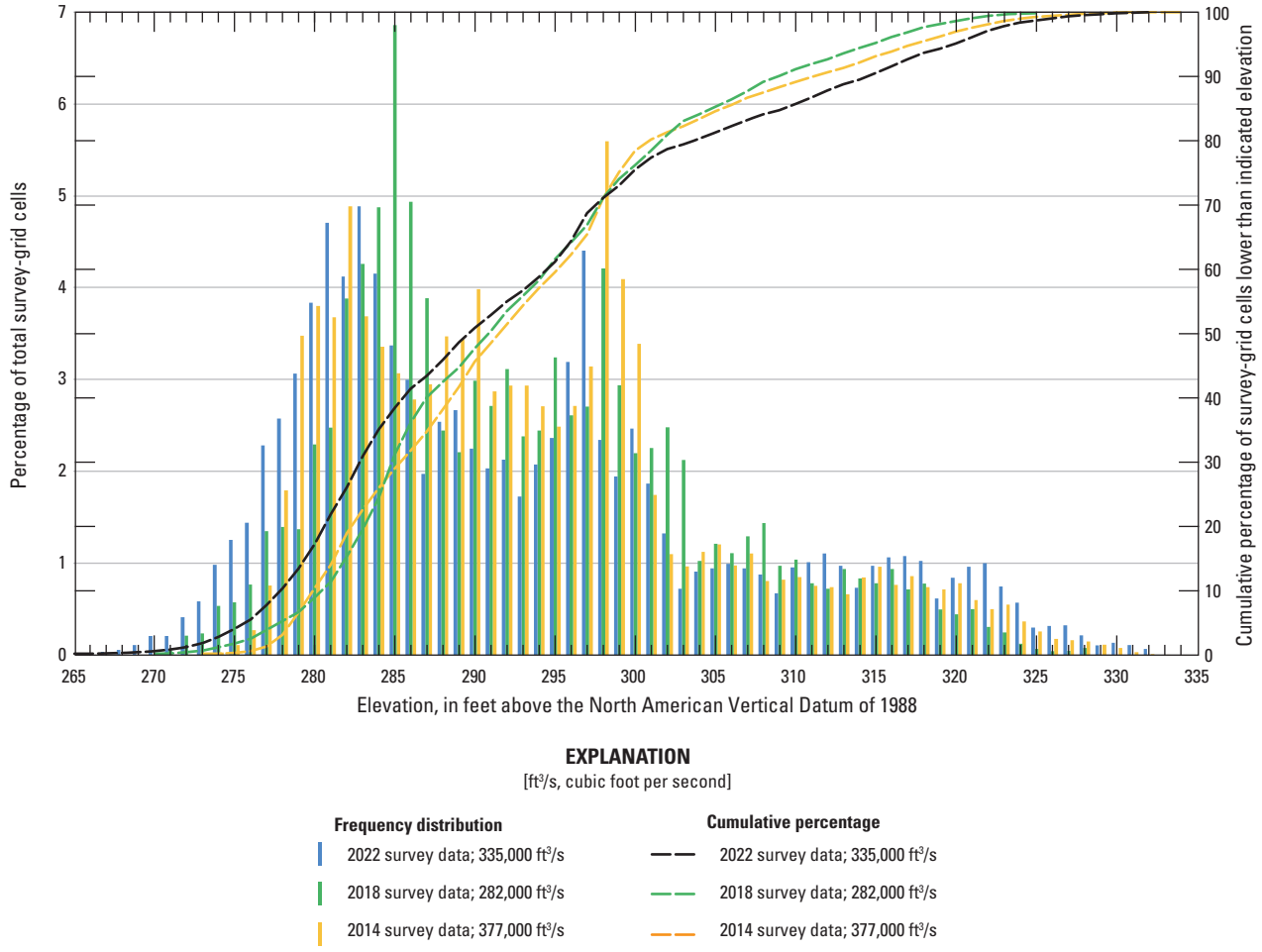

Figure 34. Frequency distribution of bed elevations for bathymetric survey-grid cells in 1-foot elevation bins on the Mississippi River near structure A5076 on State Highway 34 at Cape Girardeau, Missouri, on June 14, 2022, compared to previous surveys in 2014 and 2018 (Huizinga, 2015, 2020e, respectively).

minor horizontal positional variances between the surveys (fig. 6). The scour hole downstream from the spur dike on the left (east) bank had widened eastward between 2014 and 2022 (likely since 2018, refer to preceding paragraph), resulting in substantial erosion (fig. 37). Deposition of as much as 15 ft also was observed downstream from the tip of the spur dike (fig. 37). As with previous DoDs, deposition or scour apparent on opposing faces of a feature likely results from minor horizontal positional variances between the surveys (fig. 6).

The vertically averaged velocity vectors indicate mostly uniform flow throughout most of the reach, with localized moderate to substantial turbulence and flow reversals near the piers and the spur dike on the downstream left (east) bank (fig. 38). Velocities generally ranging from about 3 to 9 ft/s, except in these turbulent areas where velocities of as much as 12 ft/s were observed (fig. 38). Piers 3 and 4 were skewed to approach flow by about 30 degrees (table 7), causing substantial wake vortices with flow reversal and well-defined deposition ridges downstream (fig. 38).

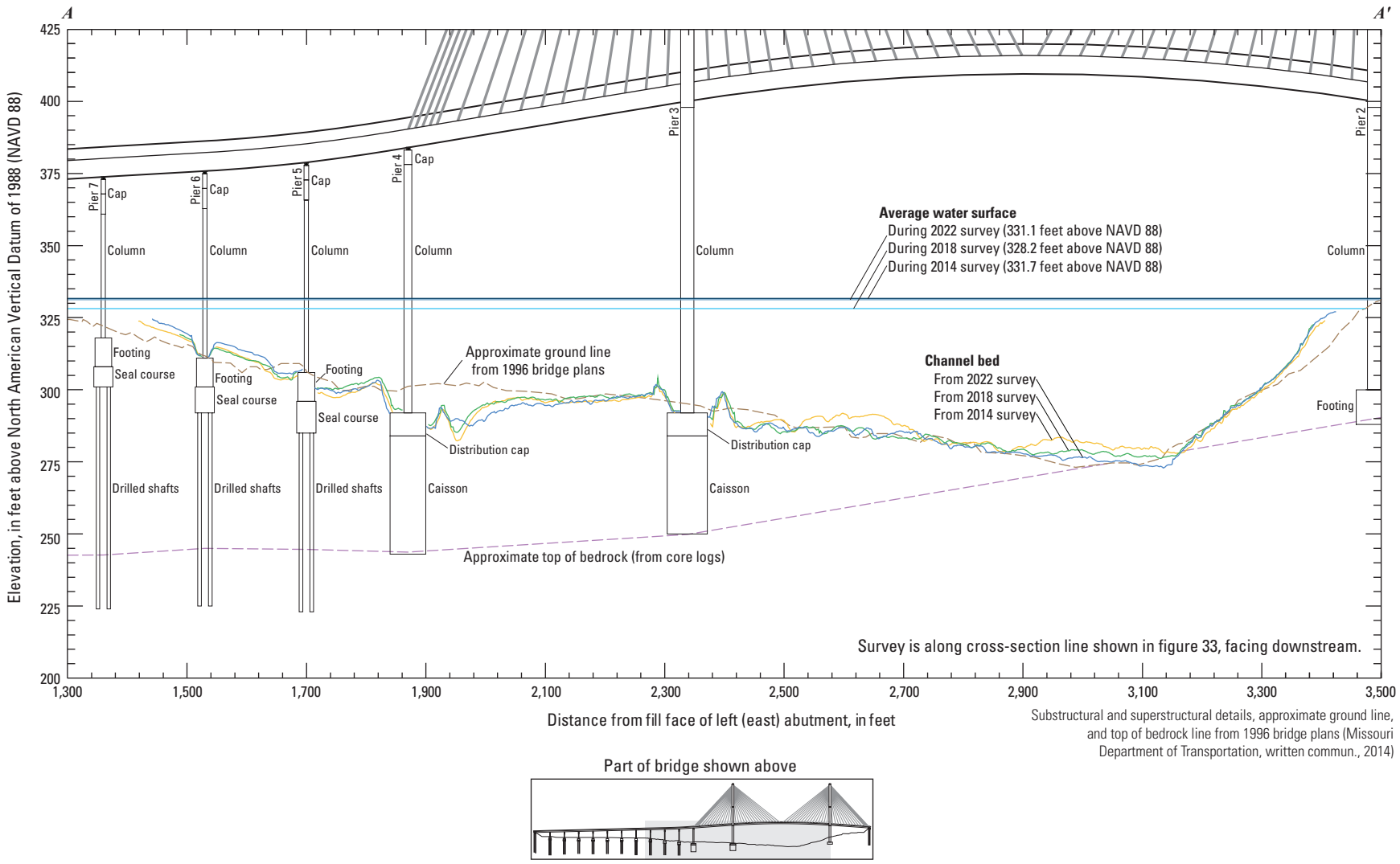

Substructural and superstructural details, approximate ground line, and top of bedrock line from 1996 bridge plans (Missouri Department of Transportation, written commun., 2014)

Figure 35. Key features, substructural and superstructural details, and surveyed channel bed of structure A5076 on State Highway 34 crossing the Mississippi River at Cape Girardeau, Missouri.

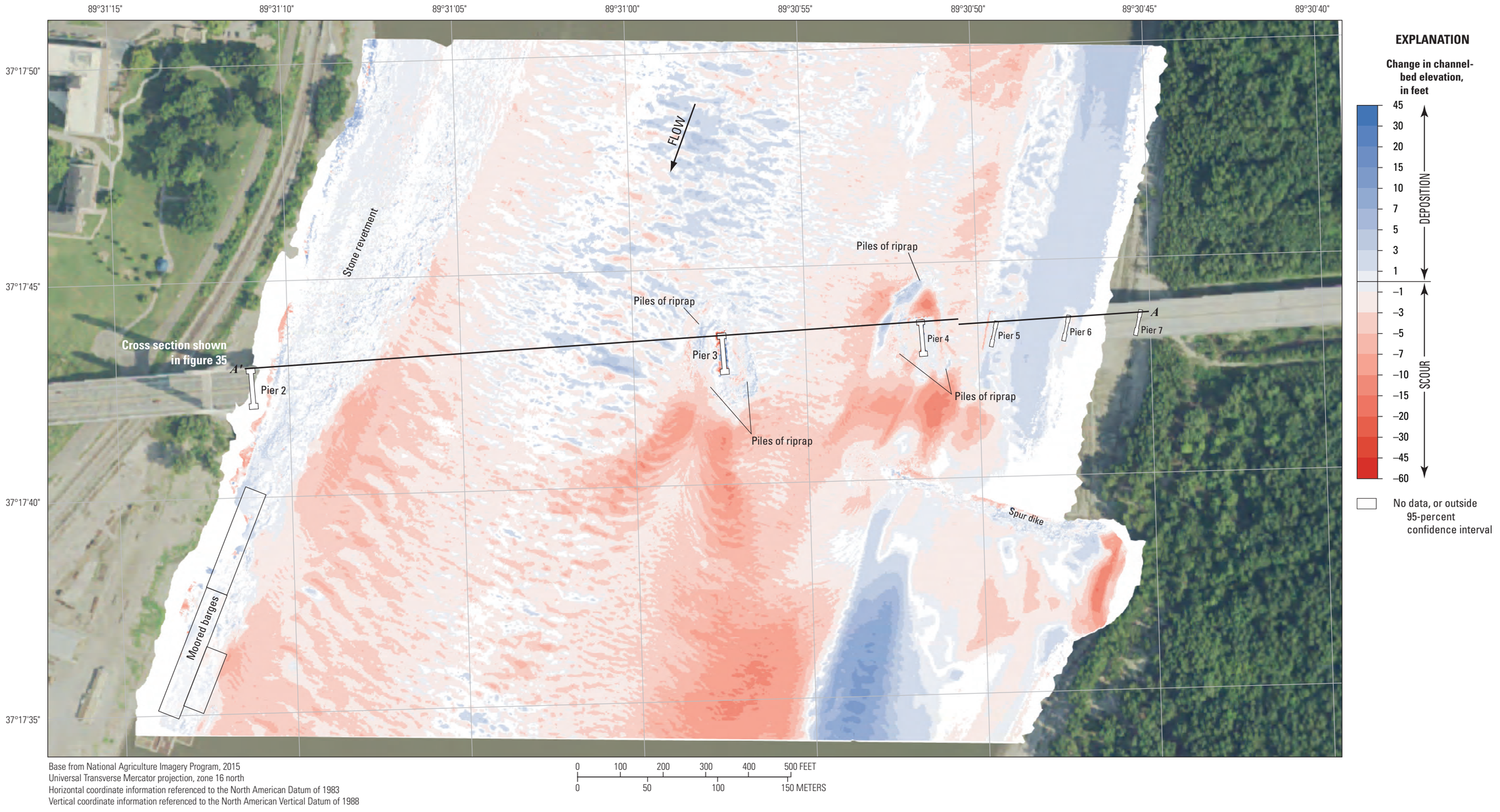

Figure 36. Difference between surfaces created from bathymetric surveys of the Mississippi River channel near structure A5076 on State Highway 34 at Cape Girardeau, Missouri, on June 14, 2022, and July 25, 2018, with probabilistic thresholding.

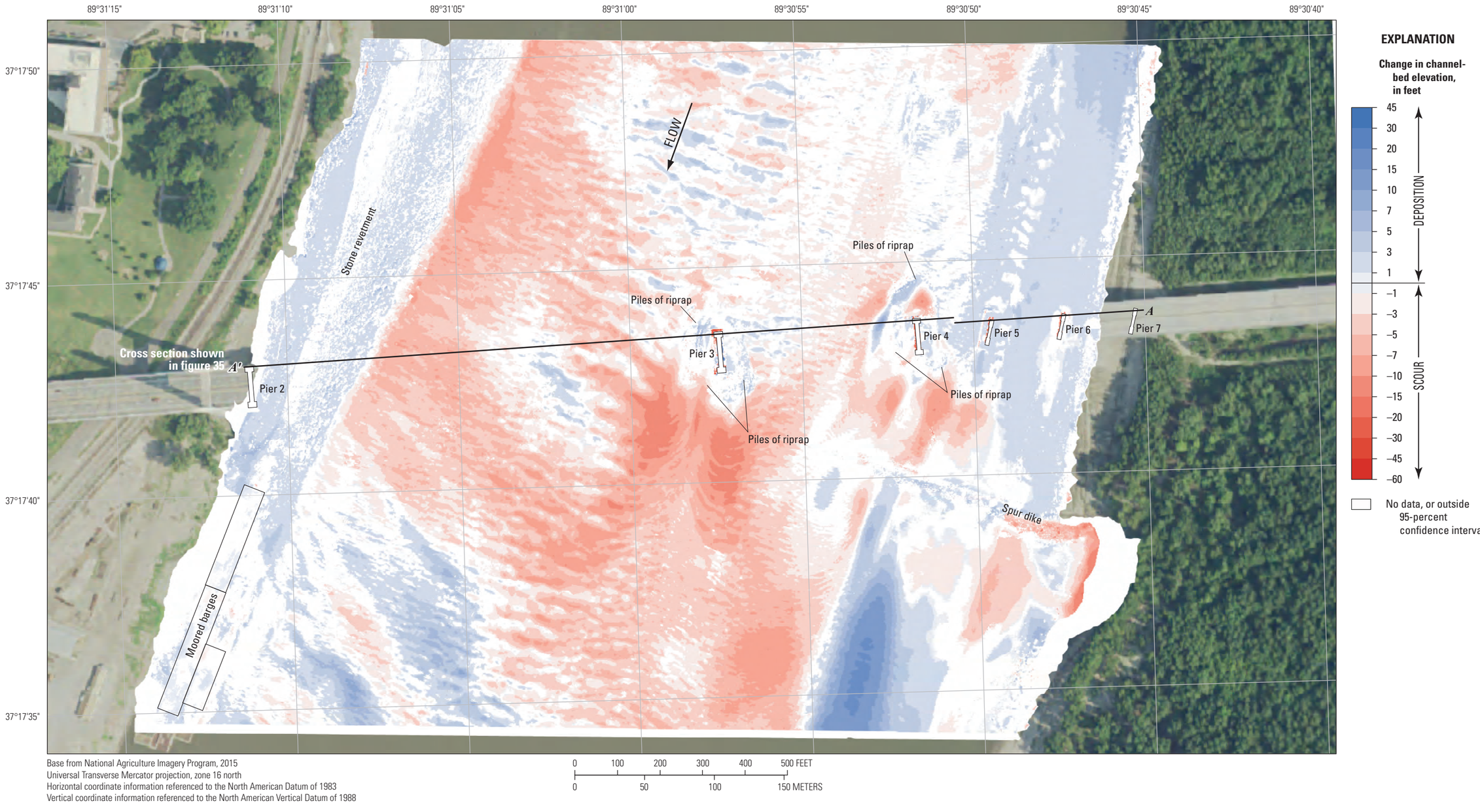

Figure 37. Difference between surfaces created from bathymetric surveys of the Mississippi River channel near structure A5076 on State Highway 34 at Cape Girardeau, Missouri, on June 14, 2022, and June 10, 2014, with probabilistic thresholding.

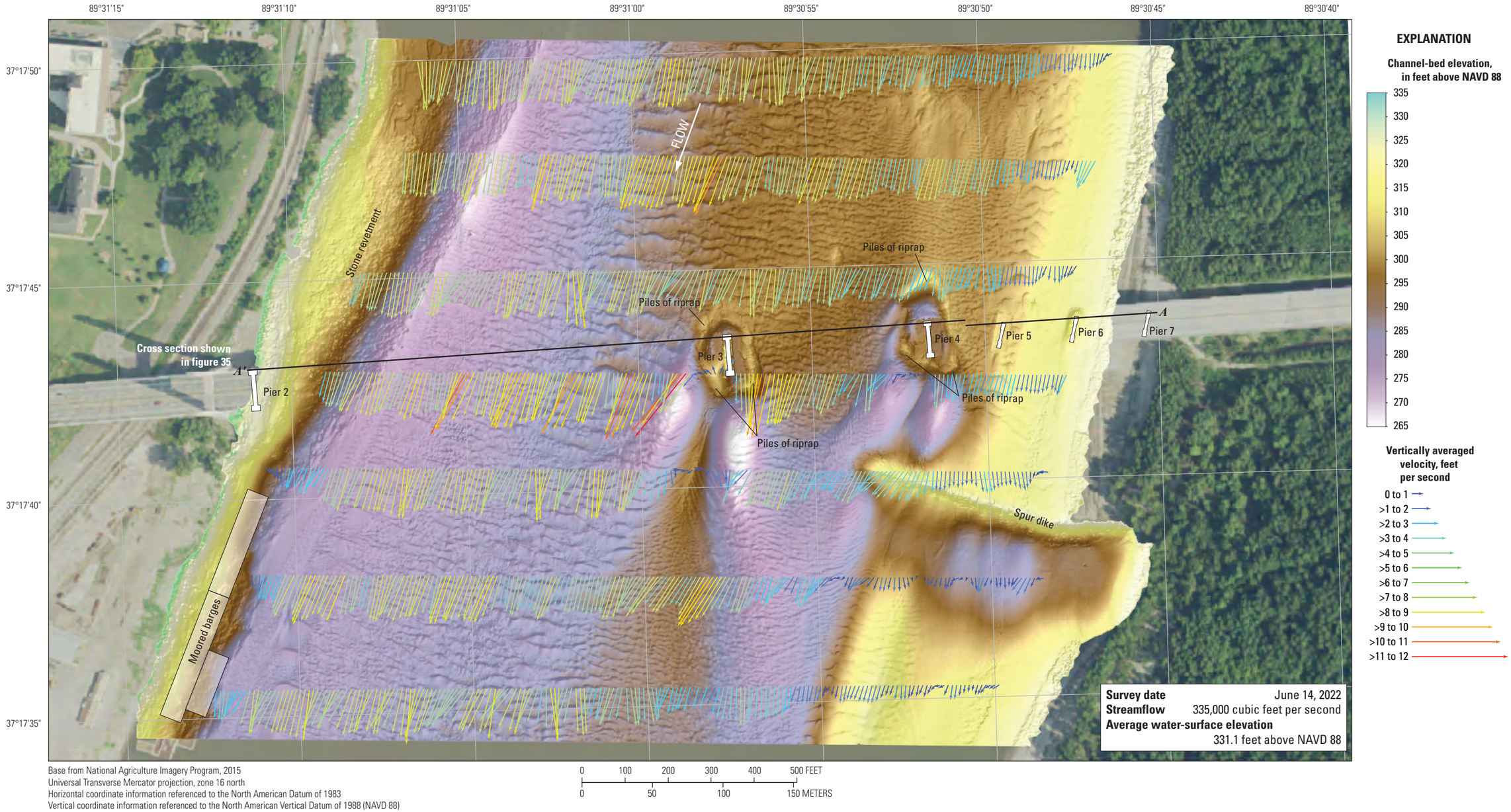

Figure 38. Bathymetry and vertically averaged velocities of the Mississippi River channel near structure A5076 on State Highway 34 at Cape Girardeau, Missouri.

Structure A1700 on Interstate 155 near Caruthersville, Missouri

Structure A1700 (site 38; table 2) on Interstate 155 crosses the lower Mississippi River at RM 838.9 (of the lower Mississippi River) near Caruthersville, Mo., in the southeastern corner of Missouri (fig. 1). The site was surveyed on June 15, 2022, when the average water-surface elevation of the river in the survey area, determined by the RTK GNSS tide solution, was 250.3 ft (table 3; fig. 39), and streamflow on the Mississippi River was about 468,000 ft^3/s during the survey (table 3).

The survey area was about 1,640 ft long and about 2,710 ft wide, extending across the active channel from the left (southeast) bank to the right (northwest) bank in the main channel (fig. 39). The upstream end of the survey area was about 675 ft upstream from the centerline of structure A1700 (fig. 39), and piers 15 through 20 were in the water. Pier 21 was in shallow water on the left bank and was not surveyed. The channel-bed elevations ranged from about 176 to 224 ft for most of the surveyed area (5th to 95th percentile range of the bathymetric data; fig. 40; table 3). A deep thalweg was present along the left (southeast) bank with one very large dune feature, and medium to large dunes with numerous small dunes and ripples were detected throughout the channel (fig. 39). As in previous surveys (Huizinga, 2015, 2020e), a stone revetment was present on both banks near the bridge (fig. 39).

The riprap blankets near piers 18 through 20 seen in previous surveys were again evident in the 2022 survey (fig. 39). Furthermore, new riprap blankets appeared to have been placed around piers 15 through 17 since 2018 (figs. 39, 1.7*F*, 1.8), enhancing stone revetment already near pier 15 and replacing the random piles of riprap observed near pier 16 in previous surveys (refer to figs. 33, 1.8 in Huizinga [2020e]). The scour holes historically observed near the various channel piers were not present in the 2022 survey (table 7). The minimum channel-bed elevation observed at piers 19 and 20 was 6 to 8 ft below the average channel-bed elevation upstream from the pier (table 7), but the cross section along the upstream bridge face indicated there had not been much change near these piers since 2011 (fig. 41). However, the riprap blankets added since 2018 near piers 15 through 17 were evident in the 2022 cross section; furthermore, it appears the original riprap blanket near pier 18 was thickened since 2018, particularly on the left side (figs. 41, 1.7*F*). Information from bridge plans indicates piers 15 to 18 are founded on piles, and piers 19 to 21 are founded on caissons, all with an unknown depth to bedrock (fig. 41; table 7). The riprap blankets near piers 19 and 20 were installed at the time of bridge construction in 1973 and appear to effectively mitigate scour near these piers (fig. 41). The new or modified riprap blankets near piers 15 through 18 appear to cover the footings and seal courses for these piers (figs. 41, 1.8). Future surveys would be helpful to determine the effectiveness of the scour mitigation.

The difference between the survey on June 15, 2022, and the previous survey on July 26, 2018 (fig. 42), indicates about 90 percent of the joint area of interest had detectable change, which means about 10 percent of the differences in the joint area of interest are equivocal and within the bounds of uncertainty (table 8). Erosion and deposition appear roughly balanced throughout most of the reach between 2018 and 2022 in the DoD (fig. 42). Substantial deposition of more than 20 ft was observed along the right (northwest) bank downstream from the bridge, with a corresponding area of as much as 20 ft of erosion adjacent to the left (southeast; fig. 42). The change in the channel-bed elevations from the new and modified riprap blankets near piers 15 through 18 is evident in the DoD, including the material added to the left side of the pre-existing blanket near pier 18 (fig. 42). The average difference between the bathymetric surfaces was –0.71 ft (table 8), indicating minor to moderate channel degradation between the 2018 and 2022 surveys. The net volume of cut in the reach from 2018 to 2022 was about 405,600 yd^3, and the net volume of fill was about 305,600 yd^3, resulting in a net loss of about 100,000 yd^3 of sediment between 2018 and 2022 (table 8). The frequency distribution of bed elevations in 2022 is most similar to the 2018 distribution, but with a slightly higher percentage of channel-bed elevations in the ranges between 182 and 194 ft, and 208 and 212 ft (fig. 40). The cross section along the upstream bridge face for 2022 also is most like the 2018 cross section, except near the new riprap blankets near piers 15 through 18, which are substantially built up (fig. 41). There is some localized erosion between piers 17 and 18, as well as erosion between piers 15 and 16 that extends to the downstream end of the reach (figs. 41 and 42). The stone revetment on the banks showed localized areas of erosion and deposition, but nearly all the indicated changes are within 3 ft of the 2018 elevation, or outside the 95-percent confidence interval (fig. 42). The left bank showed predominantly erosion, whereas the right bank showed predominantly deposition (fig. 42); however, deposition or scour apparent on opposing faces of a feature (or opposite banks) may result from minor horizontal positional variances between the surveys (fig. 6).

The difference between the survey on June 15, 2022, and the survey on June 11, 2014 (fig. 43), indicates about 86 percent of the joint area of interest had detectable change, which means about 14 percent of the differences in the joint area of interest are equivocal and within the bounds of uncertainty (table 8). Substantial erosion appears dominant throughout most of the reach between 2014 and 2022 in the DoD, with as much as 40 ft of erosion from the area near the trough of the very large dune in the thalweg near the bridge (fig. 43). As with 2018, the change in the channel-bed elevations from the new and modified riprap blankets near piers 15 through 18 is evident in the DoD, and there is additional deposition on the right side of the channel upstream from the bridge (fig. 43). Again, there is some localized erosion between piers 17 and 18, as well as erosion downstream from piers 15 and 16 that extends to the downstream end of the reach (figs. 41 and 43). The average difference between the bathymetric

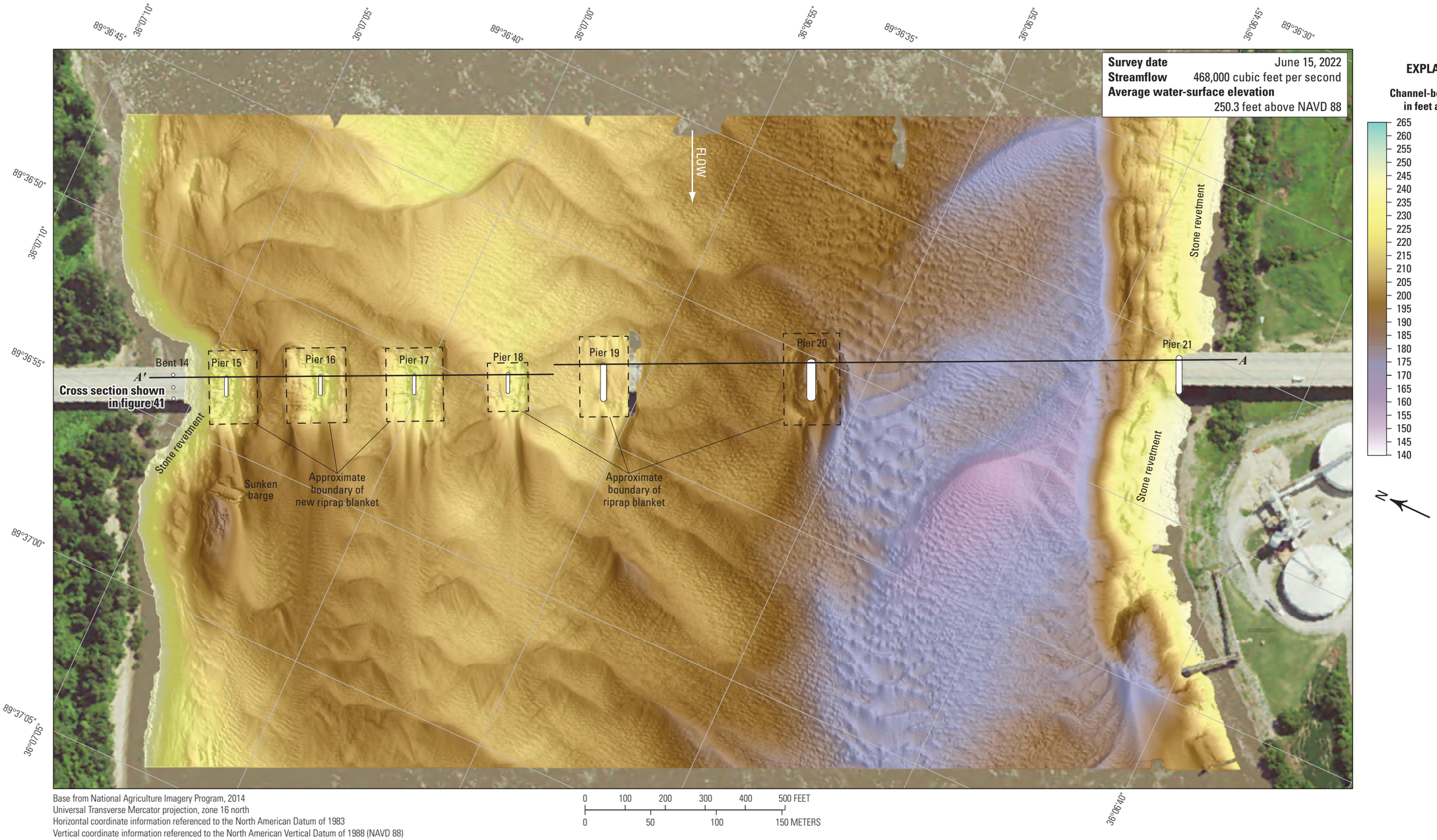

Figure 39. Bathymetric survey of the Mississippi River channel near structure A1700 on Interstate 155 near Caruthersville, Missouri.

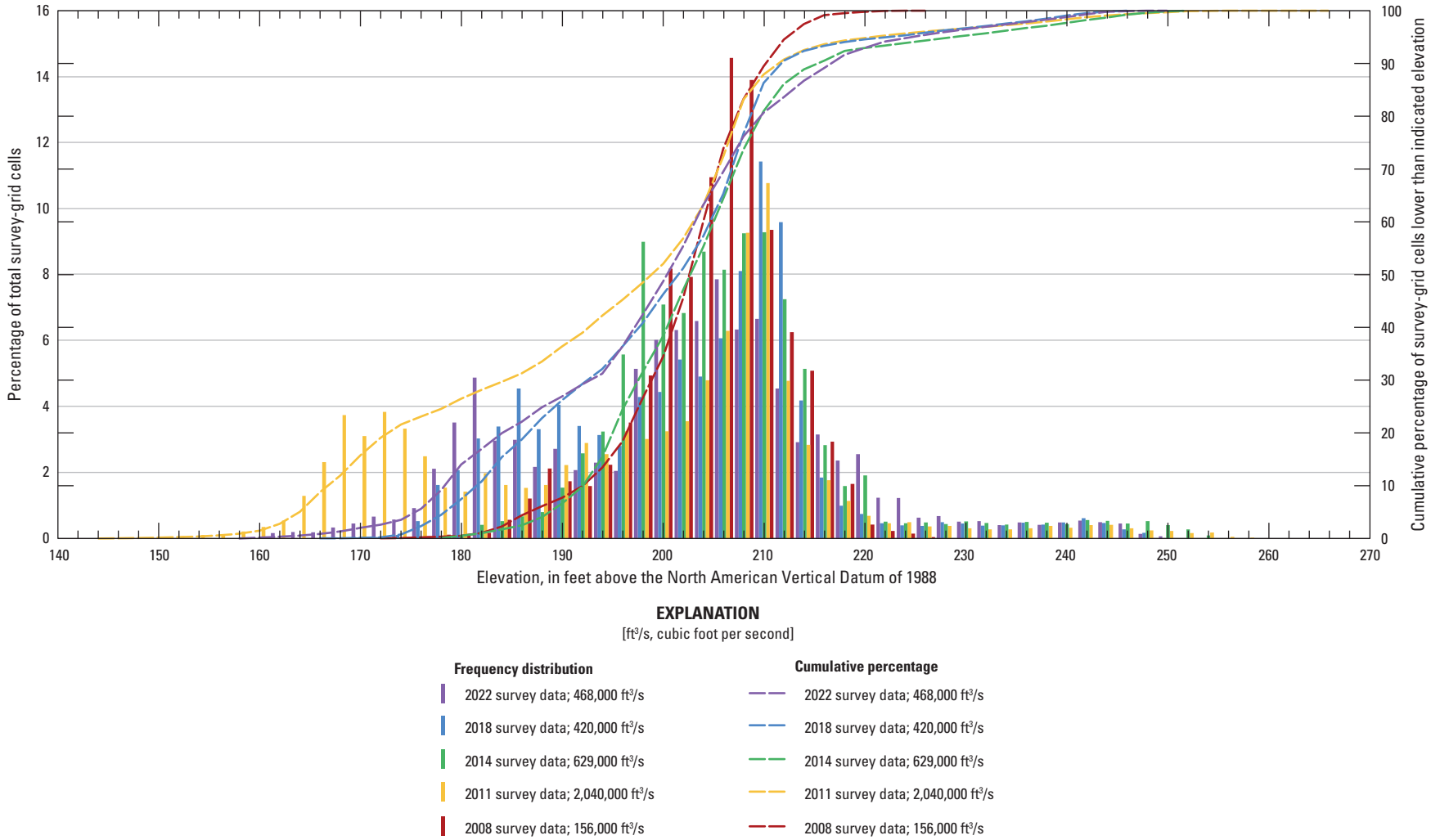

Figure 40. Frequency distribution of bed elevations for bathymetric survey-grid cells in 2-foot elevation bins on the Mississippi River near structure A1700 on Interstate 155 near Caruthersville, Missouri, on June 15, 2022, compared to previous surveys in 2008, 2011, 2014, and 2018 (Huizinga, 2014, 2020a).

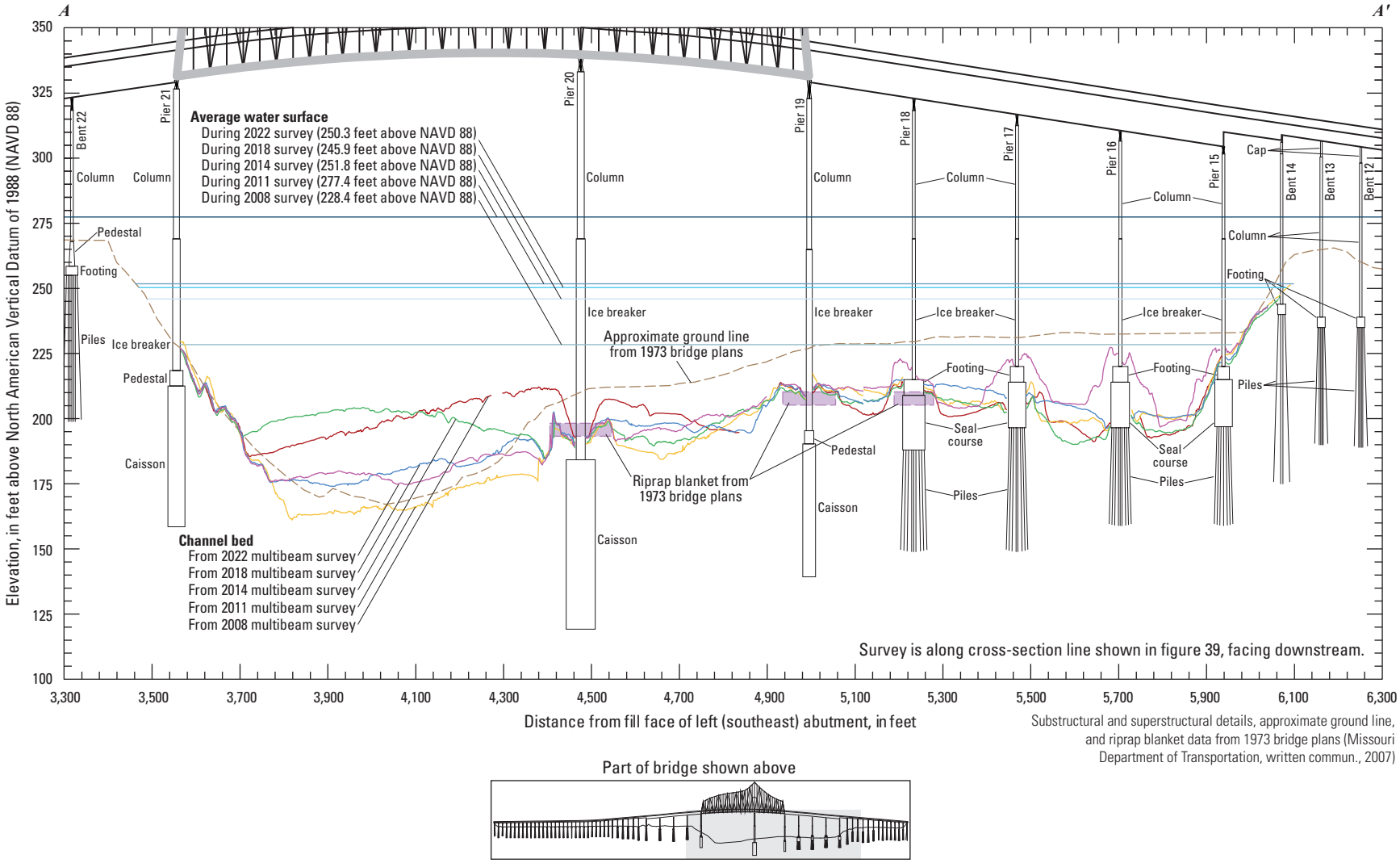

Substructural and superstructural details, approximate ground line, and riprap blanket data from 1973 bridge plans (Missouri Department of Transportation, written commun., 2007)

Figure 41. Key features, substructural and superstructural details, and surveyed channel bed of structure A1700 on Interstate 155 crossing the Mississippi River near Caruthersville, Missouri.

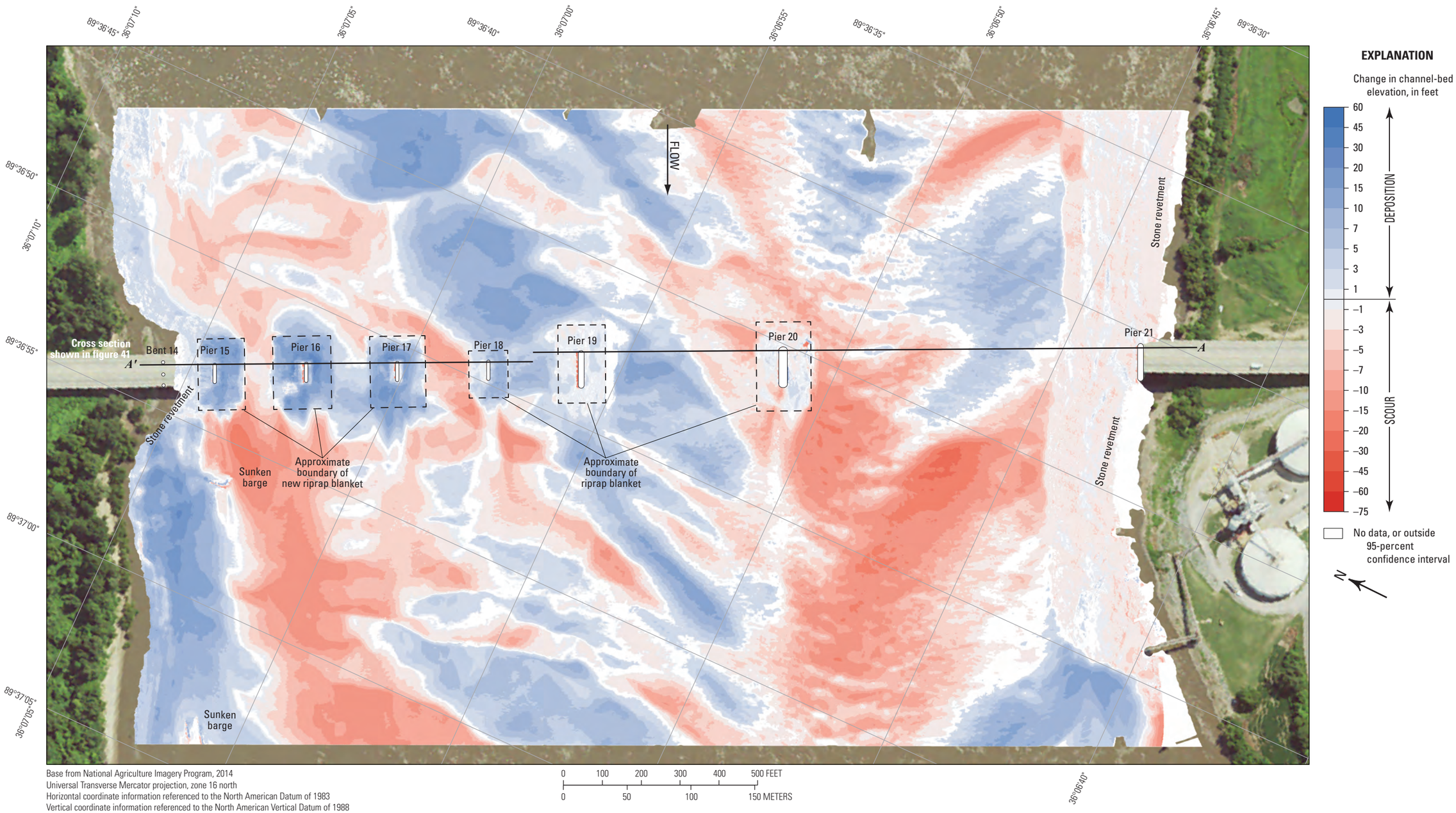

Figure 42. Difference between surfaces created from bathymetric surveys of the Mississippi River channel near structure A1700 on Interstate 155 near Caruthersville, Missouri, on June 15, 2022, and July 26, 2018, with probabilistic thresholding.

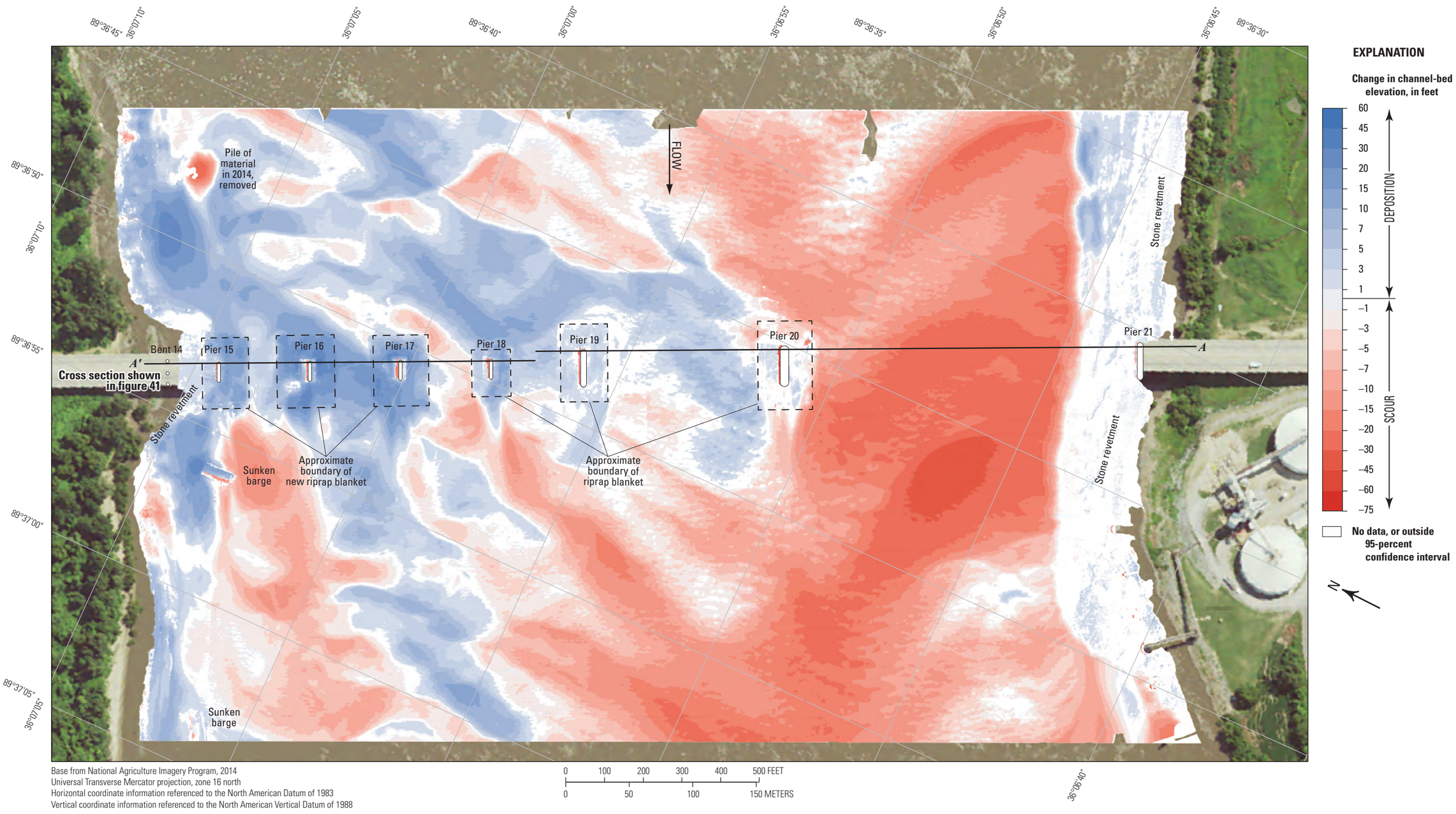

Figure 43. Difference between surfaces created from bathymetric surveys of the Mississippi River channel near structure A1700 on Interstate 155 near Caruthersville, Missouri, on June 15, 2022, and June 11, 2014, with probabilistic thresholding.

surfaces was –4.69 ft (table 8), indicating substantial channel degradation between the 2014 and 2022 surveys with a net loss of sediment of about 636,400 yd^3 between 2014 and 2022, which was the largest net loss of material of all the sites surveyed in 2022 (table 8). The frequency distribution of bed elevations in 2014 had been similar to 2008, with a narrower range of elevations than 2022 (fig. 40). The stone revetment on the left (southeast) bank showed localized areas of deposition, but much of the difference is equivocal (fig. 43). Deposition of as much as 15 ft at the base of the upstream left bank and on the right bank upstream from the bridge likely resulted from material added in these areas after the 2014 survey; the left bank deposition had been noted in Huizinga (2020e; fig. 43). As with previous DoDs, deposition or scour apparent on opposing faces of a feature (such as the piers and sunken barges, fig. 43) likely results from minor horizontal positional variances between the surveys (fig. 6).

The difference between the survey on June 15, 2022, and the survey during flooding on May 5, 2011 (fig. 44), indicates about 89 percent of the joint area of interest had detectable change, which means about 11 percent of the differences in the joint area of interest are equivocal and within the bounds of uncertainty (table 8). Substantial deposition appears dominant throughout most of the reach between 2011 and 2022 in the DoD, with as much as 30 ft of deposition in the thalweg on the left side of the channel and very localized areas of erosion near the trough of the very large dune near the bridge and on the right side of the channel downstream from the bridge, particularly downstream from piers 15 and 16 (fig. 44). The average difference between the 2011 and 2022 bathymetric surfaces was +5.83 ft (table 8), indicating substantial channel aggradation with a net gain of sediment between 2011 and 2022 of about 745,000 yd^3 (table 8), which is the largest average difference and net gain between all the surveys in this study. However, the substantial gain in sediment is to be expected because structure A1700 is the downstream-most site surveyed in Missouri (downstream from the confluences of the Missouri and Ohio Rivers) and therefore subject to the largest streamflows, the largest streamflow fluctuations, and the most substantial sediment flux, as has historically been observed at this site (table 8). The frequency distribution of bed elevations in 2011 is unique, with a higher percentage of cells at elevations 10 to 20 ft lower than 2022 (fig. 40). The stone revetment on the banks showed localized areas of moderate erosion and deposition (fig. 44). As noted in the preceding paragraph, substantial deposition at the base of the upstream left bank and on the right bank upstream from the bridge likely results from material added in these areas after the 2014 survey; however, the erratic movement of the boat and substantial depths experienced during the flood conditions at this site in 2011 likely exacerbated horizontal positional variances between the surveys (refer to the "Uncertainty Estimation" section; fig. 6).

The difference between the survey on June 15, 2022, and the earliest survey on December 10, 2008 (fig. 45), indicates about 91 percent of the joint area of interest had detectable change, which means only about 9 percent of the differences in the joint area of interest are equivocal and within the bounds of uncertainty (table 8). Substantial erosion appears dominant throughout most of the reach between 2008 and 2022 in the DoD, with as much as 40 ft of erosion from the area near the trough of the very large dune in the thalweg near the bridge and erosion along the toe of the right bank downstream from piers 15 and 16 (fig. 45). The average difference between the 2008 and 2022 bathymetric surfaces was –5.47 ft (table 8), which was the largest negative average change and indicated substantial channel degradation with a net loss of sediment between 2008 and 2022 of about 636,300 yd^3 (table 8). This average difference was very similar to 2014 and was the second largest net loss of material of all the sites surveyed in 2022. The frequency distribution of bed elevations in 2008 also was similar to 2014, with a narrower range of elevations than 2022 (fig. 40). The stone revetment on the left (southeast) bank showed localized areas of moderate erosion and deposition (fig. 45). As noted in the preceding paragraphs, substantial deposition at the base of the upstream left bank likely results from material added in that area after the 2014 survey; however, much of the apparent erosion and deposition likely results from minor horizontal positional variances between the surveys, particularly because an SBET correction was not used in this earliest survey (refer to the "Uncertainty Estimation" section; fig. 6).

The vertically averaged velocity vectors indicate substantial variability of flow throughout the channel at this site (fig. 46). Velocities ranged from about 2 to 10 ft/s, with locally lower velocities and flow reversal in numerous locations along the banks, downstream from the bank constrictions near the bridge, and downstream from the piers. The new riprap blankets near piers 15 through 17 appear to cause localized flow disturbances upstream, downstream, and between the piers (fig. 46). Additional flow disturbance may result from upwelling of flow caused by the numerous medium to large dune features present throughout the channel (Best, 2005; fig. 46).

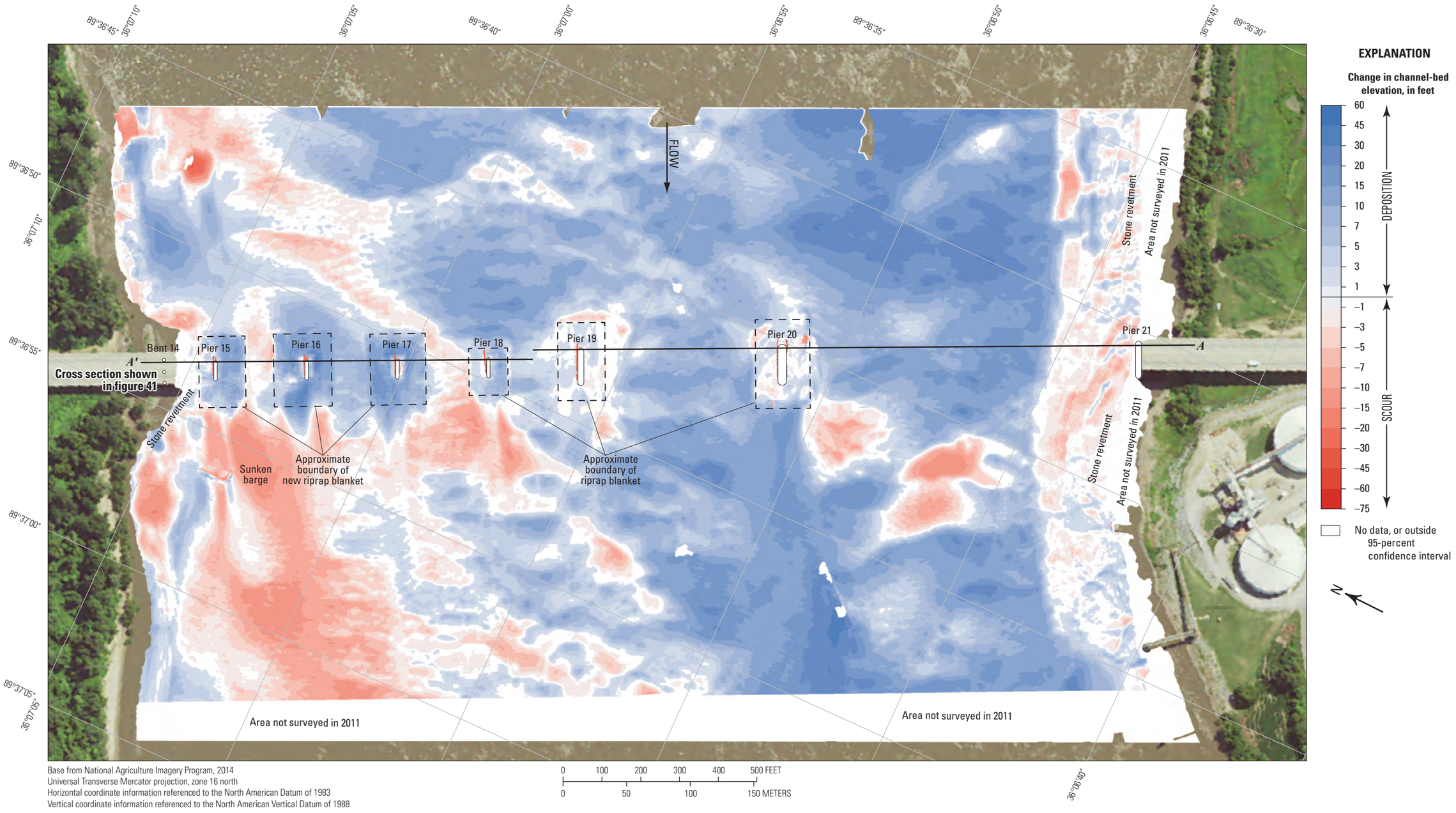

Figure 44. Difference between surfaces created from bathymetric surveys of the Mississippi River channel near structure A1700 on Interstate 155 near Caruthersville, Missouri, on June 15, 2022, and May 5, 2011, with probabilistic thresholding.

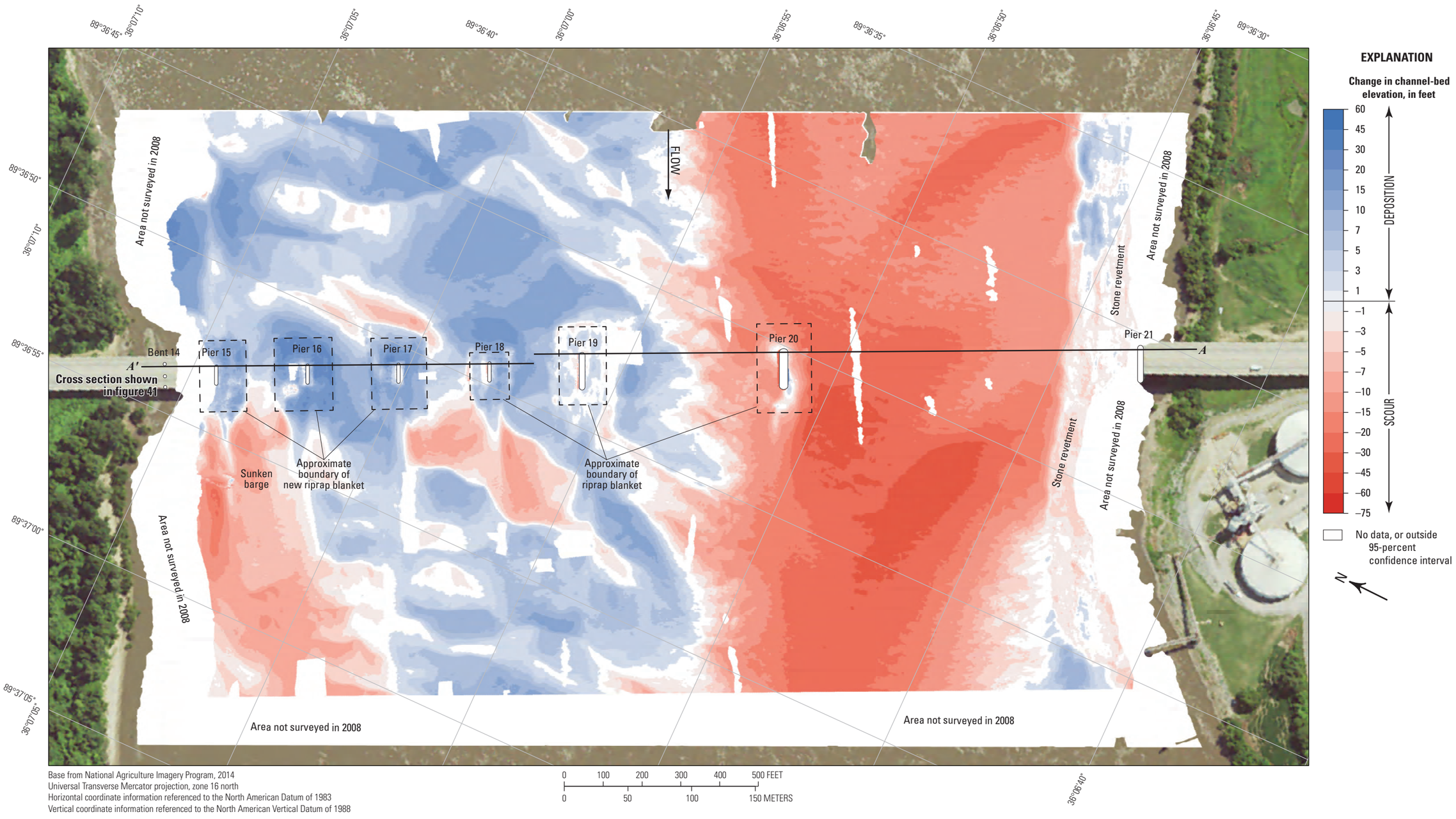

Figure 45. Difference between surfaces created from bathymetric surveys of the Mississippi River channel near structure A1700 on Interstate 155 near Caruthersville, Missouri, on June 15, 2022, and December 10, 2008, with probabilistic thresholding.

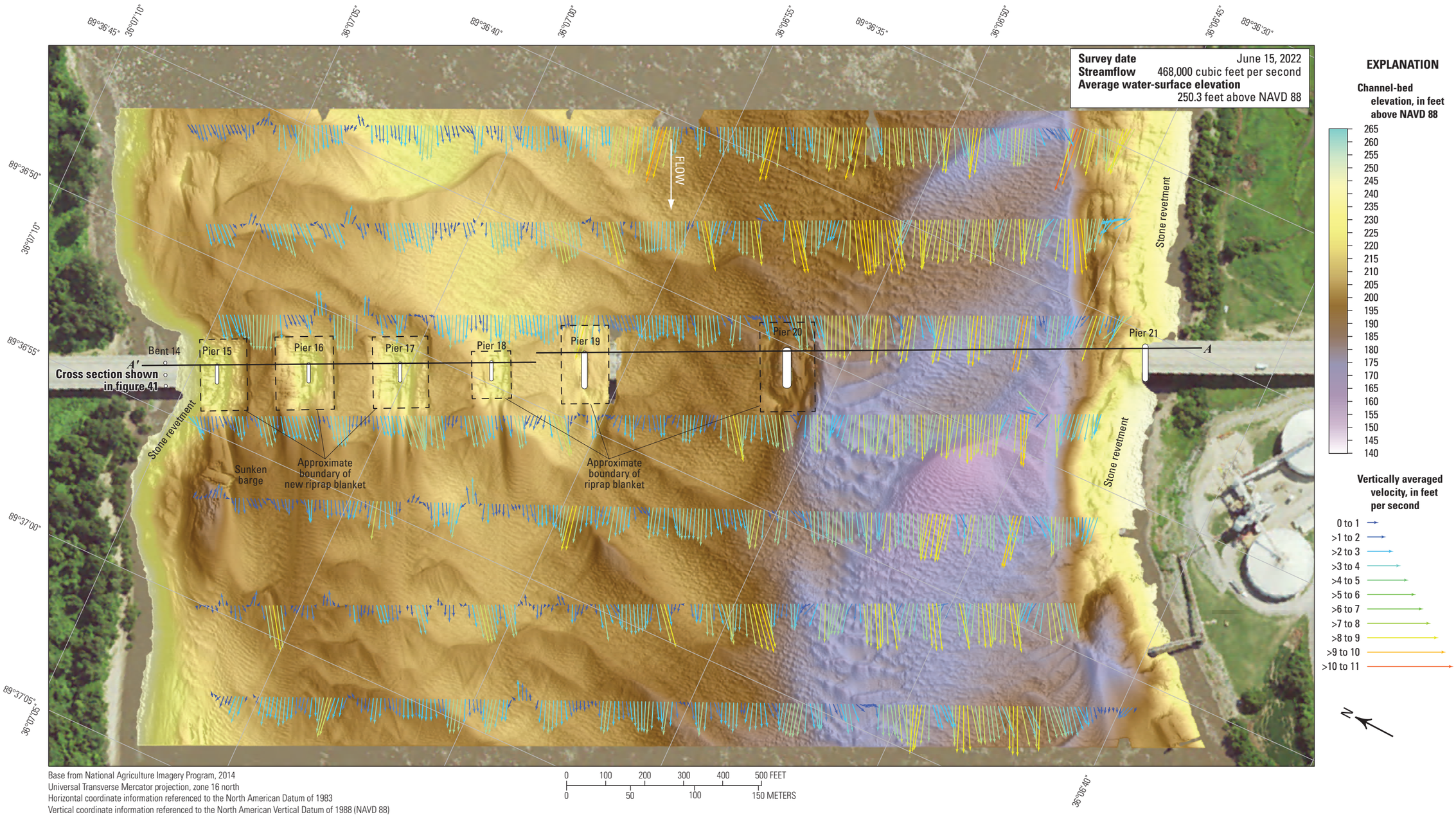

Figure 46. Bathymetry and vertically averaged velocities of the Mississippi River channel near structure A1700 on Interstate 155 near Caruthersville, Missouri.

Summary and Conclusions

Bathymetric and velocimetric data were collected by the U.S. Geological Survey, in cooperation with the Missouri Department of Transportation, near seven bridges at six highway crossings on the periphery of Missouri on June 13–22, 2022. A multibeam echosounder mapping system was used to obtain channel-bed elevations for river reaches about 1,640 feet (ft) longitudinally and generally extending laterally across the active channel from bank to bank during minor flood-flow conditions. These surveys indicated the channel conditions at the time of the surveys and provided characteristics of scour holes that may be useful for developing predictive guidelines or equations for scour hole formation. These data also may be useful to the Missouri Department of Transportation as a minor flood-flow assessment of the bridges for stability and integrity issues with respect to bridge scour during floods.

The estimated gridded uncertainty for the bathymetric surface of each survey area was computed as an estimate of the accuracy to be expected for each point with all relevant sources of error considered. An analysis of the surveys indicated that more than 90 percent of the bathymetric data at all the sites have a gridded uncertainty of less than 0.50 ft, and more than 75 percent of the channel-bed elevations at all the sites except structure A1700 near Caruthersville, Missouri (site 38), have a gridded uncertainty of less than 0.25 ft. The gridded uncertainty of the data has been decreasing with time compared to previous surveys owing to improvements in data-collection equipment and methods.

A variety of fluvial geomorphic features were detected in the channel, ranging from small ripples to large dunes that indicate moderate transport of bedload was present at all the surveyed bridges. Rock outcrops also were detected along one bank at several sites where the alluvial material of the channel bed had been washed away, which was consistent with previous surveys. Bathymetric data were collected around every pier that was in water. Scour holes were present at most piers for which bathymetry could be obtained, except those on banks or surrounded by riprap. At piers 10–11 of structure A5054 at Hannibal, Mo. (site 31), the scour holes were minor and difficult to discern from nearby dunes and ripples.

Although exposure of parts of substructural support elements was observed at several piers, at most sites the exposure likely can be considered minimal compared to the overall substructure that remains buried in bed material at these piers. The notable exceptions are piers 12 and 13 at structure L0135 on State Highway 51 at Chester, Illinois, at which the bedrock material was fully exposed around the piers. In modern construction, bridge substructural elements usually are pinned or socketed to bedrock, but full exposure of usually buried substructural elements warrants special consideration and observation.

All the bridge sites in this study were previously surveyed. Comparisons between bathymetric surfaces from the previous surveys and those of the current (2022) study indicate some correlation in channel-bed elevations with streamflow conditions; however, it is not consistent. The two sites on the Missouri River in northwest Missouri were surveyed when the river was between minor flood events. The sites on the Mississippi River on the eastern side of Missouri were surveyed when the river was receding from a minor flood peak in early June. The average difference between the bathymetric surfaces varied from 0.41 ft higher to 1.86 ft lower in 2022 than 2018, which corresponds to a gain of 15,600 cubic yards (yd^3) and a loss of 178,800 yd^3, respectively. The average difference between the bathymetric surfaces varied from 1.02 ft higher to 4.69 ft lower in 2022 than 2014, which corresponds to a gain of 22,900 yd^3 and a loss of 636,400 yd^3, respectively. Only the two sites on the Missouri River and Caruthersville were surveyed in 2011, yet the average difference between the bathymetric surfaces varied from 5.83 ft higher to 1.34 ft lower, which corresponds to a gain of 745,000 yd^3 and a loss of 55,800 yd^3, respectively. The most substantial overall net gain was between 2011 and 2022 at structure A1700 near Caruthersville, Mo. (site 38), and is expected because structure A1700 is downstream from the confluences of the Missouri and Ohio Rivers, and therefore is subject to the largest streamflows, the largest streamflow fluctuations, and the most substantial sediment flux, as has historically been observed at this site. The second most substantial overall net gain also was between 2011 and 2022, but—unexpectedly—was at the farthest upstream structure L0098 at Brownville, Nebraska (site 1). Alternatively, the most substantial overall net loss was between 2014 and 2022, and was at structure A1700 near Caruthersville, Mo. (site 38). Furthermore, the second most substantial overall net loss also was at structure A1700 near Caruthersville, Mo., between 2008 and 2022.

Pier size, nose shape, and skew to approach flow affected the size of the scour hole observed at a given pier. Piers with wide or blunt noses caused by exposed footings or caissons usually resulted in larger, deeper scour holes at those piers. For example, the exposed seal course of pier 10 of structure A3664 at St. Joseph, Mo. (site 2), the exposed footing of pier 8 of structure A5054 at Hannibal, Mo. (site 31), and the exposed caisson of pier 11 of structure L0135 at Chester, Ill. (site 36), likely contribute to the shape and depth of the scour holes near these piers and the similarity to previous surveys. Alternatively, the slightly exposed top of the footings at piers 7 and 9–11 of structure A5054 at Hannibal, Mo. (site 31) and the tops of the footings or distribution caps at piers 3–6 of structure A5076 at Cape Girardeau, Mo. (site 37), may blunt the horseshoe vortex at these piers.

When a pier was skewed to primary approach flow, the scour hole consistently was deeper and longer than at a similar pier without skew. The skew of all the piers of structure A5054 at Hannibal, Mo. (site 31) and piers 3–4 of structure A5076 at Cape Girardeau, Mo. (site 37), as well as the induced approach flow skew at pier 10 of structure A3664 at St. Joseph, Mo. (site 2), caused the scour hole to be longer and deeper on the side with impinging flow, with a defined ridge of deposition on the leeward side downstream from the pier.

New riprap blankets were observed at pier 3 of structure L0098 at Brownville, Nebr. (site 1), and piers 15–18 of structure A1700 near Caruthersville, Mo. (site 38). The presence of these features had a substantial effect on the observed scour and velocities at and near a given pier, particularly compared to elevations from previous surveys at these sites. Several other piers seemed partially surrounded by random piles of riprap or rock, which may or may not help mitigate scour near those piers. Piers 9 and 10 of structure A5054 at Hannibal, Mo. (site 31), have hummocks on either side that may be partial riprap blankets, and piers 3 and 4 of structure A5076 at Cape Girardeau, Mo. (site 37), seemed to be partially surrounded with piles of coarse material. However, the effectiveness of the scour mitigation is uncertain because the placement seems random and nonuniform.

References Cited

American Association of State Highway Transportation Officials, 2020, AASHTO LRFD bridge design specifications (9th ed.): Washington, D.C., American Association of State Highway Transportation Officials, 176 p.

Applanix Corporation, 2021, POSPac MMS GNSS-inertial tools software (rev. 17): Richmond Hill, Ontario, Canada, PUBS–MAN–001768, 239 p.

Arneson, L.A., Zevenbergen, L.W., Lagasse, P.F., and Clopper, P.E., 2012, Evaluating scour at bridges (5th ed.): U.S. Department of Transportation Federal Highway Administration Publication FHWA–HIF–12–003, Hydraulic Engineering Circular no. 18, 340 p., accessed September 30, 2022, at https://www.fhwa.dot.gov/engineering/hydraulics/pubs/hif12003.pdf.

Becker, L.D., 1994, Investigation of bridge scour at selected sites on Missouri streams: U.S. Geological Survey Water-Resources Investigations Report 94–4200, 40 p., accessed September 30, 2022, at https://doi.org/10.3133/wri944200.

Best, J., 2005, The fluid dynamics of river dunes—A review and some future research directions: Journal of Geophysical Research, v. 110, no. F4, 21 p., accessed August 21, 2023, at https://doi.org/10.1029/2004JF000218.

Brown, D.A., Turner, J.P., Castelli, R.J., and Loehr, E.J., 2018, Drilled shafts—Construction procedures and design methods: U.S. Department of Transportation Federal Highway Administration, Publication FHWA–NHI–18-024, Geotechnical Engineering Circular no. 10, 756 p., accessed August 21, 2023, at https://www.fhwa.dot.gov/engineering/geotech/nhi18024.pdf.

Calder, B.R., and Mayer, L.A., 2003, Automatic processing of high-rate, high-density multibeam echosounder data: Geochemistry, Geophysics, Geosystems (G3), v. 4, no. 6, 22 p., accessed December 8, 2023, at https://doi.org/10.1029/2002GC000486.

Densmore, B.K., Strauch, K.R., and Dietsch, B.J., 2013, Hydrographic surveys of the Missouri and Yellowstone Rivers at selected bridges and through Bismarck, North Dakota, during the 2011 flood: U.S. Geological Survey Scientific Investigations Report 2013–5087, 59 p., accessed September 30, 2022, at https://doi.org/10.3133/sir20135087.

Dietsch, B.J., Densmore, B.K., and Strauch, K.R., 2014, Repeated multibeam echosounder hydrographic surveys of 15 selected bridge crossings along the Missouri River from Niobrara to Rulo, Nebraska, during flood of 2011: U.S. Geological Survey Scientific Investigations Report 2014–5062, 53 p., accessed February 1, 2024 at https://doi.org/10.3133/sir20145062.

Esri, 2023, Resources for ArcMap (ver. 10.8): accessed September 29, 2023, at https://www.esri.com/en-us/arcgis/products/arcgis-desktop/resources.

Gilbert, G.K., and Murphy, E.C., 1914, The transportation of debris by running water: U.S. Geological Survey Professional Paper 86, 263 p., accessed September 30, 2022, at https://doi.org/10.3133/pp86.

Hughes Clarke, J.E., Mayer, L.A., and Wells, D.E., 1996, Shallow-water imaging multibeam sonars—A new tool for investigating seafloor processes in the coastal zone and on the continental shelf: Marine Geophysical Researches, v. 18, no. 6, p. 607–629, accessed November 29, 2022, at https://doi.org/10.1007/BF00313877.

Huizinga, R.J., 2010, Bathymetric surveys at highway bridges crossing the Missouri River in Kansas City, Missouri, using a multibeam echo sounder, 2010: U.S. Geological Survey Scientific Investigations Report 2010–5207, 61 p., accessed August 24, 2023, at https://doi.org/10.3133/sir20105207.

Huizinga, R.J., 2011, Bathymetric surveys at highway bridges crossing the Missouri and Mississippi Rivers near St. Louis, Missouri, 2010: U.S. Geological Survey Scientific Investigations Report 2011–5170, 75 p., accessed August 24, 2023, at https://doi.org/10.3133/sir20115170.

Huizinga, R.J., 2012, Bathymetric and velocimetric surveys at highway bridges crossing the Missouri River in and into Missouri during summer flooding, July–August 2011: U.S. Geological Survey Scientific Investigations Report 2012–5204, 166 p., accessed August 24, 2023, at https://doi.org/10.3133/sir20125204.

Huizinga, R.J., 2013, Results of repeat bathymetric and velocimetric surveys at the Amelia Earhart Bridge on U.S. Highway 59 over the Missouri River at Atchison, Kansas, 2009–2013: U.S. Geological Survey Scientific Investigations Report 2013–5177, 50 p., accessed August 24, 2023, at https://doi.org/10.3133/sir20135177.

Huizinga, R.J., 2014, Bathymetric and velocimetric surveys at highway bridges crossing the Missouri River between Kansas City and St. Louis, Missouri, April–May, 2013: U.S. Geological Survey Scientific Investigations Report 2014–5116, 79 p., accessed August 24, 2023, at https://doi.org/10.3133/sir20145116.

Huizinga, R.J., 2015, Bathymetric and velocimetric surveys at highway bridges crossing the Missouri and Mississippi Rivers on the periphery of Missouri, June 2014: U.S. Geological Survey Scientific Investigations Report 2015–5048, 81 p., accessed August 24, 2023, at https://doi.org/10.3133/sir20155048.

Huizinga, R.J., 2016, Bathymetric and velocimetric surveys at highway bridges crossing the Missouri River near Kansas City, Missouri, June 2–4, 2015: U.S. Geological Survey Scientific Investigations Report 2016–5061, 93 p., accessed August 24, 2023, at https://doi.org/10.3133/sir20165061.

Huizinga, R.J., 2017a, Bathymetric and velocimetric surveys at highway bridges crossing the Missouri and Mississippi Rivers near St. Louis, Missouri, May 23–27, 2016: U.S. Geological Survey Scientific Investigations Report 2017–5076, 102 p., accessed August 24, 2023, at https://doi.org/10.3133/sir20175076.

Huizinga, R.J., 2017b, Bathymetry and velocity data from surveys at highway bridges crossing the Missouri and Mississippi Rivers near St. Louis, Missouri, October 2008 through May 2016: U.S. Geological Survey data release, accessed August 24, 2023, at https://doi.org/10.5066/F71C1VCC.

Huizinga, R.J., 2020a, Bathymetric and velocimetric surveys at highway bridges crossing the Missouri River between Kansas City and St. Louis, Missouri, May 22–31, 2017: U.S. Geological Survey Scientific Investigations Report 2020–5018, 104 p., accessed August 24, 2023, at https://doi.org/10.3133/sir20205018.

Huizinga, R.J., 2020b, Bathymetry and velocity data from surveys at highway bridges crossing the Missouri River in Kansas City, Missouri, March 2010 through May 2017: U.S. Geological Survey data release, accessed August 24, 2023, at https://doi.org/10.5066/P9L6GW57.

Huizinga, R.J., 2020c, Bathymetry and velocity data from surveys at highway bridges crossing the Missouri River between Kansas City and St. Louis, Missouri, January 2010 through May 2017: U.S. Geological Survey data release, accessed August 24, 2023, at https://doi.org/10.5066/P94M4US7.

Huizinga, R.J., 2020d, Bathymetry and velocity data from surveys at highway bridges crossing the Missouri and Mississippi Rivers on the periphery of Missouri, December 2008 through August 2018: U.S. Geological Survey data release, accessed August 24, 2023, at https://doi.org/10.5066/P9WDI9YF.

Huizinga, R.J., 2020e, Bathymetric and velocimetric surveys at highway bridges crossing the Missouri and Mississippi Rivers on the periphery of Missouri, July–August 2018: U.S. Geological Survey Scientific Investigations Report 2020–5088, 100 p., accessed August 24, 2023, at https://doi.org/10.3133/sir20205088.

Huizinga, R.J., 2021, Bathymetry and velocity data from surveys at highway bridges crossing the Missouri River in Kansas City, Missouri, in August 2019, August 2020, and October 2020: U.S. Geological Survey data release, accessed August 24, 2023, at https://doi.org/10.5066/P96TX8AE.

Huizinga, R.J., 2022a, Bathymetric and velocimetric surveys at highway bridges crossing the Missouri River near Kansas City, Missouri, August 2019, August 2020, and October 2020: U.S. Geological Survey Scientific Investigations Report 2021–5098, 112 p., accessed August 24, 2023, at https://doi.org/10.3133/sir20215098.

Huizinga, R.J., 2022b, Bathymetry and velocity data from surveys at highway bridges crossing the Missouri and Mississippi Rivers near St. Louis, Missouri, August 3–10, 2020: U.S. Geological Survey data release, accessed April 25, 2023, at https://doi.org/10.5066/P9F04JC5.

Huizinga, R.J., 2023, Bathymetric and velocimetric surveys at highway bridges crossing the Missouri and Mississippi Rivers near St. Louis, Missouri, August 3–10, 2020 (ver. 1.1, June 2023): U.S. Geological Survey Scientific Investigations Report 2023–5050, 129 p., accessed June 1, 2023, at https://doi.org/10.3133/sir20235050.

Huizinga, R.J., 2024, Bathymetric and velocimetric surveys at highway bridges crossing the Missouri River between Kansas City and St. Louis, Missouri, May 19–26, 2021: U.S. Geological Survey Scientific Investigations Report 2024–5021, 101 p., accessed April 3, 2024, at https://doi.org/10.3133/sir20245021.

Huizinga, R.J., and Rivers, B.C., 2023a, Bathymetry and velocity data from surveys at highway bridges crossing the Missouri River between Kansas City and St. Louis, Missouri, May 19–26, 2021 (ver. 2.0, August 2023): U.S. Geological Survey data release, accessed September 8, 2023, at https://doi.org/10.5066/P9ULGQ4W.

Huizinga, R.J., and Rivers, B.C., 2023b, Bathymetry and velocity data from surveys at highway bridges crossing the Missouri and Mississippi Rivers on the periphery of Missouri, June 13–22, 2022: U.S. Geological Survey data release, accessed September 8, 2023, at https://doi.org/10.5066/P9K66GYC.

Huizinga, R.J., Elliott, C.M., and Jacobson, R.B., 2010, Bathymetric and velocimetric survey and assessment of habitat for pallid sturgeon on the Mississippi River in the vicinity of the proposed Interstate 70 Bridge at St. Louis, Missouri: U.S. Geological Survey Scientific Investigations Report 2010–5017, 28 p., accessed August 24, 2023, at https://doi.org/10.3133/sir20105017.

Huizinga, R.J., Rivers, B.C., Richards, J.M., and Waite, G.J., 2023, Bathymetric contour maps, surface area and capacity tables, and bathymetric change maps for selected water-supply lakes in north-central and west-central Missouri, 2020: U.S. Geological Survey Scientific Investigations Report 2023–5046, 52 p., accessed June 6, 2023, at https://doi.org/10.3133/sir20235046.

Huizinga, R.J., and Rydlund, P.H., Jr., 2004, Potential-scour assessments and estimates of scour depth using different techniques at selected bridge sites in Missouri: U.S. Geological Survey Scientific Investigations Report 2004–5213, 42 p., accessed August 24, 2023, at https://doi.org/10.3133/sir20045213.

HYPACK, Inc., 2020, HYPACK User Manual: Middletown, Conn., HYPACK, Inc., 2,602 p., accessed June 28, 2022, at http://www.hypack.com/File%20Library/Resource%20Library/Manuals/2020/2020-HYPACK-User-Manual.pdf.

International Hydrographic Organization, 2020, IHO standards for hydrographic surveys (6th ed.): Monaco, International Hydrographic Bureau, Special publication no. 44, 41 p., accessed February 1, 2024, at https://iho.int/uploads/user/pubs/standards/s-44/S-44_Edition_6.1.0.pdf.

Mueller, D.S., Wagner, C.R., Rehmel, M.S., Oberg, K.A., and Rainville, F., 2013, Measuring discharge with acoustic Doppler current profilers from a moving boat (ver. 2.0, December 2013): U.S. Geological Survey Techniques and Methods, book 3, chap. A22, 95 p., accessed September 30, 2022, at https://doi.org/10.3133/tm3A22.

National Marine Electronics Association, 2002, NMEA 0183—Standard for interfacing marine electronic devices (ver. 3.01). National Marine Electronics Association, 88 p., accessed February 1, 2024, at https://www.plaisance-pratique.com/IMG/pdf/NMEA0183-2.pdf.

National Weather Service, 2024, Mississippi River at Hannibal, *in* Advanced Hydrologic Prediction Service: National Weather Service database, accessed February 9, 2024, at https://water.weather.gov/ahps/. [Gage data directly accessible at https://water.weather.gov/ahps2/hydrograph.php?wfo=lsx&gage=hnnm7.]

Parsons, D.R., Jackson, P.R., Czuba, J.A., Engel, F.L., Rhoads, B.L., Oberg, K.A., Best, J.L., Mueller, D.S., Johnson, K.K., and Riley, J.D., 2013, Velocity Mapping Toolbox (VMT)—A processing and visualization suite for moving-vessel ADCP measurements: Earth Surface Processes and Landforms, v. 38, no. 11, p. 1244–1260, accessed April 27, 2023, at https://doi.org/10.1002/esp.3367.

Rivers, B.C., Huizinga, R.J., Richards, J.M., and Waite, G.J., 2023, Bathymetric contour maps, surface area and capacity tables, and bathymetric change maps for selected water-supply lakes in northeastern Missouri, 2021: U.S. Geological Survey Scientific Investigations Report 2023–5108, 63 p., accessed October 10, 2023, at https://doi.org/10.3133/sir20235108.

Riverscapes Consortium, 2022, Geomorphic change detection software: Riverscapes Consortium, accessed September 2022 at https://gcd.riverscapes.net.

Rydlund, P.H., Jr., 2009, Real-time river channel-bed monitoring at the Chariton and Mississippi Rivers in Missouri, 2007–09: U.S. Geological Survey Scientific Investigations Report 2009–5254, 27 p., accessed August 24, 2023, at https://doi.org/10.3133/sir20095254.

Simons, D.B., and Richardson, E.V., 1966, Resistance to flow in alluvial channels: U.S. Geological Survey Professional Paper 422–J, 61 p., accessed April 27, 2023, at https://doi.org/10.3133/pp422J.

Simon, Li and Associates, 1985, Seasonal effects of river stage-discharge relations at selected gages, final report: Fort Collins, Colo., prepared for U.S. Army Corps of Engineers, Contract No. DACW43–85–D–0017, 96 p.

U.S. Army Corps of Engineers [USACE], 2004a, Upper Mississippi River System flow frequency study, appendix E: Rock Island, Ill., U.S. Army Corps of Engineers, accessed September 25, 2023, at https://www.mvr.usace.army.mil/Portals/48/docs/FRM/UpperMissFlowFreq/App.%20E%20Kansas%20City%20Dist.%20Hydrology_Hydraulics.pdf.

U.S. Army Corps of Engineers [USACE], 2004b, Upper Mississippi River System flow frequency study, appendix C: Rock Island, Ill., U.S. Army Corps of Engineers, accessed September 25, 2023, at https://www.mvr.usace.army.mil/Portals/48/docs/FRM/UpperMissFlowFreq/App.%20C%20Rock%20Island%20Dist.%20Mississippi%20River%20Hydrology_Hydraulics.pdf.

U.S. Army Corps of Engineers [USACE], 2004c, Upper Mississippi River System flow frequency study, appendix D: Rock Island, Ill., U.S. Army Corps of Engineers, accessed September 25, 2023, at https://www.mvr.usace.army.mil/Portals/48/docs/FRM/UpperMissFlowFreq/App.%20D%20St.%20Louis%20Dist.%20Hydrology_Hydraulics.pdf.

U.S. Army Corps of Engineers [USACE], 2013, Engineering and design—Hydrographic surveying: Washington D.C., U.S. Army Corps of Engineers, manual no. EM 1110–2–1003, 560 p., accessed September 25, 2023, at https://www.publications.usace.army.mil/Portals/76/Publications/EngineerManuals/EM_1110-2-1003.pdf?ver=gDGVUj_0XR2sXHiIpQZv2Q%3d%3d.

U.S. Geological Survey [USGS], 2023a, USGS water data for the Nation: U.S. Geological Survey National Water Information System database, accessed September 25, 2023, at https://doi.org/10.5066/F7P55KJN.

U.S. Geological Survey [USGS], 2023b, USGS streamgage statistics for station 06818000: U.S. Geological Survey WaterWatch toolkit, accessed September 25, 2023, at https://waterwatch.usgs.gov/index.php?sno=06818000&ds=dv01d_por&btnGo=GO&m=sitempnn.

U.S. Geological Survey [USGS], 2023c, USGS streamgage statistics for station 07020500: U.S. Geological Survey WaterWatch toolkit, accessed September 25, 2023, at https://waterwatch.usgs.gov/index.php?sno=07020500&ds=dv01d_por&btnGo=GO&m=sitempnn.

Glossary

bent A vertical, load-bearing, intermediate bridge substructure unit between the ends of a bridge used to support the bridge at intermediate intervals, typically consisting of two or more piles (referred to as a "pile bent") or columns, each supported by an individual footing, pile, or drilled shaft.

caisson An older type of bridge foundation consisting of a watertight retaining structure used as the foundation of a bridge pier, constructed in such a way that the water can be pumped out, keeping the work environment dry while the ground under the caisson is excavated and the caisson "sunk" into final position below the ground line. Upon reaching its final position, the caisson is backfilled with sand or gravel for added weight and stability.

cap The upper or bearing part of a bridge pier or bent, usually made of concrete or hard stone and designed to distribute concentrated loads from the bridge superstructure evenly over the columns of the pier or bent.

cofferdam A temporary retaining structure used in pier and pylon construction to retain water and support the sides of an excavation where water is present. A cofferdam generally consists of vertical sheet piling around the perimeter of a bracing system and a bottom seal course. Once sealed, the water can be pumped out, keeping the work environment dry while the footing, columns, and other substructural elements are built.

column The primary part of a bridge bent, pier, or pylon used to convey the load of the bridge superstructure to the foundation.

dolphin An isolated structure for berthing and mooring of vessels away from the river bank. A dolphin generally consists of a group of piles, or a cylinder of sheet piling filled with gravel or concrete, and sometimes is used in conjunction with a moored service or loading dock.

drilled shaft A cylindrical shaft that is drilled into the ground as a bridge foundation, typically extending through the alluvial material into underlying rock and filled with reinforced concrete.

footing A part of the foundation of a bridge bent, pier, or pylon used to transmit the load from the column to the ground, either directly or indirectly through piles or drilled shafts.

pedestal A transitional element occasionally used in a bridge pier or pylon, typically found between the column and a footing or caisson.

pier A vertical, load-bearing, intermediate bridge substructure unit between the ends of a bridge used to support the bridge at intermediate intervals, consisting of a single column or shaft, or multiple columns connected with a strut or solid web, and generally supported by a single footing.

pile A long, narrow cylinder or beam made of wood, metal, or concrete used as part of the foundation of a bridge, typically driven into the ground from above and integrated into a seal course or footing of a pier, or the cap of a pile bent. Groups of piles also are used as mooring dolphins.

pylon A tower-like vertical, load-bearing substructural unit that usually supports the cables of a suspension bridge or a cable-stayed bridge. A pylon typically extends above the bridge superstructure.

seal course The base of a newer type of bridge foundation, created when a cofferdam used to build the foundation is "sealed" with concrete at the underwater ground level to prevent water from entering the cofferdam from below.

spur dike linear structure usually constructed of piled stone projecting from the bank in a river to redirect the river's own energy to protect the bank from erosion and to direct the axis of flow.

stone revetment A facing of stone, concrete units, or slabs built to protect a bank or other feature against erosion by wave action, currents, and surges.

strut A horizontal intermediate bridge substructure unit used to connect and brace two or more columns or shafts of a pier.

substructure The part of a bridge that supports the superstructure and transmits the load of the superstructure and deck to the ground through the foundations.

superstructure The part of a bridge that supports the bridge deck, and connects one substructural element to another and thereby transmits the load of the deck and anything on the deck to the substructure.

water year A continuous 12-month period selected to present data relative to hydrologic or meteorological phenomena during which a complete annual hydrologic cycle normally occurs. The water year used by the U.S. Geological Survey runs from October 1 through September 30 and is designated by the year in which it ends.

Appendix 1. Shaded Triangulated Irregular Network Images of the Channel and Side of Pier for Each Surveyed Pier

Shaded triangulated irregular network images of the channel and side of pier were prepared for each surveyed pier at structure L0098 at Brownville, Nebraska (fig. 1.1); dual bridge structure A3664 at St. Joseph, Missouri (fig. 1.2); structure A5054 at Hannibal, Mo. (figs. 1.3, 1.4); structure L0135 at Chester, Illinois (fig. 1.5); structure A5076 at Cape Girardeau, Mo. (fig. 1.6); and structure A1700 near Caruthersville, Mo. (figs. 1.7, 1.8).

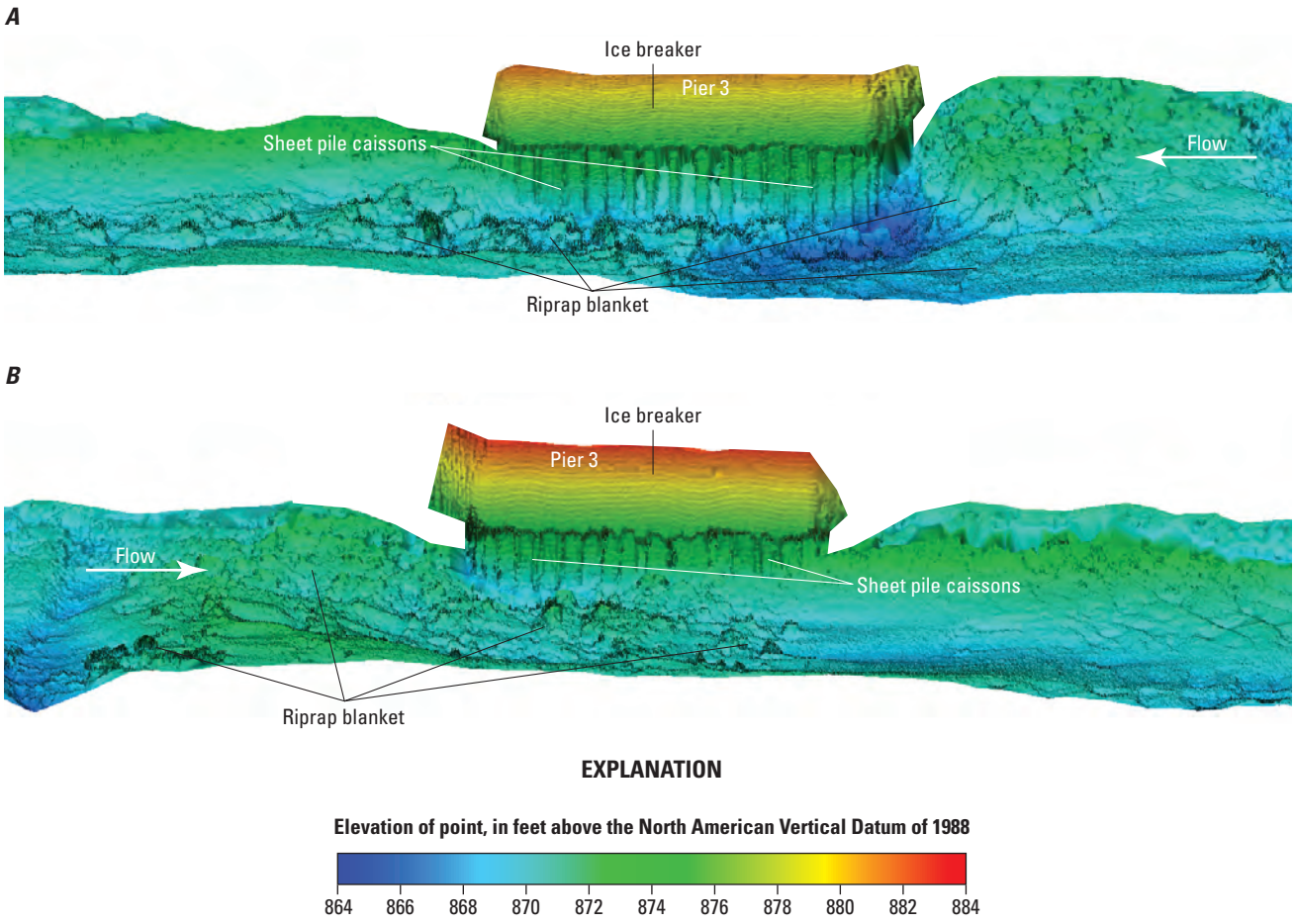

Figure 1.1. Shaded triangulated irregular network visualization of the channel bed and main channel pier of structure L0098 on U.S. Highway 136 over the Missouri River at Brownville, Nebraska. *A*, Left (northeast) side of pier 3. *B*, Right (southwest) side of pier 3.

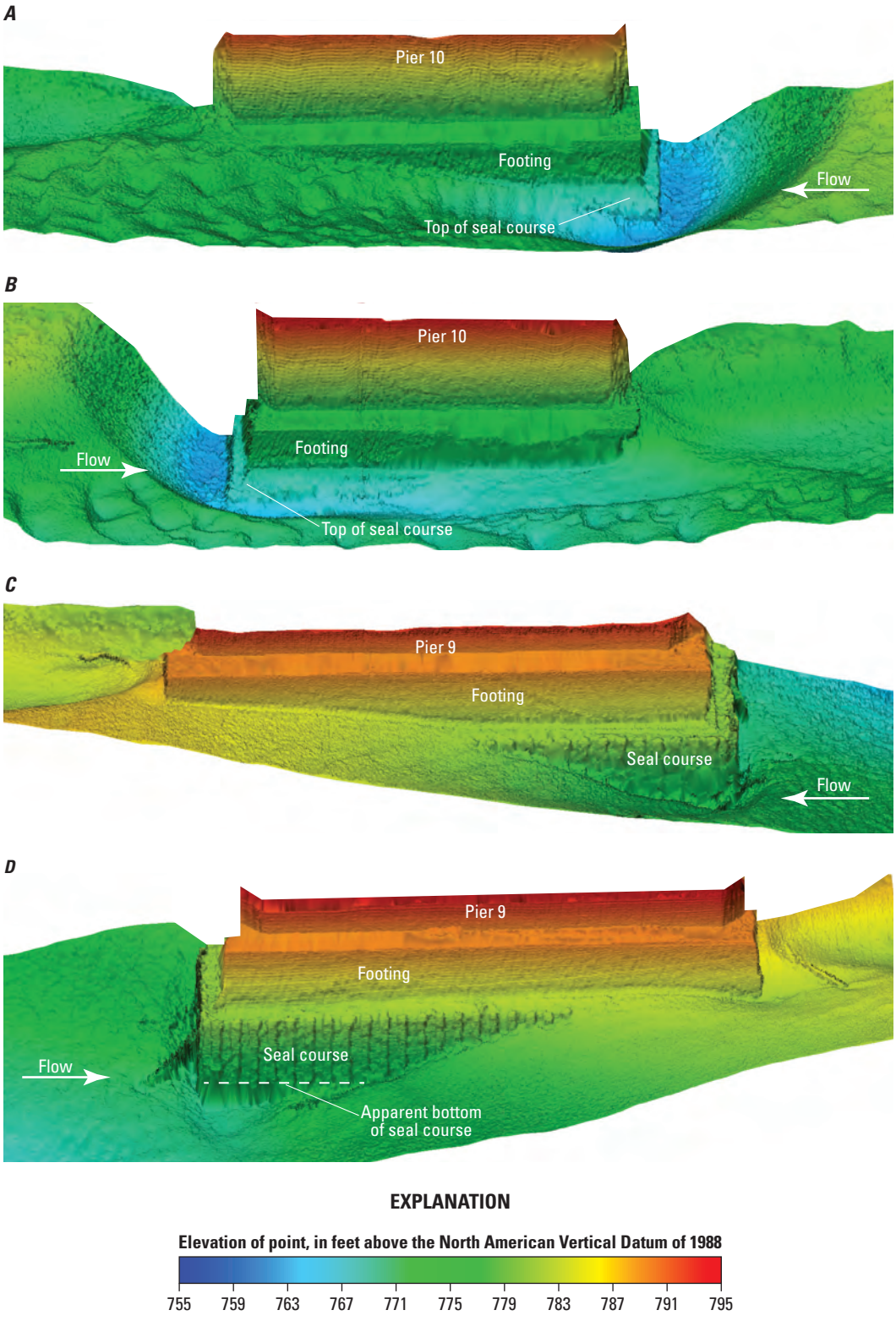

Figure 1.2. Shaded triangulated irregular network visualization of the channel bed and piers of dual bridge structure A3664 on U.S. Highway 36 over the Missouri River at St. Joseph, Missouri. *A*, Left (east) side of pier 10. *B*, Right (west) side of pier 10. *C*, Left (east) side of pier 9. *D*, Right (west) side of pier 9. (Note: point cloud data for pier 8 were too sparse to create a visualization).

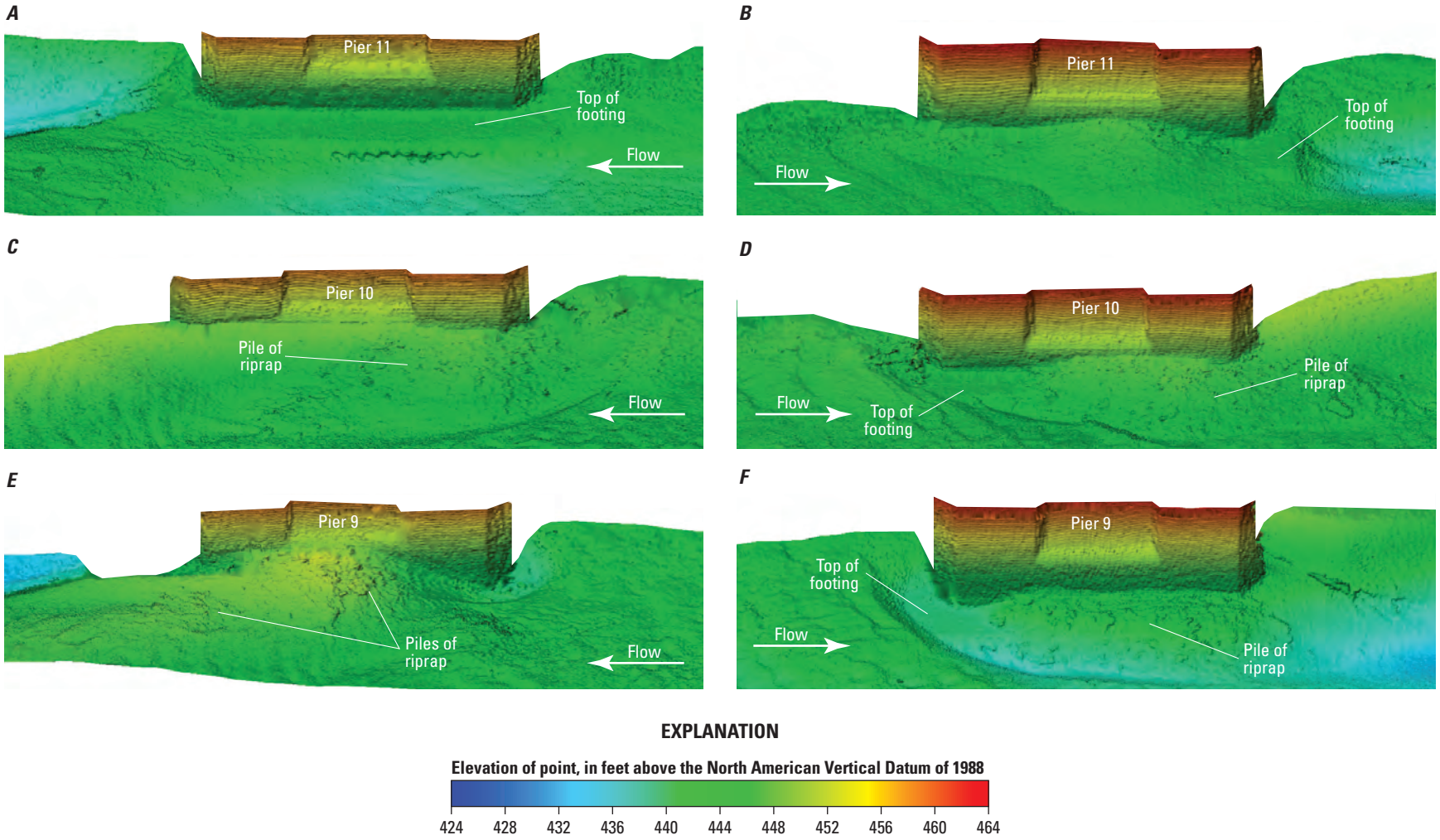

Figure 1.3. Shaded triangulated irregular network visualization of the channel bed and left main channel piers of structure A5054 on Interstate 72 over the Mississippi River at Hannibal, Missouri. *A*, Left (northeast) side of pier 11. *B*, Right (southwest) side of pier 11. *C*, Left (northeast) side of pier 10. *D*, Right (southwest) side of pier 10. *E*, Left (northeast) side of pier 9. *F*, Right (southwest) side of pier 9.

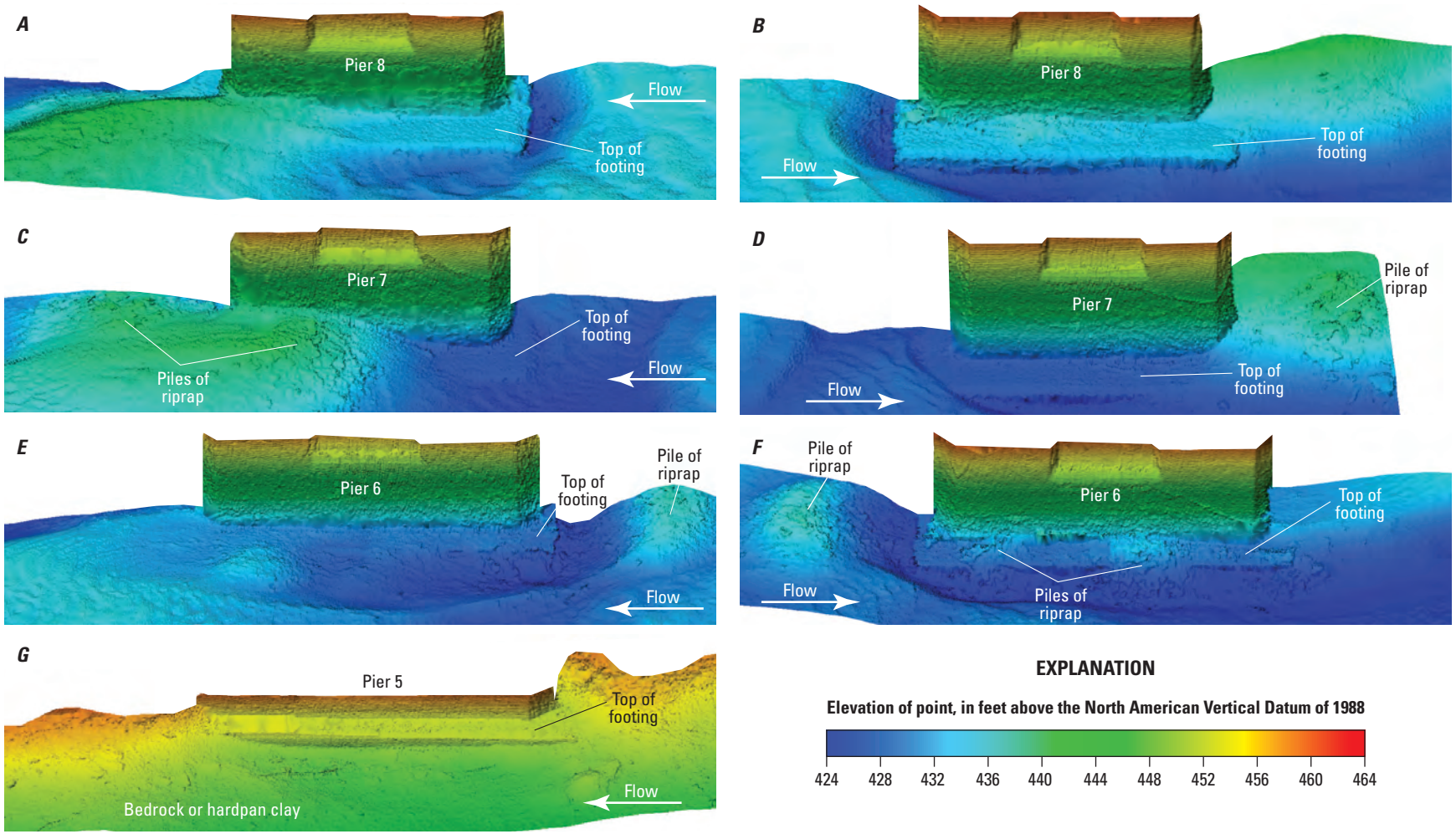

Figure 1.4. Shaded triangulated irregular network visualization of the channel bed and right main channel piers of structure A5054 on Interstate 72 over the Mississippi River at Hannibal, Missouri. *A*, Left (northeast) side of pier 8. *B*, Right (southwest) side of pier 8. *C*, Left (northeast) side of pier 7. *D*, Right (southwest) side of pier 7. *E*, Left (northeast) side of pier 6. *F*, Right (southwest) side of pier 6. *G*, Left (northeast) side of pier 5.

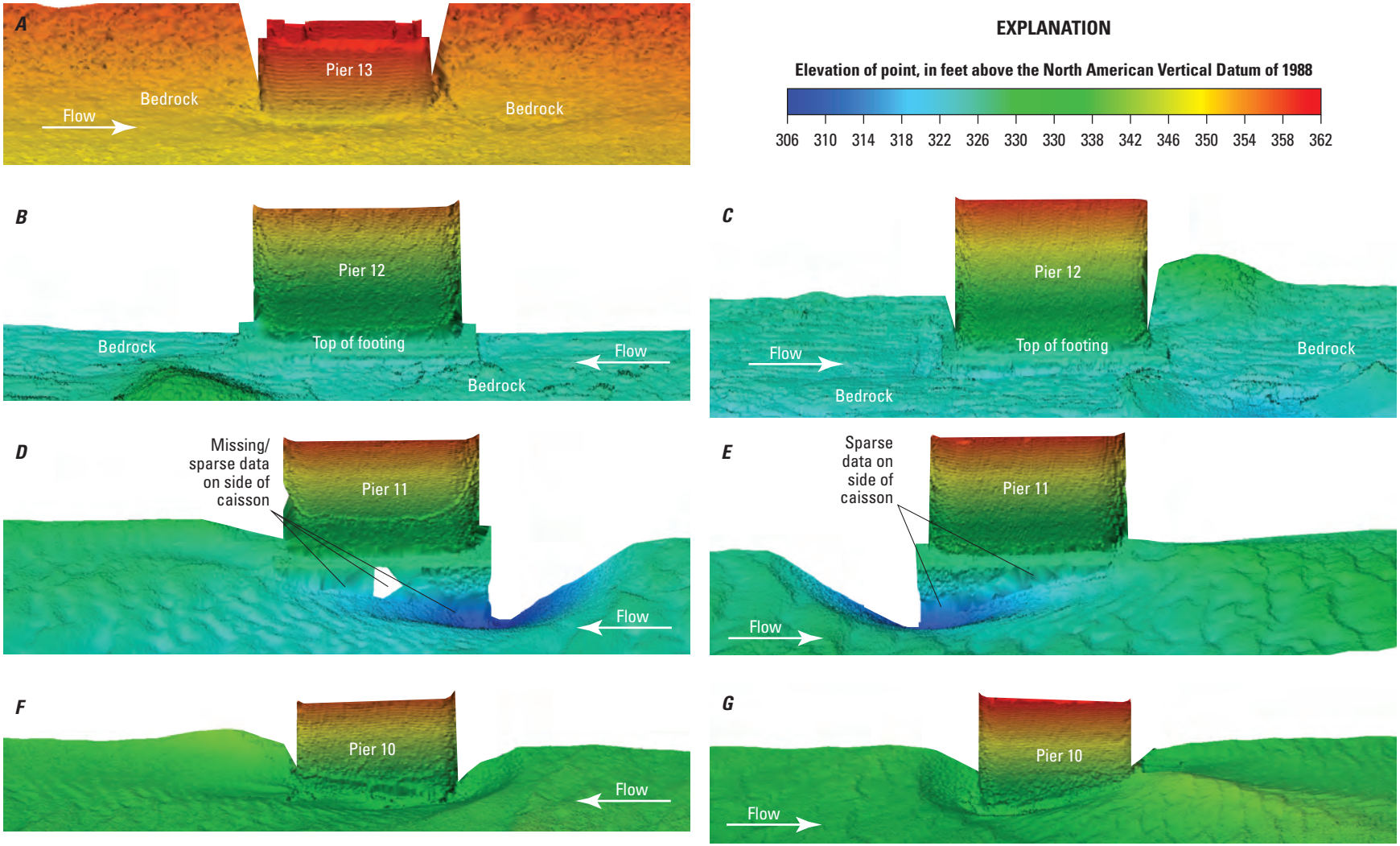

Figure 1.5. Shaded triangulated irregular network visualization of the channel bed and main channel piers of structure L0135 on State Highway 51 over the Mississippi River at Chester, Illinois. *A*, Right (southwest) side of pier 13. *B*, Left (northeast) side of pier 12. *C*, Right (southwest) side of pier 12. *D*, Left (northeast) side of pier 11. *E*, Right (southwest) side of pier 11. *F*, Left (northeast) side of pier 10. *G*, Right (southwest) side of pier 10.

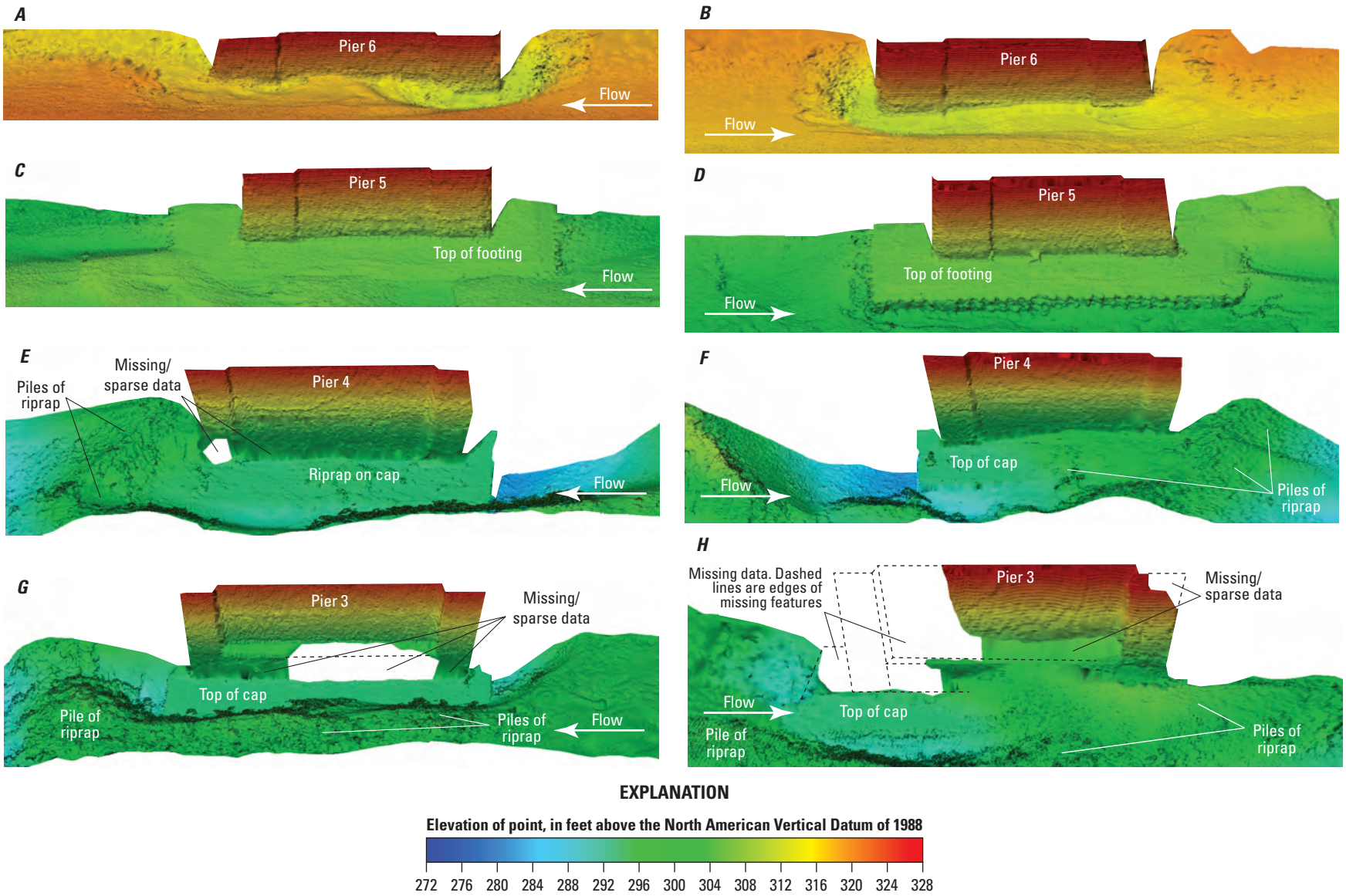

Figure 1.6. Shaded triangulated irregular network visualization of the channel bed and main channel piers of structure A5076 on State Highway 34 over the Mississippi River at Cape Girardeau, Missouri. *A*, Left (east) side of pier 6. *B*, Right (west) side of pier 6. *C*, Left (east) side of pier 5. *D*, Right (west) side of pier 5. *E*, Left (east) side of pier 4. *F*, Right (west) side of pier 4. *G*, Left (east) side of pier 3. *H*, Right (west) side of pier 3.

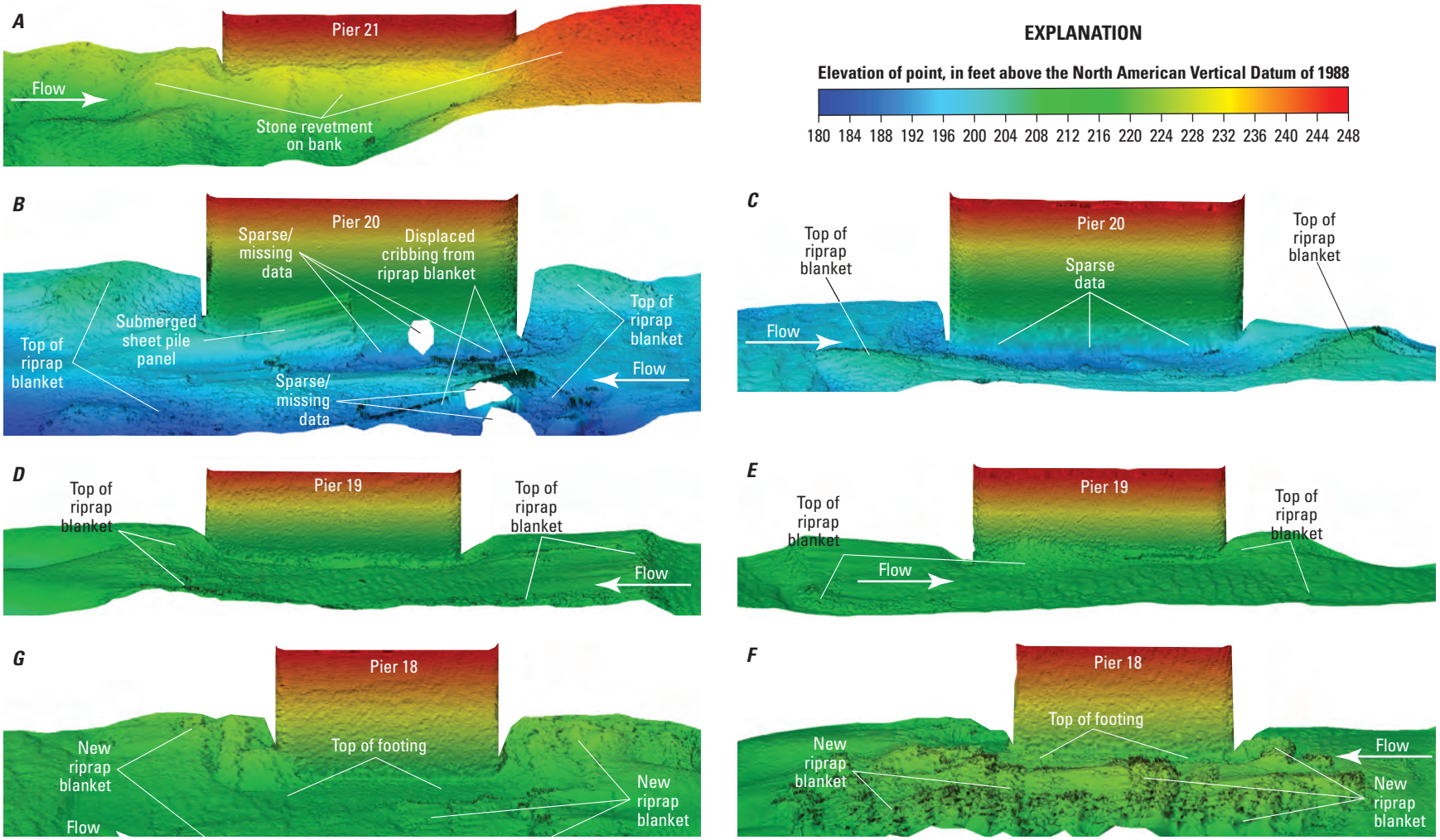

Figure 1.7. Shaded triangulated irregular network visualization of the channel bed and left main channel piers of structure A1700 on Interstate 155 over the Mississippi River near Caruthersville, Missouri. *A*, Right (northwest) side of pier 21. *B*, Left (southeast) side of pier 20. *C*, Right (northwest) side of pier 20. *D*, Left (southeast) side of pier 19. *E*, Right (northwest) side of pier 19. *F*, Left (southeast) side of pier 18. *G*, Right (northwest) side of pier 18.

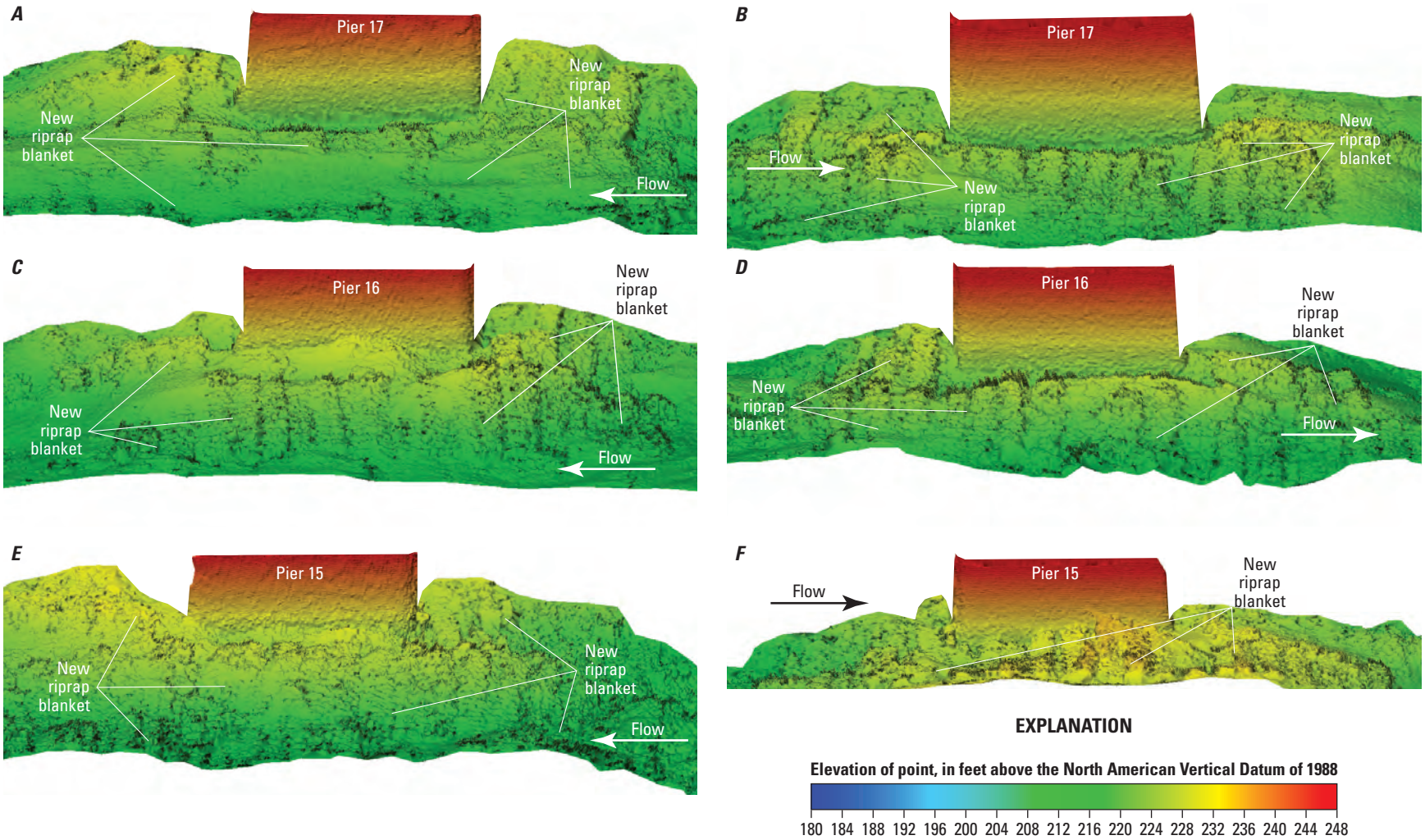

Figure 1.8. Shaded triangulated irregular network visualization of the channel bed and right main channel piers of structure A1700 on Interstate 155 over the Mississippi River near Caruthersville, Missouri. *A*, Left (southeast) side of pier 17. *B*, Right (northwest) side of pier 17. *C*, Left (southeast) side of pier 16. *D*, Right (northwest) side of pier 16. *E*, Left (southeast) side of pier 15. *F*, Right (northwest) side of pier 15.

For more information about this publication, contact:
Director, USGS Central Midwest Water Science Center
1400 Independence Road
Rolla, MO 65401
573–308–3667

For additional information, visit: https://www.usgs.gov/centers/cm-water

Publishing support provided by the
Rolla Publishing Service Center

ISSN 2328-0328 (online)
https://doi.org/10.3133/sir20245032